



저작자표시-비영리-변경금지 2.0 대한민국

이용자는 아래의 조건을 따르는 경우에 한하여 자유롭게

- 이 저작물을 복제, 배포, 전송, 전시, 공연 및 방송할 수 있습니다.

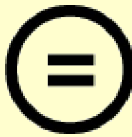
다음과 같은 조건을 따라야 합니다:



저작자표시. 귀하는 원저작자를 표시하여야 합니다.



비영리. 귀하는 이 저작물을 영리 목적으로 이용할 수 없습니다.



변경금지. 귀하는 이 저작물을 개작, 변형 또는 가공할 수 없습니다.

- 귀하는, 이 저작물의 재이용이나 배포의 경우, 이 저작물에 적용된 이용허락조건을 명확하게 나타내어야 합니다.
- 저작권자로부터 별도의 허가를 받으면 이러한 조건들은 적용되지 않습니다.

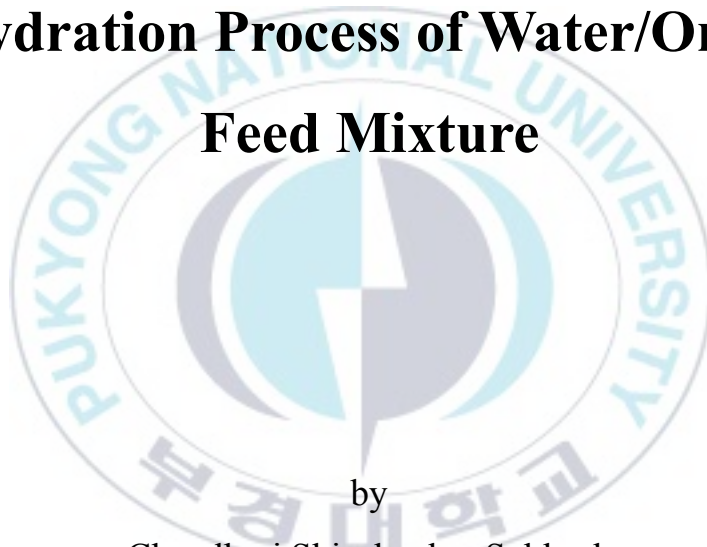
저작권법에 따른 이용자의 권리는 위의 내용에 의하여 영향을 받지 않습니다.

이것은 [이용허락규약\(Legal Code\)](#)을 이해하기 쉽게 요약한 것입니다.

[Disclaimer](#)

Thesis for the Degree of Doctor of Philosophy

**Synthesis and Evaluation of PVA Based
Membrane for Pervaporation
Dehydration Process of Water/Organic
Feed Mixture**



by

Chaudhari Shivshankar Subhash

Department of Industrial Chemistry Engineering

The Graduate School

Pukyong National University,

February 22, 2019

**Synthesis and Evaluation of PVA Based
Membrane for Pervaporation
Dehydration Process of Water/Organic
Feed Mixture**

Advisor: Prof. Shon MinYoung

by

Chaudhari Shivshankar Subhash

A thesis submitted in partial fulfillment of the requirement

For the degree of

Doctor of Philosophy

In Department of Industrial Chemistry Engineering, The Graduate School,

Pukyong National University

January 2019

Synthesis and Evaluation of PVA Based Membrane for Pervaporation
Dehydration Process of Water/Organic Feed Mixture

A dissertation

by

Chaudhari Shivshankar Subhash

Approved by:

Prof. Myung Jun Moon (Chairman)

Prof. Jun Hyuk Lim (Member)

Prof. Dong Wook Chang (Member)

Prof. Seong Il Ryu (Member)

Prof. Min Young Shon (Member)

February 22, 2019

Index.....	I
List of table.....	V
List of Figure.....	VI
Abbreviations.....	X
Abstract.....	XII

1. Introduction

1.1 Purpose of the study.....	3
1.1.1 Synthesis and Evaluation of PVA based membrane.....	3
1.1.2 Dehydration of water/organic mixtures.....	4
1.2 Objective of present study.....	17
1.3 Plan of work.....	17
Reference.....	18

2. Research Background and Literature Survey

2.1 Membrane separation processes.....	21
2.2 Pervaporation- Membrane Separation process.....	23
2.3 Factor affecting polymer membrane performance in pervaporation.....	27
2.3.1 Effect of operating condition.....	27
2.3.2 Effect of permeant size.....	30
2.3.3 Effect of membrane thickness.....	30
2.3.4 Membrane swelling.....	31
2.3.5 Membrane crystallinity.....	31
2.3.6 Free Volume.....	31
2.4 Classification of pervaporation process and materials and application.....	32
2.5 PVA based membrane.....	34
Reference.....	39

3. Pervaporation dehydration of isopropanol by using the blend membrane prepared from the PVA and PVAm

3.1 Introduction.....	42
3.2 Experimental.....	43
3.2.1 Preparation of the crosslinked PVA/PVAm blende membrane.....	45
3.2.2. Swelling measurement.....	48
3.2.3 Pervaporation apparatus and measurement.....	49
3.3 Result and Discussion.....	51
3.3.1 Membrane characterization.....	51
3.2.2 Pervaporation.....	60
3.2.2.1 Effect of PVAm Addition.....	60
3.2.2.2 Effect of temperature.....	65
3.2.2.3 Effect of feed composition.....	69
3.2.2.4 Effect of membrane thickness.....	72
3.2.2.5 Comparison of PV performance with other studies.....	75
3.4 Conclusion.....	77
Reference.....	78
4. Pervaporation dehydration of acetonitrile by using the blend membrane prepared from the PVA and PVAm	
4.1 Introduction.....	80
4.2 Experimental.....	83
4.2.1 Preparation of the crosslinked PVA/PVAm blend membrane.....	83
4.2.2 Degree of membrane sorption in acetonitrile/water feed mixture.....	85
4.2.3 Pervaporation apparatus and measurements.....	85
4.3 Result and Discussion.....	87
4.3.1 Membrane Characterization.....	87
4.3.2 Membrane swelling and Sorption Study.....	87
4.4 Pervaporation.....	89
4.4.1 Effect of PVAm content in PVA/PVAm ratios on PV performance for water/ACN mixture.....	89
4.4.2 Effect of feed composition on separation performance for water/ACN mixture.....	94

4.4.3 Effect of feed temperature on separation performance for water/ACN mixture.....	99
4.4.4 Comparison of pervaporation results with other studies.....	105
4.5 Conclusion.....	107
Reference.....	108

5. Pervaporation dehydration of water/isopropanol mixtures using M-STA loaded PVA/PVAm mixed matrix membrane.

5.1 Introduction.....	110
5.2 Experimental.....	114
5.2.1 Preparation of the preparation of m-STA particle.....	114
5.2.2 Preparation of the M-STA loaded PVA/PVAm mixed matrix membranes	115
5.2.3 Swelling Degree Measurement.....	118
5.2.4 Pervaporation apparatus and measurements.....	118
5.3 Result and Discussion.....	119
5.3.1 Membrane Characterization.....	119
5.4 Pervaporation.....	129
5.4.1 Effect of M-STA Loading.....	129
5.4.2 Effect of feed concentration.....	133
5.4.3 Effect of operating temperature on the membrane performance in pervaporation...	136
5.4.4 Membrane durability study.....	141
5.5 Conclusion.....	143
Reference.....	144

6. Pervaporation separation of a water/acetic acid mixture using in situ synthesized silver nanoparticles in PVA/PAA membrane

6.1 Introduction.....	146
6.2 Experimental.....	149
6.2.1 Membrane preparation.....	149
6.2.2 Membrane absorption Study.....	151
6.2.3 Swelling degree measurement.....	151

6.2.4 Pervaporation apparatus and measurements.....	151
6.3 Result and Discussion.....	152
6.3.1 Characterization.....	152
6.4 Pervaporation.....	164
6.4.1 Effect of Ag nanoparticles on the pervaporation performance of the PVA/PAA membrane.....	164
6.5 Conclusion.....	169
Reference.....	170

7. Summary and Conclusion

7.1 Summary.....	173
7.2 Conclusion.....	174



List of Table

Table 1.1 Pervaporation Membrane and there pervaporation performance in separation of water/IPA.....	8
Table 1.2 Pervaporation Membrane and there pervaporation performance in separation of water/Acetonitrile mixture.....	12
Table 1.3 Pervaporation Membrane and there pervaporation performance in separation of water/acetic acid mixture.....	16
Table 2.1 Separation process by membranes.....	22
Table 2.2 Advantages and disadvantages associated with PVA based membrane.....	36
Table.3.1 Abbreviations of blended PVA and PVAm membranes.....	47
Table 3.2 Pervaporation performances of PVA/PVAm blend membrane compared with other studies.....	76
Table.4.1 Abbreviations of blended PVA and PVAm membranes for water/acetonitrile separation.....	84
Table 4.2 Comparison table for the pervaporation performance of PVA/PVAm blend membrane with other studies for acetonitrile separation.....	106
Table.5.1 Abbreviations of MSTA loading in PVA/PVAm blended membranes.....	116

List of Figure

Figure 1.1 Schematic pervaporation method.....	2
Figure 1.2 Isopropanol manufacture process flow diagram.....	5
Figure 1.3 Acetonitrile manufacture process flow diagram.....	10
Figure 1.4 Flow chart of acetic acid manufacturing process by fermentation of ethanol...14	
Figure 1.5 Flow chart of acetic acid manufacturing process by (Monsanto process) carbonylation of methanol.....	15
Figure 2.1 Mass transport mechanism across the membrane.....	25
Figure 2.2 the solution diffusion model for PV transport.....	26
Figure 2.3 the Pore flow model for PV transport.....	27
Figure 2.4 Classification of pervaporation process.....	33
Figure 2.5 Chemical structure of polyvinyl alcohol.....	35
Figure 2.6 Polyvinyl alcohol modification methods.....	37
Figure 3.1 Schematic diagram of pervaporation apparatus.....	50
Figure 3.2 Proposed Chemical crosslinking reaction for PVA/PVAm blend membranes..52	
Figure 3.3 FTIR (ATR mode) spectra for PVA and PVA crosslinked membrane a) and PVA, PVA/PVAm blend uncrosslinked and crosslinked membranes b).....	53
Figure 3.4 XRD pattern of PVA, PVAm0, PVAm0.5, PVAm1, PVAm1.5 membranes.....	55
Figure 3.5 DSC curve of PVA0, PVAm0.5, PVAm1, PVAm1.5 membranes.....	57
Figure 3.6 SEM (surface and cross-sectional) micrographs for PVA (a, c) and PVAm1.5 (b, d).....	59
Figure 3.7 Effect of PVAm addition on the degree of swelling using a feed composition of 85 wt. % IPA at 30 °C, thickness: 70 µm.....	62
Figure 3.8 Effect of PVAm addition on the pervaporation flux and separation factor. Feed composition: 85% IPA, 70 µm thickness at 30 °C.....	63
Figure 3.9 Total flux and the fluxes of water and IPA as a function of PVAm addition.....	64
Figure 3.10 Effect of temperature on the pervaporation flux and separation factor. Feed composition: 85% IPA, 70 µm thickness.....	67

Figure 3.11 Variation of $\ln J_{\text{Water}}$ and $\ln J_{\text{IPA}}$ with temperature for PVAm1.5 membrane, Feed: 85% IPA solution.....	68
Figure 3.12 Effect of feed on swelling degree. Temperature: 60 °C 85% IPA, 70 μm thickness.....	70
Figure 3.13 Effect of feed on the pervaporation flux and separation factor. Temperature: 60 °C, 70 μm thickness.....	71
Figure 3.14 Permeation flux as a function of Reciprocal of membrane thickness, PVAm1.5, Feed: 85/15 IPA/water at 40 °C.....	73
Figure 3.15 Effect of membrane thickness on flux and separation factor. Temperature: 40 °C, Feed: 85% IPA/water.....	74
Figure 4.1 Variation of degree of swelling with different wt. % of water in the feed for different PVAm blend membranes.....	88
Figure 4.2 Influence of PVAm content in blend membranes of PVA on permeation flux and separation factor for Acetonitrile dehydration at 30 °C, thickness ~65 μm	91
Figure 4.3 Effect of PVAm content in blend membranes of PVA on individual fluxes of water, acetonitrile and water wt. % in permeate.....	92
Figure 4.4 Influence of PVAm content in blend membranes of PVA on pervaporation separation index (PSI).....	93
Figure 4.5 Effect of feed composition on pervaporation performance for water-acetonitrile mixture by MB1.5 at 30 °C, 65 μm	96
Figure 4.6 Effect of feed composition on pervaporation performance for water-acetonitrile mixture by MB1.5 on individual fluxes of water, acetonitrile.....	97
Figure 4.7 Comparison of vapor-liquid equilibrium curve with pervaporation experimental results of MB1.5 membranes for water-acetonitrile mixtures at 30 °C.....	98
Figure 4.8 Effect of temperature on pervaporation flux and separation factor for water acetonitrile by MB1.5 membrane, feed composition: 85/15 w/w acetonitrile/water.....	101
Figure 4.9 Effect of temperature on pervaporation flux and separation factor for water acetonitrile by MB1.5 membrane, feed composition: 90/10 w/w acetonitrile/water.....	102
Figure 4.10 Variation of $\ln J_{\text{water}}$ and $\ln J_{\text{Acn}}$ with temperature at 85/15 acetonitrile feed composition.....	103

Figure 4.11 Variation of $\ln J_{\text{water}}$ and $\ln J_{\text{Acn}}$ with temperature at 90/10 acetonitrile feed composition.....	104
Figure 5.1 FTIR (ATR mode) spectra for (a) STA, melamine and melamine- STA complex.....	121
Figure 5.2 XRD patterns for M-STA particles and M0-MSTA, M4-MSTA, M8-MSTA and M12-MSTA membranes.....	123
Figure 5.3 SEM surface micrographs for (a) M0-MSTA (b) M8-MSTA membranes and (c) M-STA particles and (d) SEM-EDS spectra for M-STA particles.....	125
Figure 5.4. 3D AFM images for (a) M0-MSTA, (b) M4-MSTA, (c) M8-MSTA (d) M12-MSTA membranes.....	126
Figure 5.5 Effect of M-STA loading on contact angle of water and swelling degree of the membranes.....	128
Figure 5.6 Effect of M-STA loading on the pervaporation flux and separation factor. Feed composition: 80% IPA, at 60 °C.....	131
Figure 5.7 Effect of M-STA loading on the individual contents of water and IPA (%) in the permeate solution. Feed composition: 80% IPA, at 60 °C.....	132
Figure 5.8 Effect feed composition on the pervaporation flux, M0-MSTA and M8-MSTA membranes, at 60 °C.....	134
Figure 5.9 Effect feed composition on the separation factor, M0-MSTA and M8-MSTA membranes, at 60 °C.....	135
Figure 5.10 Effect of temperature on pervaporation flux and separation factor, M8-MSTA membranes, Feed composition: 80% IPA.....	138
Figure 5.11 Individual fluxes of water and IPA as function of temperature, M8-MSTA membranes, Feed composition: 80% IPA.....	139
Figure 5.12 Variation of $\ln J_{\text{water}}$ and $\ln J_{\text{IPA}}$ with temperature for M8-MSTA membrane, Feed: 80% IPA solution.....	140
Figure 5.13 Plot of time against flux and water in the permeate (%) for durability of membrane (M8-MSTA) at Feed composition: 86/14 IPA/water (w/w), at 30 °C.....	142
Figure 6.1 FTIR spectra for PVA/PAA and silver composite membranes.....	154

Figure 6.2 Effect of silver nanoparticle content on the water contact angle for the PVA/PAA membrane.....	155
Figure 6.3 UV-vis absorption spectra for silver composite and virgin PVA/PAA membranes.....	157
Figure 6.4 SEM micrographs of PVA/PAA (a) and silver composite membranes (MAg0.75 – (b), MAg 1.5 – (c), MAg2.25 – (d)).....	159
Figure 6.5 SEM-EDS spectrum of the in situ synthesized Ag nanoparticles in the PVA/PAA composite membrane (MAg0.75).....	160
Figure 6.6 Membrane water absorption as a function of time ($s^{1/2}$) for the PVA/PAA and silver composite membranes.....	163
Figure 6.7 Effect of silver nanoparticle content on the pervaporation flux and separation factor. Feed composition: 20% acetic acid, 50 μm thickness at 40 °C.....	166
Figure 6.8 Effect of silver nanoparticle content on the degree of swelling for PVA/PAA membranes using a feed composite of 80 wt. % acetic acid at 40 °C, thickness: 50 μm	167
Figure 6.9 Total flux and the fluxes of water and acetic acid as a function of silver nanoparticle content.....	168

Abbreviation

PV	Pervaporation
PVA	Polyvinyl alcohol
PVAm	Polyvinyl amine
PAA	Polyacrylic acid
STA	Silicotungstic acid
M-STA	Melamine modified silicotungstic acid
Ag Nps	Silver nanoparticle
IPA	Isopropyl alcohol (Isopropanol)
ACN	Acetonitrile
AA, (AcOH)	Acetic acid
SD	Swelling Degree
α	Separation Factor
$J_{(IPA, ACN, AA)}$	Flux ($\text{kg}/\text{m}^2\text{h}$) (Total, Isopropanol, Acetonitrile and Acetic acid)
Q	Weight of permeated solution collected in cold trap
A	Effective of membrane (m^2)
t	Pervaporation operation time (second)
P_w and F_w	Weight fraction of water in permeate and feed
F_I and P_I	Weight fraction of Isopropanol in feed and permeate
F_A and P_A	Weight fraction of Acetic acid in feed and permeate
F_{Acn} and P_{Acn}	Weight fraction of Acetonitrile in feed and permeate
$PSI = J \cdot \alpha$	Pervaporation separation index
m_s and m_d	mass of the swelled and dried membranes
Ap	Pre-exponential Factor
Ep	Energy of activation for permeation (kJ/mol)
T ($^{\circ}\text{C}$)	Temperature (degree Celsius)
μm	Micrometer

XRD	X-ray Diffraction Study
FTIR-ATR mode	Fourier transform infrared (attenuated total reflection)
SEM	Scanning Electron Microscopy
EDS	Energy dispersive X-ray spectroscopy
AFM	Atomic force microscopy
UV	Ultra violet spectroscopy
DSC	Differential Scanning Colorimetry



Synthesis and Evaluation of PVA Based Membrane for Pervaporation Dehydration Process of Water/Organic Feed Mixture

Shivshankar S Chaudhari

Department of Industrial Chemistry, The graduate school
Pukyong National University

Abstract

In this worked PVA based hydrophilic membranes were prepared using different methods for pervaporation dehydration of water/isopropanol, water/acetonitrile and water/acetic acid mixtures. All the membrane were characterized by different technique such as, scanning electron microscopy, X-ray diffraction analysis, contact angle measurements, Differential scanning calorimetry, Fourier transform infrared spectroscopy and swelling degree measurements. Among them blending membrane from PVA/PVAm were used for separation of water/isopropanol mixture and acetonitrile mixtures. In pervaporation output, membrane with blending ratio (PVA: PVAm 5:1) showed optimum performance in both of water/IPA and water/Acetonitrile feed system. Further in the next study, in order to upgrade the pervaporation output for the same membrane (PVA: PVAm 5:1.5), it was further upgrade using the loading of modified silico-tungstic acid (MSTA) particle in to it. For that, the modified silicotungstic acid particle were prepared using melamine and silicotungstic acid complexation in aqueous media. In pervaporation separation water/isopropanol mixture, it was concluded that the 8 wt. % loaded MSTA loaded showed the optimum pervaporation performance. It was found that separation using the pervaporation membrane for water/isopropanol was economically inexpensive in comparison to the distillation. Since due to relative volatility of water and acetic acid mixture their separation using the distillation is economically and energetically expensive so mixed matrix membrane using the PVA and in situ synthesized Silver nano particle were prepared and pervaporation separation of water/acetic acid were successfully done.

물/유기용액의 투과 증발 탈수공정을 위한 PVA 기반의 분리막 합성 및 성능 평가
연구

Shivshankar S Chaudhari

부경대학교 대학원 공업화학과

요 약

본 연구에서는 다양한 방법으로 친수성을 갖는 폴리비닐알콜을 기반으로 한 분리막을 제작하였으며 water/isopropanol, water/acetonitrile 그리고 water/acetic acid 혼합물에서 물을 선택적으로 분리할 수 있는 투과증발 실험을 실시하였다. 제작한 분리막은 X-ray diffraction analysis, contact angle measurements, Differential scanning calorimeter, Fourier transform infrared spectroscopy 그리고 swelling degree 를 측정하여 분리막의 특성을 분석하였다. 제작한 분리막 중 PVA/PVAm 분리막은 water/isopropanol 과 water/acetonitrile 혼합 용액의 투과증발 연구에 사용하였으며 PVA: PVAm 5:1 의 조건에서 최적화 된 투과증발 성능을 확인하였다. 기존 PVA/PVAm 분리막의 투과증발 성능 개선을 위하여 수계에서 melamine 과 silicotungstic acid 를 반응시킨 Modified silico-tungstic acid (MSTA) 입자를 제조하였으며 PVA/ PVAm 막에 첨가하여 water/isopropanol 혼합물의 투과증발 실험을 진행하였다. 실험 결과 MSTA 가 8 wt% 첨가된 분리막에서 우수한 투과증발 성능을 나타내었다. 실험 결과 투과증발막을 이용한 water/isopropanol 혼합물의 분리는 증류법에 비해 경제적인 공정임을 알 수 있었다. Water 와 acetic acid 의 상대적인 휘발성 차이로 인하여 증류공정을 이용한 분리는 에너지 소모가 많은 공정으로 알려져 있다. 본 연구에서는 PVA 분리막에 in situ 로 Silver nano 입자를 합성하여 분리막을 제조하였으며 water/acetic acid 의 투과증발에 적용하였다. 결과적으로 water 를 분리하는데 있어 효과적인 방법임을 확인하였다.

1. Introduction

Convective separation techniques, such as distillation, azeotropic distillation, play an important role in the dehydration of organic solvents such as alcohols and esters in the chemical industries. However, these processes are energy-intensive and lead to uneconomical pathways. Alternatively, pervaporation, a membrane-based separation technique for liquid separation, usually uses polymeric or inorganic or organic-inorganic hybrid dense membranes as a separating barrier. Generally, pervaporation is employed in three categories for the separation of organics: 1) Dehydration of organic solutions, e.g., alcohols, acetic acid, ethylene glycol; 2) Separation of organic-organic liquids, e.g., aliphatic-aromatic, alcohol-alcohol; 3) Removal of volatile organics from diluted organic streams. It has valuable advantages compared to distillation or azeotropic distillation. A pervaporation system can be used effectively to break azeotropes or separate liquids with different volatilities without any physical difficulty since it is a very simple process. Moreover, it does not have any environmental side effects, as well as pervaporation requires pressure to be maintained on the permeate side, which creates a partial pressure difference between the membrane sides that serves as the driving force for diffusion. As shown in Figure 1.1, either side of the membrane is a liquid and on the other side is a vapor permeate. In pervaporation, selective sorption and diffusion occur across the membrane under the influence of a chemical potential gradient. Therefore, unlike other membrane-based separation processes, in pervaporation, phase change from liquid on the feed side to gaseous on the permeate side occurs. So basically, sorption is a thermodynamic property that depends on the chemical affinity of the membrane with certain liquid components, and diffusion is a kinetic property that depends on the size and motion and permanence gap in the polymer chain matrix of the membrane, which determine the efficiency of any membrane. [1]

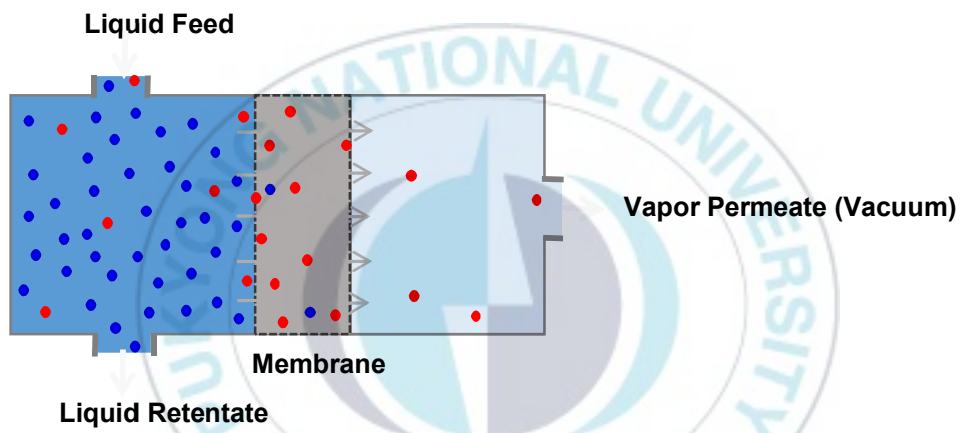


Figure 1.1 Schematic diagram pervaporation separation method.

1.1 Purpose of the study

1.1.1 Synthesis and Evaluation of PVA based membrane

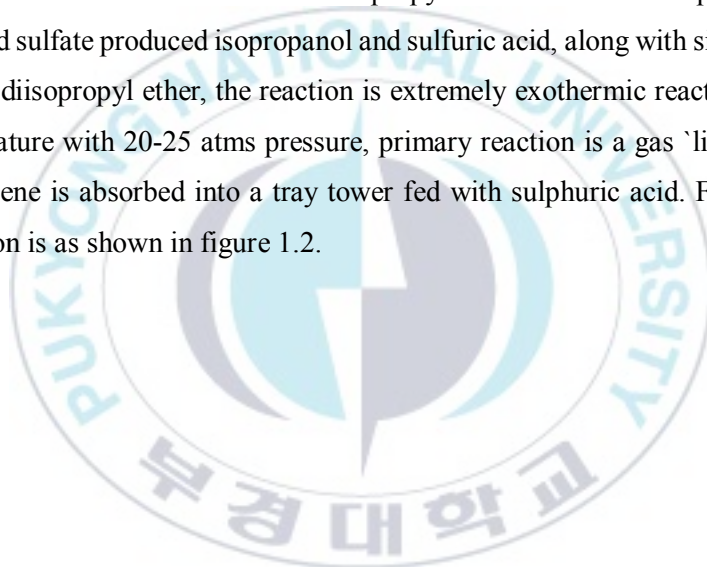
Similar to other membrane based separation, in the pervaporation, chemical nature of membrane determine its application and permeation performance. For the dehydration of organics such as alcohols, acetonitrile and acetic acid, polyvinyl alcohol preferred due to its affinity with water [2-4]. The high affinity of PVA with water provide a high selectivity, but it should be controlled because membrane performance can declined adversely if has excessive affinity, since the PVA membrane swell in the water. [5]. So, PVA membranes has always been crosslinked with the certain crosslinking agent to control the swelling. Crosslinking is a method of connection of PVA polymer chain with covalent bonding by chemical agent to reduce the flexibility. Although the membrane swelling can be controlled by crosslinking but in that case membrane permeation performance reduce abruptly due to the formation close compact structure and increased in the rigidity of the PVA membrane. Additionally it also reduces the free volume in the PVA based membrane. Although the PVA based crosslinked membrane has most widely explore in the dehydration of organics. However looking at the performance the PVA based membrane in the literatures for the pervaporation dehydration organics. It is necessary to enhance its PV performance by several modifying method such as blending method, physical mixing of inorganic or organic nano particle in the PVA membrane matrix. And evaluation of their performance in the pervaporation dehydration organics. So in that way, it could be possible to simultaneously increase a permeability and selectivity of the PVA membranes.

1.1.2 Dehydration of water/organic mixtures

Organics, for example isopropanol, acetonitrile and acetic acid have a several application in chemical industries. But in their production and purification by convectional method is a very complex process and require the tremendous amount energy.

Production process of isopropanol, concentration by azeotropic distillation and economic of pervaporation and hybrid pervaporation distillation process.

Isopropanol is produced from hydration of propylene. In the first step Isopropyl acid sulfate is produced from the sulfation of propylene. In the next step, hydrolysis of Isopropyl acid sulfate produced isopropanol and sulfuric acid, along with side reaction take place yield a diisopropyl ether, the reaction is extremely exothermic reaction, operated at room temperature with 20-25 atms pressure, primary reaction is a gas `liquid reaction in which propylene is absorbed into a tray tower fed with sulphuric acid. Flow diagram of IPA production is as shown in figure 1.2.



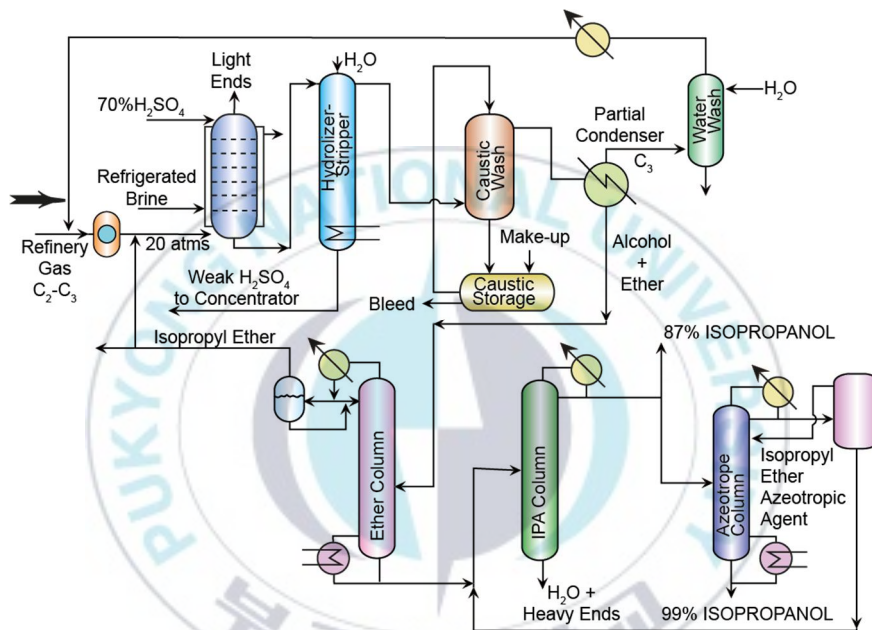


Figure 1.2 Isopropanol manufacture process flow diagram [6]

As we can observed from the flow diagram of isopropanol production process. In the bottom product consisting of isopropyl alcohol and water is sent to an isopropyl alcohol column that produces water and heavy ends as the bottom product and 87% isopropanol-water azeotrope mixture as the top product is formed. Therefore, in order to separate the azeotrope, it should sent to an azeotropic distillation column that uses isopropyl ether as an azeotropic agent to obtain 99 % isopropanol as the bottom product. [6-7]. Since water and isopropanol form an azeotrope because they have same composition in vapor and liquid phase [8-9]. The normal distillation process can not apply for concentration of IPA. So azeotropic distillation is apply, however it this case it require third component as entrainer (isopropyl ether), which become more energy intensive process resulted in to the higher cost of production. [8]. On the other hand pervaporation is less energy process, which can be alternative to separation of azeotropes. It has a less environment side effect than distillation. [10]. In pervaporation the separation is not based on the relative volatility of the components in the mixture, but only depends on the relative affinity of the components for the membrane [11]. A vacuum is kept on the permeate side of the membrane while the feed side of the membrane is kept at atmospheric or elevated pressure so a pressure difference is created over the membrane which is the driving force for the pervaporation process. The component(s) that permeates through the membrane evaporates while passing through the membrane because the partial pressure of the permeating component(s) is kept lower than the equilibrium vapor pressure. V. V. Hoof and group studied the economic comparison between the azeotropic distillation and different hybrid system combining distillation with pervaporation for dehydration of isopropanol. They have applied two different type of membrane, polymer [PERVAP 2510, Sulzer Chem Gmbh] and Ceramic membrane [NaA type zeolite, Mitsui and Co.] for pervaporation separation water and IPA. In their conclusion, it was reported that the economic point of view hybrid system distillation-pervaporation with ceramic was the most interesting process with saving in total costs of 49% in comparison to the azeotropic distillation [12]. Therefore, several research group are continuously exploring the different pervaporation membrane for the pervaporation dehydration of water/IPA mixture in azeotropic composition range. Table 1.1 shows pervaporation output for pervaporative

separation water and IPA mixture by some of studies. It is obvious from the table that, it always have difficulty to make synergy between flux and selectivity in pervaporation due to flux and selectivity term are contradictory to each other. So necessary to explore more alternative membrane for pervaporation separation of water/IPA at azeotropic composition range.

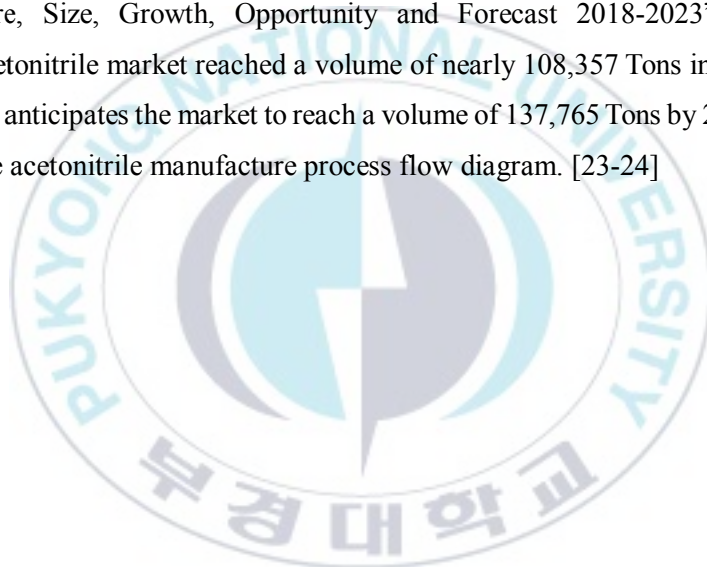


Table 1.1 Pervaporation Membrane and there pervaporation performance in separation of water/IPA mixture

Membranes	Feed(%) composition,(w/w) Isopropyl alcohol/Water	Temperature (°C)	Flux(J) (Kg/m ² h)	Separation factor(∞)	Reference
P84/ aerosol Silica	90/10	30	0.121	80	[13]
PVA-PNIPAAm Grafting	12/88	40	0.011	95	[18]
PVA/MWNT	90/10	30	0.168	882	[19]
ZIF-90 Incorporation	85/15	60	0.109	5668	[20]
Surface modification of chitosan with PBI	80/20	25	0.15	221	[21]
Matrimid/MgO	82/18	100	0.63	700	[14]
TETA-TMC	90/10	25	0.37	171	[15]
MPDSA/TMC	70/30	25	0.7	755	[16]
Pervap 2201	85/15	60	0.22	400	[17]

Production process of Acetonitrile, concentration by azeotropic distillation and economic of pervaporation or hybrid pervaporation distillation process.

Acetonitrile, also known as methyl cyanide, ethyl nitrile and cyan methane, is a colorless chemical compound with the formula CH_3CN . In the production of acrylonitrile it is produced as a by-product. Acetonitrile has a sweet, ethereal in odour. It is very important as it acts as a vital intermediate in the pharmaceutical industry. For example, it is used as a derivative in the production of sulpha pyrimidine and Vitamin B1. It also finds application as a raw material for manufacturing aromatizes, epoxy hardeners and agriculture pesticides. A new research report by IMARC Group, titled “Acetonitrile Market: Global Industry Trends, Share, Size, Growth, Opportunity and Forecast 2018-2023” estimates that the global acetonitrile market reached a volume of nearly 108,357 Tons in 2017 [22]. The report further anticipates the market to reach a volume of 137,765 Tons by 2023. The figure 1.3 shows the acetonitrile manufacture process flow diagram. [23-24]



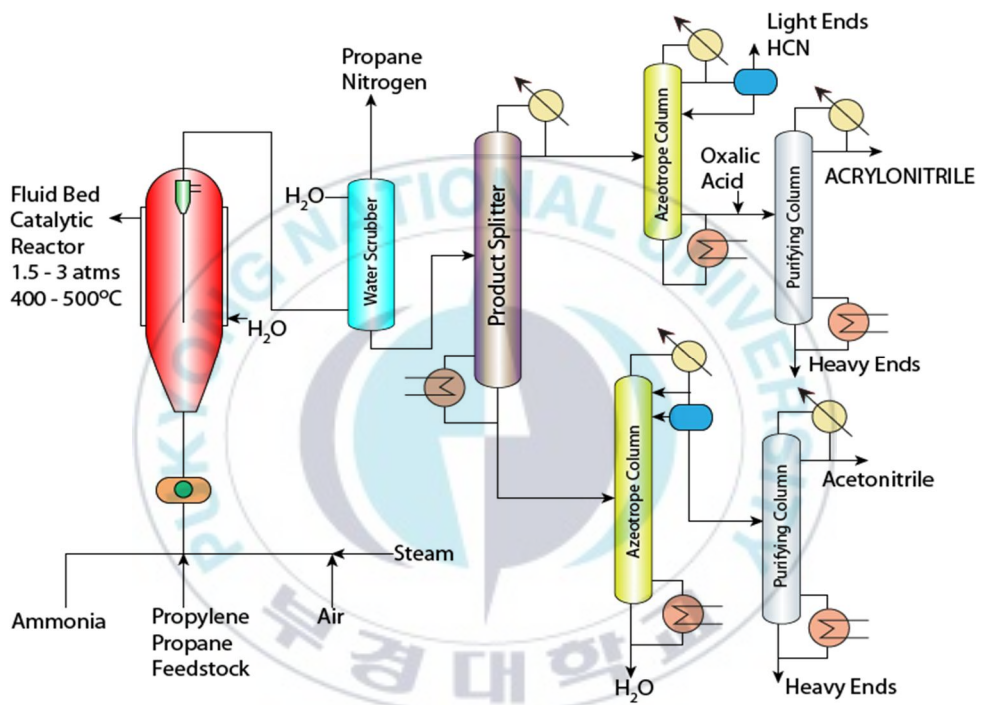


Figure 1.3 Acetonitrile manufacture process flow diagram [24]

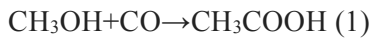
As it seen from the fig 1.3 that, the bottom product from the product splitter enters an azeotropic column which produces water as a bottom product. The total condenser in this column generates both aqueous and organic layers. The organic layer is rich in acetonitrile and heavy ends whereas the aqueous layer is sent back as a reflux to the azeotropic column. The bottom product from the acetonitrile azeotropic column enters a purification unit where distillation principle enables the separation of acetonitrile from the heavy ends. Overall, the purification of acetonitrile process is very complex process, it spend tremendous amount of energy. [23-24]. As explained in the above section, pervaporation or hybrid process of distillation and pervaporation can save the energy as it is membrane based separation process [25], the separation is based on the different on the different affinity of membrane with separating component [26]. It has several merits over the traditional distillation, it reduce the energy demand because only that liquid is need to be vaporized that intend to separation. Simple process, driven by only vacuum pump, it has lower capital coast [27]. Pervaporation separation for water-acetonitrile mixture in azeotropic composition range has not been broadly studied as compared to the alcohols-water separation. The table 1.2 shows the pervaporation performance result of the some of the studied. As, at look at the table 1.4 getting higher flux with selectivity is difficult by any of the membranes, so it is necessary to develop and study the more alternative membrane for the acetonitrile membranes.

Table 1.2 Pervaporation Membrane and there pervaporation performance in separation of water/acetonitrile mixture

Membrane	Feed(%) composition,(w/w) Water/Acetonitrile	Temper ature (°C)	Flux(J) (Kg/m ² h)	Separation factor(∞)	Thickness (μ)	Reference
PVA-FeO ₃ /FeO ₂ Incorporation	10-32	35	0.02-0.20	20-700	45	[28]
Zeolite filled(PVA/Polyan iline S-IPN	10-50	30	0.03-0.09	3-69	40	[29]
PAN-IA- Copolymerization	1.2-24	30	0.028-0.23	35-409	40	[30]

Production process of acetic acid, concentration by azeotropic distillation and economic of pervaporation or hybrid pervaporation distillation process

Acetic acid is important chemical has been constant used in the chemical industries. It is been produced from the oxidative fermentation of ethanol by bacteria (acetobacter) and by carbonylation of methanol by rhodium or iridium catalyst [Monsanto process]



As observed from, figure 1.4 and 1.5 in the production of acetic acid, at the final stage acetic acid yield a very dilute concentration acetic acid, in order to concentrate of acetic acid the extraction and distillation is been used. Due to the closed to unity of relative volatility of acetic acid to water although it does not form the azeotropes with water but still it is difficult to separate [31]. Because in distillation of acetic acid and water the water being taken off as distillate, this spend tremendous amount of energy and additionally it require large number of plate and large column. So Azeotropic distillation has been employed as alternative to distillation for pervaporation separation of water acetic acid but this leads to impurities and moreover it is still energy intensive process. Therefore so called hybrid system consist of the simple distillation can used to concentrate up to 90% of acetic acid and followed applying the pervaporation as a viable alternative, capable of saving significant energy saving. D. Horbez and groups [32] have studied and simulated the energy efficiency of hybrid PV-Distillation for acetic acid production and concluded that pervaporation can improve the distillation for acetic acid-water separation and energy gain up to 20% is achievable. The table 1.3 shows the pervaporation performance result of the some of the studies for the water/acetic mixture in more than 90% acetic concentration in the feed by verity of membranes. As, at look at the table 1.5 getting higher flux with selectivity is difficult by any of the membranes. Additionally, it shows the tremendous need of exploring the alterative membrane for acetic acid dehydration process. So it is necessary to develop and study the more alternative membrane for the Acetic /water feed system.

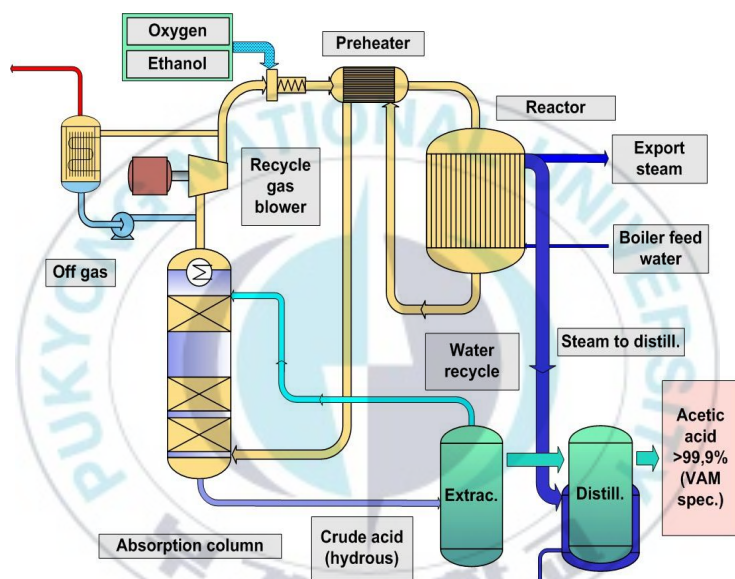


Figure 1.4 Flow chart of acetic acid manufacturing process by fermentation of ethanol. [33]

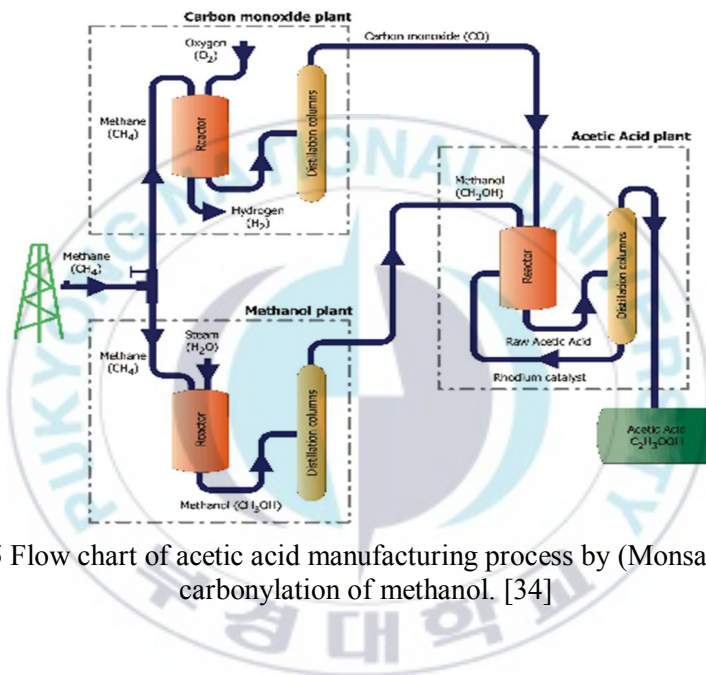


Figure 1.5 Flow chart of acetic acid manufacturing process by (Monsanto process) carbonylation of methanol. [34]

Table 1.3 Pervaporation Membrane and there pervaporation performance in separation of water/acetic acid mixture

Membranes	Feed(%) composition,(w/w) Acetic acid /Water	Temper ature (°C)	Flux(J) (Kg/m ² h)	Separation factor(∞)	Reference
PVA-Formaldehyde	90/10	30	0.14	5.3	[35]
PVA-Glutaraldehyde	90/10	30	0.10	9	[35]
PVA-Polyacrylamide grafted (93%)	90/10	45	0.098	5.63	[36]
Na-alginate-HDM crosslinked	85/15	70	0.26	161	[37]
Polycarbonate	97/3	25	0.04	∞	[38]
TPX	80/20	25	0.088	79	[39]
Mordenite-Alumina	90/10	80	0.05	50	[40]
Silica-alumina	90/10	100	0.05	5.9	[41]
Pervap 2205	90/10	30	0.33	61	[42]
Pervap 1005 (Sulzer Chemtech)	90/10	80	0.88	48	[43]

1.2 Objective of present study

The aim of this research

- 1 Synthesis and evaluation of hydrophilic PVA based membrane for separation of water/IPA, water/ACN and water/ AA feed mixture.
- 2 Physicochemical characterization for developed polymer membrane.
- 3 Pervaporation separation and optimization of developed membrane for water/ IPA, water/ACN and water/AA feed mixture.
- 4 Upgradation of membrane pervaporation performance for separation water/IPA mixture.

1.3 Plan of work

- 1 Preparation and characterization of modified polyvinyl alcohol membrane using different method.
 - Blending with polyvinyl amine and crosslinking by glutaraldehyde.
 - Mixed matrix membrane preparation using the Melamine modified STA particle in to the PVA/PVAm blend membrane.
 - Mixed matrix membrane using in situ synthesized Silver nanoparticle in the PVA/PAA polymer matrix.
- 2 Pervaporation run for the water/IPA, water/Acetonitrile and water/AA separation using prepared membrane at their azeotropic concentration range.
- 3 Analysis of the permeate composition as well as evaluation of flux, separation factor with help of instrumental analysis techniques.(Gas chromatograph)

Reference

- [1] S. Sourirajan, S. Bao, T. Matsuura, An approach to membrane separation by pervaporation, in proceeding of second international conference on pervaporation, 251, Process in the chemical industry, ed. R. A. Bakish, Bakish Mat. Cor. Englewood, NJ, 209 (1987)
- [2] F. Kursun, N. Isiklan, J. Ind. Eng. Chem. 41 (2016) 91-104
- [3] M. K Mandal, S. B. Sant, P. Bhattacharya, Colloids surface. A 373 (2011) 11-21.
- [4] N. Isiklan, O. Sanli, Chem. Engi. Proce. Intensi. 44 (2005) 1019-1027.
- [5] R. W. Bakers, Membrane Technology and applications, 2nd ed. John Wiley & Son Ltd. New York (2004).
- [6] Kirk R. E., Othmer D. F., Encyclopedia of Chemical Technology, John Wiley and Sons, 1999-2012
- [7] I. Dryden C. E., Outlines of Chemical Technology, East-West Press, 2008
- [8] Brunjes A.S.; Bogart M.J.P, The Binary Systems Ethanol-n-Butanol, Acetone-Water and Isopropanol-Water. Ind.Eng.Chem. 35 (1943) 255-260.
- [9] Lebo R.B.: Properties of Mixtures of Isopropyl Alcohol and Water. J.Am.Chem.Soc. 43 (1921) 1005-1011
- [10] S. F. Lipinzki, R. W. Field, P. K. Ten, and Pervaporation based hybrid process, a review of process design, J. Membr. Sci. 153 (1993) 183-210.
- [11] M. Mulder, Basic principle of membrane technology, second. Edition, Kluwer, Academic Publishers, Dordrecht, 1998.
- [12] V. V. Hoof, L. V. Abeele, A. Buekenhoudt, C. Dotremont, R. Leysen, Economic comparison , Separ. Purif. Technol. 37 (2004) 33-39.
- [13] O. Bakhtiari, S. Mosleh, T. Khosravi, T. Mohammadi, Mixed matrix membrane for pervaporative separation, Desalin. Water. Treat 41 (2012) 45-52.
- [14] L. Y. Jiang, T. S. Chung, R. Rajgopalan, AIChE 53 (2007), 1745-57.
- [15] S. H. Huang, W. S. Hung, D. J. Liaw, C. H. Lo, W. C. Chao, C. C. Hu, C. L. Li, K. R. Lee, J. Y. Lai, Sep. Purif. Technol. 7 (2010) 40-72
- [16] S. T. Kao S. H. Huang, D. J. Liaw, W. C. Chaw C. C. Hu, C. L. Li, D. M. Wang, Polym. Journal, 8 (2010) 242.

- [17] D. V. Baelen, B. V. Bruggen, K.V. Dungen, J. Degreve, C. Van-decastleele, *Chem. Engi. Sci.* 60 (2005) 1583-1590.
- [18] J. W. Rhim, S. W. Yeom, S.W. Kim and K. H. Lee, *J. Appl. Polym. Sci.*, 1997, 63, 521.
- [19] M. Amirilargani, M. A. Tofighy, T. Mohammadi and B. Sadatnia, *Ind. Eng. Chem. Res.*, 2014, 53, 12819
- [20] D. Hua, Y. Ong, Y. Wang, T. Yang and T. Chung, *J. Membr. Sci.* 2013, 453, 155.
- [21] Y. J. Han, K. H. Wang, J. Y. Lai, Y. L. Liu, *J. Membr. Sci.* 2014, 463, 17.
- [22] A.Rajan, IMARC group, United States. <http://www.digitaljournal.com/pr/3803564>
- [23] C. E. Dryden, *Outlines of Chemical Technology*, East-West Press, 2008
- [24] R. E. Kirk, D. F. Othmer, *Encyclopedia of Chemical Technology*, John Wiley and Sons, 1999-2012
- [25] M. T. Gomez, A. Klein, J. Repke, G. Wozny, *Desalination*, 224 (2008) 28-33.
- [26] F. Lipinzki, R. W. Field, P. K. Ten, and Pervaporation based hybrid process, a review of process design, *J. Membr. Sci.* 153 (1993) 183-210.
- [27] M. Mulder, *Basic principle of membrane technology*, second ed. Kluwer academic publishers, Dordrecht, 1998, P.336.
- [28] M. K Mandal, S. B. Sant, P. Bhattacharya, *Colloids surface. A* 373 (2011) 11-21.
- [29] B. V. Naidu, S. D. Bhat, M. Sairam, V. Wali, D. P. Sawant, S. B. Halligudi, N. N. Mallikarjuna, T. M. Aminabhavi, *J. Appl. Polym. Sci.* 96 (2005) 1968-1978.
- [30] P. Das, S. K. Ray, *J. Membr. Sci.* 507 (2016) 81-89.
- [31] Dortmund data Bank, *Thermophysical data for process design*.
- [32] C. Serval, D. Roizard, E. Favre and D. Horbez, *Ind. Engi. Chem. Research.* 53 (2014) 7768-7779.
- [33] D.D. Guzman, *Wacker licenses bio acetic acid process*, Article from green chemical blog (2010).
- [34] *Celanese Acetic acid plant*, Nanjing (2006).
- [35] N. Durmaz-Hilmioglu, A. E. Yildirim, A. S. Sakaoglu, S. Tulbentci, *Chemi. Eng. Proce.* 40 (2001) 263.
- [36] T. M. Aminabhavi, H. G. Naik, *J. Appl. Polym. Sci.* 83 (2003) 244.
- [37] X. P. Wang, *J. Membr. Sci.* 170 (2000) 71.

- [38] J. Huang, M. L. Tu, Y. C. Wang, C. L. Li, K. R. Lee, J. Y. Lai, *Eur. Polym. J.* 37 (2001) 527.
- [39] Y. C. Wang, J. F. Lee, *Water. Sci. Technol.* 38 (1998) 463.
- [40] G. Li, E. Kikuchi, M. Matsukata, *Sep. Purif. Technol.* 32 (2003) 199.
- [41] M. Asaeda, M. Ishida, T. Waki, *J. Chem. Eng. Jpn.* 38 (2005) 336.
- [42] P. S. Rao, A. Krishnaiya, B. Smitha, S. Sridhar, *Sep. Purif. Technol.* 41 (2006) 979.
- [43] D. Gorri. A. Urriaga, I. Ortiz, *Ind. Eng. Chem. Res.* 44 (2005) 977



2. Research Background and Literature survey

This chapter to briefly explain the membrane separation process having a main focus on the pervaporation, factor affecting the membrane separation process and details of mass transport in pervaporation process and introduction of PVA membrane development.

2.1 Membrane separation processes.

Membrane have a gained a considerable attention in chemical technology and are used in a broadly in variety of application. The key function of membrane is, it has ability to control the permeation of certain species through it. Mainly in separation application the goal is to allow one component of a mixture to permeate the membrane freely, while retarding permeation of other components. A membrane defined as a it is a semipermeable selective barrier which, under the influence certain driving force allow a preferential passage of one or more molecule, particles or gas from mixture of either gaseous or liquid or solution [1]. The performance of membrane generally evaluated in terms of flux which is explain the amount of mass transfer across the membrane and selectivity which derive the capability of membrane to separation of one or more species. It is possible to distinguish membrane separation process because driving force for the separation across the membranes are different. Microfiltration, ultrafiltration, nano filtration and reverse osmosis are the pressure driven operation. And Dialysis, pervaporation, forward osmosis, gas separation are concentration gradient operation. Some other process such as electro dialysis, membrane electrolysis, fuel cell are electric potential gradient process and membrane distillation operate in temperature gradient. Table 2.1 describe the details of membrane separation process depicted by et al Baker [1]

Table 2.1 Separation process by membranes

Process	Driving Force	Species size(range)	Application
Vapor Permeation	Partial pressure difference	Molecular scale (< 1nm)	Separation of azeotropic mixture
Pervaporation	Partial pressure difference (concentration gradient)	Molecular scale (< 1nm)	Separation of azeotropes, aromatic/aliphatic and esterification
Gas Separation	Partial pressure difference	Molecular scale (< 1nm)	Separation of gases inorganic/organic
Electro dialysis	Electrode potential gradient process (ΔE)	< 5nm	Brackish/large scale desalination /salt production
Dialysis	Concentration gradient	< 5nm	Separation of salt and micro solute from solution
Reverse osmosis (RO)	Pressure driven process (ΔP)	< 5nm	To remove <u>ions</u> , <u>molecules</u> and larger particles from drinking water
Ultrafiltration	Pressure driven process (ΔP)	1~ 5nm	Concentrating macromolecular (10^3 - 10^6 <u>Da</u>) solutions
Nano filtration	Pressure driven process (ΔP)	5~10 nm	Water softening (Cation removal), purification gas condensate,
Microfiltration	Pressure driven process (ΔP)	0.1~10 μm	Sterilization of liquids, Petroleum refining

2.2 Pervaporation-Membrane Separation process

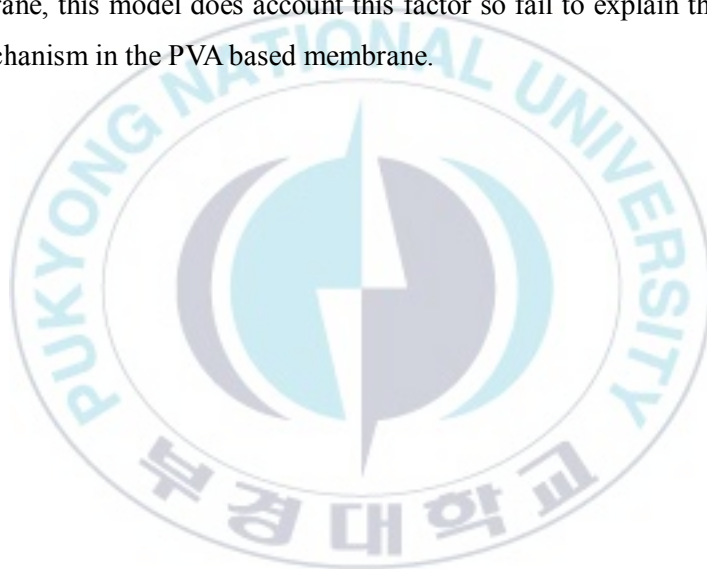
Pervaporation is a membrane based separation process has been very popular and gaining an acceptance in different chemical industries. Since it is a unique process tool for separation and recovery of liquids mixtures. Commercially it is recognized for the dehydration of hydrocarbon to yield the high purity organics such an ethanol, isopropanol, and ethyl alcohol. In separation of azeotropes (e.g. Water) and mixture of small difference in relative volatility pervaporation play effective role over its separation by distillation or extraction due these process turn in to energy intensive process. Additionally it quite easy to make a hybrid system using distillation and pervaporation. In that case concentration of target component of mixture obtained up to less than 30 % to the by distillation later pervaporation play effective role concentrate the resultant mixture. [2]

Pervaporation can be define as it is separation by membrane of two or more component in the liquid phase through the non-porous membrane where transportation mechanism take place due to the chemical potential gradient. [3]. Mass transport in the pervaporation membrane can be explain by solution diffusion model [4]. Generally there are three steps through separation take place in the pervaporation membrane. [Please ref. Fig 1.1]

- 1) In the first step selective sorption of components to the feed side of the membrane
- 2) Selective diffusion of the components across the membrane
- 3) Desorption of component to the permeate side of the membrane.

As can see from the figure 2.1 and 2.2 that, the pressure and temperature remain constant so no phase change is possible within the membrane means linear pressure profile across the membrane thickness and on permeate side there is change in pressure and temperature at permeate interface. Therefore chemical potential across the membrane can be expressed as concentration gradient and the driving force achieved by lower partial pressure at the permeate side either by applying vacuum or by using sweeping of inner gas. So, according to the solution diffusion model, separation between permeants obtained because of differences in the amount of dissolution of components and rate of diffusion of components across the membrane. The solution diffusion model is most widely used accepted transport model in pervaporation separation [3].

In 1987, Sourirajan [5] proposed the pore flow model to explain the pervaporation transport mechanism, basically in this model permeants are separated by pressure driven convective flow through the tiny pore where one permeant is excluded from some of the pore in the membrane through which other permeant move. In the pore flow model the phase change occur from the liquid to vapor at certain thickness of the membrane after feed liquid enter in the membrane pore and later vapor phase transported across the remaining length of pore and emerge on the permeate side therefore as per this model total mass transfer (flux) is depend on the pressure gradient (Please ref. figure 2.2). However, in hydrophilic membranes (PVA), swelling of membrane occurred at higher water content in the membrane, this model does account this factor so fail to explain the pervaporation transport mechanism in the PVA based membrane.



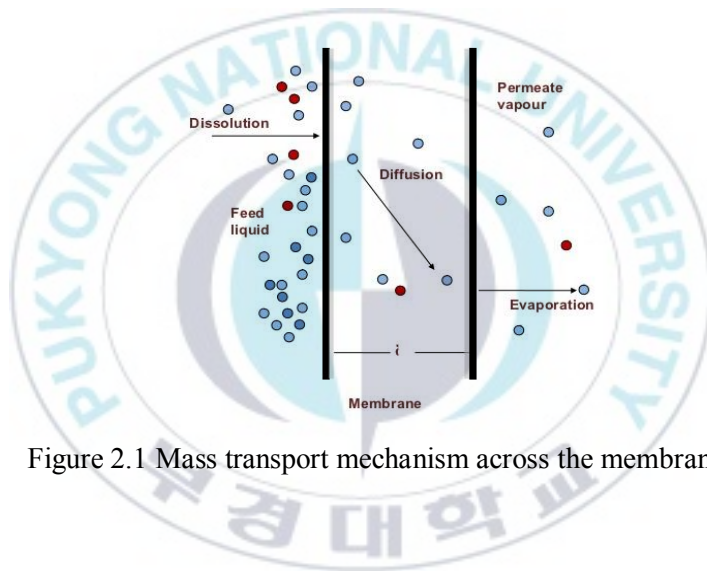


Figure 2.1 Mass transport mechanism across the membrane

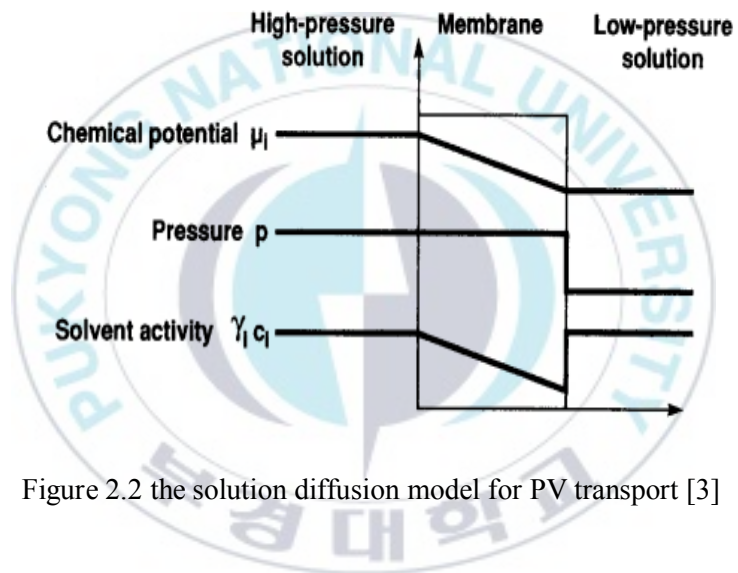


Figure 2.2 the solution diffusion model for PV transport [3]

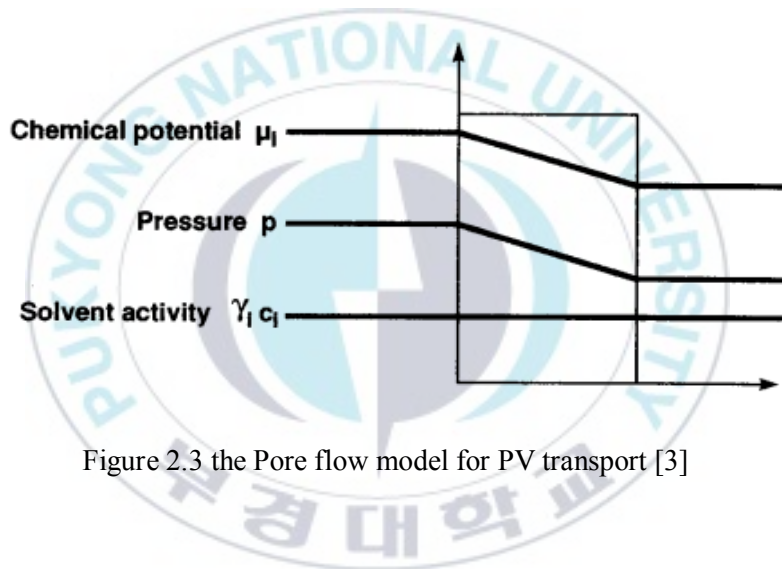


Figure 2.3 the Pore flow model for PV transport [3]

2.3 Factor affecting polymer membrane performance in pervaporation

Pervaporation performance of any membrane evaluated by total flux (permeation rate of component) and selectivity of membrane for particular component to which intend to separate in comparison to another and the pervaporation separation index. The pervaporation flux, separation factor and pervaporation separation index of each membrane was calculated using following three equations:

$$\text{Flux } (J) = \frac{Q}{A \times t} \quad (2)$$

Where, Q is the weight of permeated solution collected in the cold trap and the flux is calculated with respect to effective area (A) in time t.

$$\text{Separation Factor } (\alpha) = \frac{P_i/P_j}{F_i/F_j} \quad (3)$$

Where, P_i , P_j , F_i and F_j are the weight fractions of component i (in this study water is target component) and j (organics = IPA or Acetonitrile or Acetic acid) solution in the permeated solution and the feed solution, respectively. In addition, the pervaporation separation index was calculated from the following equation:

$$\text{Pervaporation Separation Index (PSI)} = J \times (\alpha - 1) \quad (4)$$

Where, J and α , are the flux and separation factor, respectively. Generally pervaporation performance are influence by following parameters. [6-11]

2.3.1 Effect of operating condition

Operating feed temperature, Feed composition, flow rate, and partial pressure difference are the major factors that affect the pervaporation flux and separation factor and PSI of membranes.

2.3.1.1 Feed Composition

In theoretical aspect, to separate the any liquid mixture in all composition range can be possible by pervaporation. Nevertheless the pervaporation generally most efficient in removing minor component from organic-water azeotropes, close boiling point mixture, or isomers or aliphatic/aromatic mixture [12-13]. According to solution diffusion model, the chemical potential gradient across the membrane characterized by concentration gradient is a driving force in pervaporation operation. Sorption process at feed and membrane interface and diffusion transport of permeating component that depend on concentration is influence by chemical potential gradient. In general, polymer membrane swelled with high concentration of desired component and which increase the polymer chain gap (void). Therefore, membrane performance is decrease in terms of separation (selectivity) but on other hand the permeation is faster (Flux) because easy permeation of desired and undesired component.

2.3.1.2 Feed Temperature

Pervaporation process is greatly affected by feed temperature. The mass transport across the membrane generally increase with increase of feed temperature. The reason behind that, with the increase of feed temperature, it boost the polymer chain mobility in matrix and energies the permeants [14-15] and hence increases the driving force for permeation. Additionally, when more energy supply to the permeants it is easy to vaporization of them because in the pervaporation phase change occur from liquid to vapor phase at permeate side this result in the higher permeate rate.

2.3.1.3 Flow rate

In pervaporation operation, on feed side the if feed solution does not have constant circulation, concentration polarization take place because concentration gradient created due to boundary layer on the membrane surface and in that boundary layer concentration permeating component decreases [3, 16]. In that case decrease in concertation of component to be permeated in boundary layer hence concentration polarization works

against separation achieved by the membrane with reducing the flux and separation factor. Therefore it is necessary to use high turbulent flow rate on feed side.

2.3.1.4 Permeate pressure

In pervaporation process permeate side of membrane generally kept to the vapor pressure of selective component and feed side generally kept as atmospheric pressure to obtain the driving force with creating partial pressure difference. Due to this pressure on permeate side affect the pervaporation performance. In general lower the downstream pressure increase the driving force for the mass transfer across the membrane. [3, 17]

2.3.2 Effect of permeant size

According to the solution diffusion model, the sorption and diffusion of components controls the pervaporation performance. Where sorption depends on the chemical characteristic of polymer and permeating component however diffusion of permeating components strongly concern with the size and shape of permeating molecules and also molecule aggregation within polymer. So it is obvious, at an instant, separation of binary feed mixture, molecule with smaller in molecular size desirably move faster in comparison to the molecule with high molecular size. [18]

2.3.3 Effect of membrane thickness

Similar to Fick's law of diffusion, membrane thickness affect the pervaporation flux but not considerably selectivity. This can explain that, smaller the path length for diffusion increase the mass transport across the membrane, however selectivity depends on the preferential sorption so with decrease of membrane does not affect the selectivity. From many of studies has been done to investigate the effect of membrane performance as function of membrane thickness they have reported flux is inversely proportional membrane thickness however separation remain unaffected [19]

2.3.4 Membrane swelling

The polymeric membrane performance has greatly affected by the swelling of membrane. The membrane swelling occurred from higher affinity for certain species of membrane in feed. Membrane with high degree of swelling disintegrate the polymer matrix in membrane due to plasticization of it and that resulted in to the decrease in the membrane selectivity. So degree of swelling must be controlled. [4, 17, 20]

2.3.5 Membrane crystallinity

During the membrane formation in polymer membrane due to low degree polymerization, strong intermolecular forces (hydrogen bonding), symmetrical linear chain, slow rate of cooling, orientation of molecule yield a crystalline region in the membrane along with amorphous region call semicrystalline membrane. For example, in PVA membrane consist of flexible PVA backbone is favorable for the close packing and crystallization due to presence of linear chain with strong hydrogen bonding. Generally, membrane with high degree of crystallinity reduces the membrane swelling due to crystallite behave as a physical crosslinked due to close packing and which reduces the permeation rate. [21]

2.3.6 Free volume

The free volume of a polymer is the sum of the many small spaces between in the polymer chain in the amorphous, non-crystalline materials. The free volume of a polymer can be determined by measuring the polymers specific volume, then calculating the occupied volume of groups that form the polymer.[1] Thermal motion of polymer chain create a tiny pore in the amorphous region call the free volume, that appear and disappear at same time when the permeating transportation take place across the membrane. So larger the free volume increases the permeate rate of permeants.

2.4 Classification of pervaporation process and materials and application.

Pervaporation separation for particular feed system is classified into different processes. In hydrophilic pervaporation, the target compound is water removed from the aqueous-organic mixture by preferential permeation across the membrane. Most commonly used materials are polyvinyl alcohol, polyether amide, chitosan and ionic polymers. The possible interaction with water is hydrogen bonding, ion-dipole interaction. Hydrophilic membrane used for breaking of azeotropes, dehydration liquids mixture with close boiling point, dehydration of multi component, water removal in esterification process [20].

In hydrophobic pervaporation, from the diluted stream of aqueous-organic mixture, the organic compound are target and separate through the membrane. Common material used for the hydrophobic pervaporation are polydimethyl siloxane (PDMS), Polybutadiene etc. the possible interaction is hydrophobic- hydrophobic interaction. Uses of hydrophobic pervaporation are the waste water treatment, recovery of aromatic in food technology, separation of compound from the fermentation broth in bio technology. [22-25]

Target organophilic pervaporation, it is an organic-organic separation, from that the one of organic compound is target to separate through the membrane from other. The common membrane material used for such separation are PDMS, polyurethane, chitosan, polyether amide etc. Application for the target organophilic pervaporation is separation of ethanol from the ethyl tertiary butyl ether, separation of methanol from the methyl tertiary butyl ether, aliphatic -aromatic mixture separation in petroleum industry. Figure 2.4 illustrate the classification of pervaporation. [24]

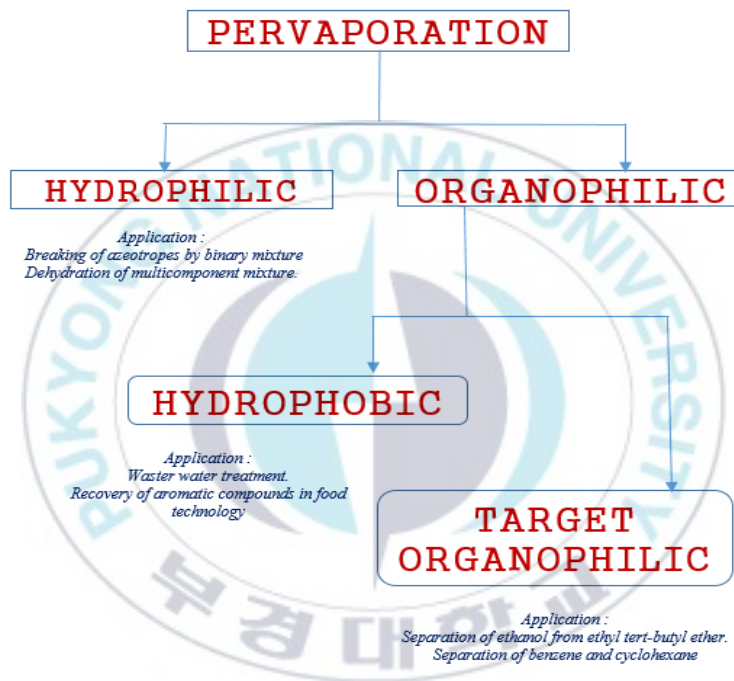
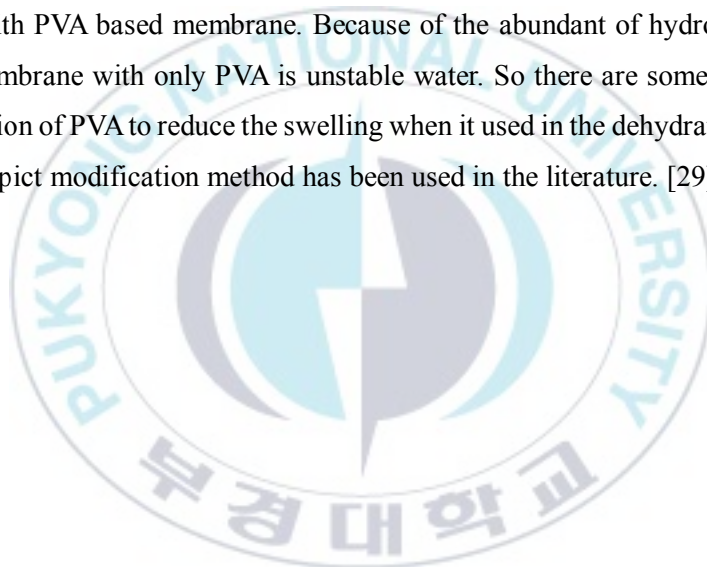


Figure 2.4 Classification of pervaporation process

2.5 PVA based membrane.

Polyvinyl alcohol is most popular material for pervaporation dehydration process. Commercial PVA is typically made by hydrolysis of poly (vinyl acetate) or PVAC. The chemical structure of PVA as shown in figure 2.5 PVA exhibit excellent membrane forming ability, excellent processability, high abrasion strength, high hydrophilicity due to numerous hydroxyl group in its polymer backbone, flexibility and elongation, tensile strength. [26-27] Due to its hydrophilicity it shows the excellent permselectivity for water in pervaporation. Membrane based on the PVA is commercially available [28] therefore it was the natural choice for the study. The table 2.2 shows that advantage and disadvantages associated with PVA based membrane. Because of the abundant of hydroxyl moieties in the PVA, membrane with only PVA is unstable water. So there are some technique used for modification of PVA to reduce the swelling when it used in the dehydration application. Figure 2.6 depict modification method has been used in the literature. [29]



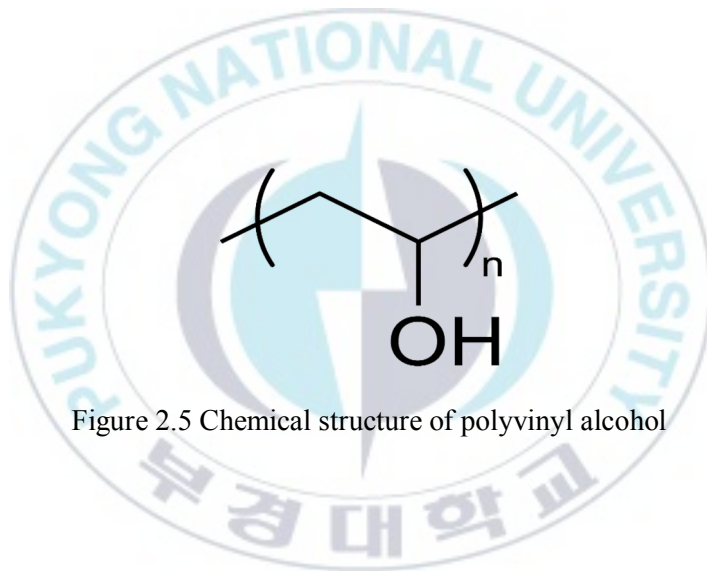


Figure 2.5 Chemical structure of polyvinyl alcohol

Table 2.2 Advantages and disadvantages associated with PVA based membrane

Advantages	Disadvantages
Excellent hydrophilicity	High degree of swelling
Permeability to water, good mechanical property	Permeability to ions
Thermal resistance	Compaction under the pressure
Resistance to chemical	Low flux when highly crosslinked
Require Low operating pressure	
Film forming ability	

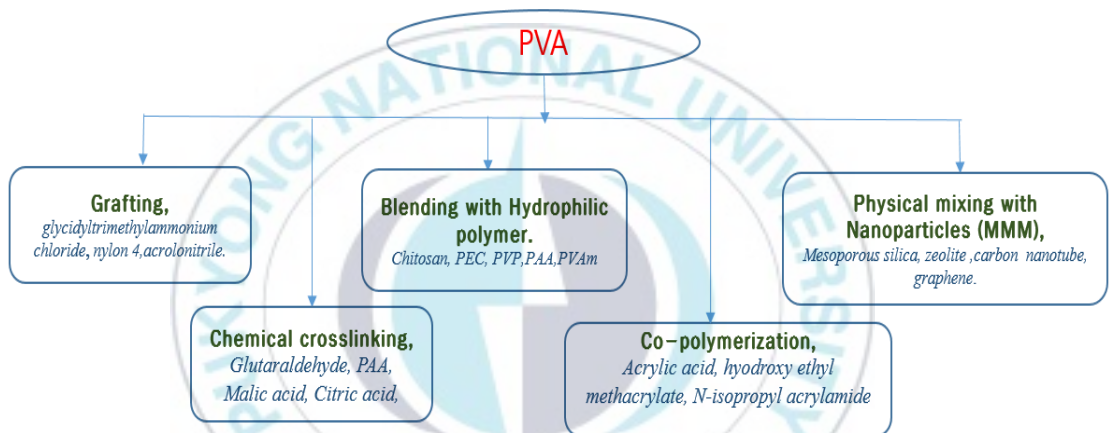


Figure 2.6 Polyvinyl alcohol modification methods

Grafting

It is modification technique where oligomeric chain are attached side chain branches irregularly on to polymer main chain. Usually the grafting done by covalent bonding by chemical reaction or by irradiation. Graft polymers are a branched copolymer where the components of the side chain are structurally different than that of the main chain. [30-31]

Crosslinking

There are several chemical reagent used for the chemical crosslinking of PVA chain. It is usually done chemical reaction, heat treatment, irradiation, Freeze thaw inducement crystallization, etc. However due to the excessive crosslinking can cause membrane brittleness which affect the pervaporation performance. Crosslinking technique and reagent play important role in the membrane preparation. [29]

Blending

PVA membrane has been blended with several polymer such as chitosan, polyacrylic acid, polyvinyl pyrrolidone (PVP). Due to the blending of two polymers yield new material that combine the properties of two polymers. It is possible to obtain desire hydrophilicity or hydrophobicity by blending in that case membrane characteristic can be adjust for the particular feed system. [32]

Copolymerization

It is the technique which has goal as polymer blending, except due to the covalent bonding of two polymer resulted the higher mechanical strength of the membrane. [33-34]

Physical mixing of nanoparticles (MMM)

This is an advance method in which inorganic or organic filler embedded in to the PVA polymer matrix, with without covalent bonding to improve the physicochemical of properties of the membrane. Example zeolite, carbon nano tube, graphite or mesoporous silica particles. [35-36]

Reference.

- [1] R. W. Bakers, Membrane Technology and applications, 2nd ed. John Wiley & Son Ltd. New York (2004).
- [2] G. H. Koops, Dehydration of acetic acid by pervaporation (1992) Netherlands
- [3] J. G. Wiljmans, R. W. Baker, The solution-diffusion model: A review, *J. Membr. Sci.* 107 (1995) 1–21.
- [4] M. H. V. Mulder, C. A. Smolders, Pervaporation solubility aspect of Solution diffusion model, *Sep. and Purif. Methods.* 15 (1986) 1
- [5] S. Sourirajan, S. Bao, T. Matsuura, An approach to membrane separation by pervaporation, in proceeding of second international conference on pervaporation, 251, Process in the chemical industry, ed. R. A. Bakish, Bakish Mat. Cor. Englewood, NJ, 209 (1987)
- [6] I. Cabasso, Ultrastructure of asymmetric membrane and composite membranes, A. F. Turbak (Ed), Synthetic membranes, Vol 1. Desalination, ACS Symp. Ser No. 153, ACS, Washington, DC, 267 (1981)
- [7] R. C. Binning, R. J. Lee, J. F. Jennings, E. C. Martin, Separation of Liquid mixture by permeation, *Ind. Eng. Chem.* 53 (1961) 45.
- [8] R. Guo, C. Hu, B. Li, Z. Jiang, *J. Membr. Sci.* 289 (2007) 209-218.
- [9] J. P. G. Villaluenga, T. Mohammadi, A Review, on the separation benzene/cyclohexane mixture by pervaporation, *J. Membr. Sci.* 169 (2000) 159-174.
- [10] W. Yoshida, Y. Cohen, Ceramic supported polymer membrane for pervaporation of binary mixture, Organic/organic mixture *J. Membr. Sci.* 213 (2003) 145-157
- [11] M. K. Mandal, S. B. Sant, P. Bhattacharya, Dehydration of aqueous acetonitrile solution by pervaporation using PVA-iron oxide nanocomposite membrane, *Colloids surface. A* 373 (2011) 11-21.
- [12] M. H. V. Mulder, T. A. Franken, C. A. Smolders, *J. Membr. Sci.* 23 (1985) 41.
- [13] T. Johnson, S. Thomas, *J. Membr. Sci.* 155 (1999) 133-145.
- [14] P. S. Rachipudi, A. A. Kittur, S. K. Choudhari, J. G. Varghese, M. Y. Kariduraganavar, *Eur. Polym. J.* 45 (2009) 3116-3126.
- [15] R. Y. M. Huang, C. K. Yeom, *J. Membr. Sci.* 51 (1990) 273–292.

- [16] X. Feng, R. Y. M. Huang, *J. Membr.Sci.* 92 (1994) 201-208.
- [17] B. Smitha, D. Suhanya, S. Sridhar, *J. Membr.Sci.* 241 (2004) 1-21.
- [18] R. Y. M. Huang, V. J. C. Lin, *J. Appl. Polym. Sci.* 12 (1968) 2615-2631.
- [19] J. P. G. Villaluenga, M. Khayet, P. Godino, B. Seoane, J. I. Mengual, *Sep. Sci. Purif. Tech.* 47 (2005) 80-87.
- [20] S. Semenova, H. Ohya, K. Soontarapa, *Desalination*, 110 (1997) 251-286.
- [21] R. Gref, Q. T. Nguyen, P. J. Neel, Transport properties of polyvinyl alcohol, *J. Appl. Polym. Sci.* 49 (1993) 209-218.
- [22] G. Liu, G. Lin, S. Liu, H. Zhou, W. Wei, W. Jin, *Chem. Engi. Proc. Intensi.* 86 (2014) 162-172
- [23] R. W. Field, V. Lobo, Hydrophobic pervaporation, *Ann. N. Y. Acad. Sci.* 986 (2003) 401-410.
- [24] M. Peng, L. M. Vane, S. Liu, *J. Hazard. Mater.* B98 (2003) 69-90.
- [25] V. S. Cunha, M. L. L. Paredes, C. P. Borges, A. C. Habert, R. Nobrega, *J. Membr. Sci.* 31 (2002) 277-290.
- [26] K. Halake, M. Birajdar, B. S. Kim, H. Bae, C. Lee, Y. J. Kim, S. Kim, H. Kim, S. Ahn, S. An, J. Lee, *Ind. Eng. Chem.* 20 (2014) 3913-3918.
- [27] P. D. Chapman, T. Olivera, A. G. Livingston, K. Li, *J. Membr. Sci.* 318 (2008) 5-37.
- [28] S. Chemtech, Pervaporation membranes for organic separation instruction for storage, Handling Commissioning, Sulzer Chemtech, GmbH.
- [29] B. Bolto, T. Tran, M. Hoang, Z. Xie, *Progress Polym. Sci.* 34 (2009) 969-981.
- [30] A. Sajjan, H. G. Premakshi, M. Y. Kariduraganavar, *J. Ind. Eng. Chem.* 25 (2015) 151-161
- [31] W. Y. Chiang, Y. H. Lin, *J. Appl. Polym. Sci.* 110 (1996) 211.
- [32] K. Rao, M. C. S. Subha, M. Sairam, N. N. Mallikarjuna, T. M. Aminabhavi, *J. Appl. Polym. Sci.* 103 (2007) 1918.
- [33] F. Kursun, N. Isiklan, *J. Ind. Eng. Chem.* 41 (2016) 91-104.
- [34] L. Liang, *J. Membr. Sci.* 106 (1995) 167-182.
- [35] G. Wu, M. Jiang, T. Zhang, Z. Jia, *J. Membr. Sci.* 507 (2016) 72-80.

[36] E.J. Flynn, D. A. Keane, P. M. Tabari, M. A. Morris, Sep.Purif.Technol.118 (2013) 73-80.



3. Pervaporation dehydration of isopropanol by using the blend membrane prepared from the PVA and PVAm

3.1 Introduction

Over the last few decades, of the many membrane separation processes, pervaporation (PV) has attracted significant attention in both academia and industry. Distillation processes for azeotropic mixtures and solvents with similar volatilities require a tremendous amount of energy. In contrast, membrane-based separation processes are both feasible and economical [1]. Pervaporation follows solution diffusion principles [2], where liquid mixtures are separated preferentially by phase changes through dense organic [3] and organic-inorganic composite membranes [4, 5] during mass transport. Consequently, pervaporation is distinct from other membrane separation processes. Pervaporation applications include the separation of water-organic mixtures (alcohol dehydration) [5, 6], the separation of organic-organic mixtures [7] and the separation of diluted dissolved organic residues from wastewater streams [8].

To date, pervaporation has only been commercialized for the dehydration of various alcohols, such as ethanol and isopropanol (IPA). Isopropanol has numerous applications; for example, it is used as a solvent in the pharmaceutical industry because of its low toxicity. In addition, isopropanol is a major ingredient in gas dryer fuel additives. Isopropanol forms an azeotrope with water, forming a boiling mixture at 80.37 °C at an isopropanol composition of 87.7 wt. %. Consequently, to separate azeotropes, pressure swing distillation or a third component used as an entrainer is required in extractive or azeotropic distillation [9], and both processes are unfeasible and uneconomical with unfavorable side effects. Therefore, pervaporation or hybrid systems combining pervaporation with distillation have been explored. Hoof et al. reported a hybrid distillation-pervaporation system using a ceramic membrane that saves 49% of the cost of separation compared to

azeotropic distillation [10]. Because of the numerous applications of IPA, several pervaporation membranes have been explored for its dehydration using different methods. For example, Zhao et al. studied polyelectrolyte complex (PEC) materials for membrane preparation. Because PECs are formed by the mixing of oppositely charged polyelectrolytes via electrostatic forces, they form effective hydrophilic channels for the dehydration of alcohols [11]. They have successfully prepared different polyelectrolyte complex membranes (PECMs) that showed remarkable pervaporation performance in comparison to the polyanion and polycation membranes from which the polyelectrolytes (PECs) were formed, by using homogeneous PECs [12], blending PEC solutions with different polymer solutions, and preparing solution-processable PECs [13]. However, the mechanical properties of the PEC membranes proved to be poor over the long operation times necessary for a pervaporation experiment; in addition, polyelectrolyte membranes are not stable under various processing conditions because polyelectrolyte materials cause coacervation in aqueous media, arising from the electrostatic attraction between opposing charges. The mechanical strength of the membranes could be enhanced by the incorporation of silica, inorganic nanoparticles [14], and carbon nanotubes [15]. However, these nanocomposite membranes are affected by the poor dispersion of the nanomaterial in the polymer matrix and the aggregation of nanoparticles, and these effects have a severe impact on the membrane pervaporation performance.

Poly (vinyl alcohol) (PVA) is an aliphatic, semi-crystalline material frequently used as a base material for the preparation of hydrophilic membranes. It is inherently hydrophilic because of the many hydroxyl groups in the polymer main chain. Furthermore, it is suitable for membrane preparation because of its excellent chemical stability and film-forming ability [16, 13]. However, in aqueous feed mixtures, PVA membranes undergo excessive swelling; thus, PVA is always modified using methods such as chemical crosslinking [17], polymer grafting, blending with different polymers, the formation of PVA copolymers [18, 19, 20, 21], and thermal treatment. Membranes prepared from the blending of different polymers show promising pervaporation performance. In blended films, the intrinsic chemical, physical, mechanical, and morphological properties of each film are combined, so it is possible to fine-tune membrane properties through blending. For example,

Ariyaskul et al. prepared PVA membranes blended with chitosan for the pervaporation and separation of water-isopropanol mixtures, and they have reported that a membrane containing 75% chitosan (CS) shows the best results [20]. Aminabhavi et al. reported chitosan and hydroxypropyl cellulose (HPC) blend membranes, crosslinked with a urea-formaldehyde solution, for the PV dehydration of IPA. They have found that a CS-HPC blend membrane showed superior PV separation performance to that of a plain chitosan membrane [21]. Among the chitosan, poly (ethylamine), poly(allyl amine), the poly(vinyl amine) contain highest amount of NH_2 groups, and allow the preparation of very hydrophilic membranes [22]. These studies prompted us to prepare blended membranes from poly (vinyl alcohol) and poly(vinyl amine) (PVAm). Because membranes prepared from PVAm (commercially available as PVAm HCl) are usually sticky, swollen, and highly viscous, it is not possible to form films using poly (vinyl amine) alone. In contrast, PVA has excellent film-forming properties, a high tensile strength, flexibility, and stability in organic solvents. Both PVAm and PVA are hydrophilic, containing amine NH_2 and OH functional groups in their main chains; consequently, the combination of these polymers may yield a high-quality pervaporation membrane for dehydration processes. There are some studies in the literature related to the PVA/PVAm blended membrane. The fixed carrier transport (FSC) membrane for CO_2 separation were reported by Hagg and Deng [23,24,25]. They have found that the membrane prepared from the blending of PVA/PVAm providing good membrane stability and mechanical strength. Since PVAm has a high density of primary amine moieties while blending with PVA form polymer network by entanglement of PVA chains with PVAm chains. Hu et al. have studied the use of PVA/PVAm blend membranes containing carbon nanotubes for the dehydration of ethylene glycol; however, the focus of their study was the effect of the CNTs in the membrane on PV performance [26].

In this study, we have focused on the preparation of membrane blend membrane from PVA and PVAm crosslinked with glutaraldehyde at mild temperatures for the pervaporation dehydration of water-isopropanol mixtures. We have used PVA as the base polymer and added PVAm in various proportions. The resulting membranes were characterized by infrared (IR) spectroscopy, swelling studies, scanning electron microscopy (SEM) analysis,

differential scanning calorimetry (DSC), and X-ray diffraction (XRD). Finally, the membranes were applied to the pervaporation of an isopropanol-water mixture under a range of conditions to determine the optimum conditions for enhancing membrane performance.

3.2 Experimental.

Materials

Poly (vinyl alcohol) with a molecular weight of 88000-97000 and a 98-99% degree of hydrolysis was purchased from Alfa Aesar, USA. Poly (vinyl amine) (PVAm) (Lupamin-9095, M_w 340000, 10 wt. % solution) was donated by BASF Indonesia. Isopropyl alcohol (99.5 wt. %) was obtained from Dae-Jung Chemicals & Metal Co, Korea. Silico tungstic acid hydrate $[H_4(Si(W_3O_{10})_{10})_4] \cdot nH_2O$ and melamine were obtained from the Sigma Aldrich. Ultrapure water (Puris, Expe-RO EDI water system) was used. A 35 wt. % ready-made solution of poly (acrylic acid) with a molecular weight of 250,000 was purchased from Sigma Aldrich, USA. Silver nitrate powder (99.9%) was purchased from Kojima Chemical Co., Ltd., Japan.

3.2.1 Preparation of the crosslinked PVA/PVAm blend membranes

The homogeneous PVA and PVA/PVAm blend membranes were prepared by dissolving PVA (4 g) powder in water (96 g) with continuous stirring at 75 °C for 6 h. The resultant polymer solution was filtered to remove residual undissolved particles. The solution was then kept overnight to remove any air bubbles. Following the resting period, the solution was cast in a Petri dish and dried at 40 °C. Subsequently, the membrane was pulled away from the Petri dish, and the films were crosslinked in a crosslinking bath containing 90/10/4/1 vol. % IPA/water/glutaraldehyde (25%) solution and catalytic hydrochloric acid at 50 °C for 1 h. The thickness of the resulting membrane was 70 μm , abbreviated as PVAm0. In order to prepared blend membrane, the 4 wt. % PVAm solution was obtained by diluting the 40 g of PVAm solution to 100 g of water, mixed well using constant stirring with magnetic stirrer at room temperature for 2 hrs.

The resultant solutions were blended with the PVA solutions in different amounts but maintaining the same amount of PVA solution. The membrane abbreviations were listed in the Table.3.1.As the amount of PVAm added to the membranes increased, mechanically instability and brittleness developed. Consequently, the addition of PVAm was limited to 30 g. To crosslink the blended membranes, we followed the same procedure as that for PVAm0. All membranes were stored at 40 °C in a drying oven until use.



Table.3.1 Abbreviations of blended PVA and PVAm membranes

Abbreviation	Ratio in the membrane (g/g)	
	PVA (Polyvinyl alcohol)	PVAm(polyvinyl amine)
PVAm0	100	0
PVAm0.5	100	10
PVAm1.0	100	20
PVAm1.5	100	30

Pervaporation set up and Characterization technique

Infrared spectroscopy.

The resulting homogeneous crosslinked PVA and PVA/PVAm membranes were scanned using an ATR-FTIR spectroscopy (ATR mode of FT-IR, Nicolet iS10, USA) over a wavenumber range of 400-4000 cm^{-1} to observe the spectral changes in IR spectra for characterisation of the membrane. Each spectrum for each sample was collected by aggregating 32 scan at resolution of 2 wavenumbers.

X-ray diffraction studies of blends membrane.

The X-ray diffractogram of incorporated PVA/PVAm blend membranes were recorded using X-ray diffractometer (Rigaku Japan, D/Max 2500). The dried membrane samples with uniform thickness were mounted on the sample holder then the patterns were recorded in range of 0-50 at a speed of 5°/min

Differential scanning calorimetry

The thermal properties of PVA and PVAm blend membranes were measured by differential scanning calorimetry (Perkin Elmer (USA), Pyris-1). A sample weight range of 5-8 mg was used, and the samples were heated from 50 °C to 300 °C at a heating rate of 10 °C/min.

Scanning electron microscope (SEM).

The surface morphology of PVA/PVAm Blend membranes were observed by SEM analysis that produces image of a sample by scanning it with a focus beam of electron [Teskan, Czech, Vega II, and LSU]. Specimens for analysis were prepared by gold coating to make film conductive.

3.2.3 Swelling degree measurements

The dried membrane samples were immersed in bottle containing the 50 cm^3 of different water/isopropanol mixtures for 48 h, at a 30, 40, 50 and 60 °C temperatures. They were then removed from the solutions, wiped with dry tissue paper, and the weight of the

swelled membrane was measured immediately. The swelled membrane was then dried to constant weight under vacuum at 25 °C. The swelling degree was calculated using the following equation:

$$SD = \frac{m_s - m_d}{m_d} \quad (1)$$

Where, m_s and m_d are the mass of the swelled and dried membranes, respectively.

3.2.3 Pervaporation apparatus and measurements

The pervaporation apparatus designed for the present study is shown in figure 3.1. The membranes were placed on a membrane cell and fixed. The effective area of membrane was 19.64 cm². The membrane cell was composed of two compartments – one connected to a feed tank, and other connected to the downstream side (vacuum pump). The feed tank was maintained at the desired temperature (40 °C) in water bath, and the feed mixture was continuously circulated using a pump (100 rpm) through the membrane cell. The pressure in the downstream side was maintained less than 10 mbar using a vacuum pump. The permeated solution was collected in a cold liquefied nitrogen trap and then weighed. The feed mixture composition was ranged from 10-30wt. % of acetic acid in water. The composition of permeated solution was analysed using gas chromatography (with TCD detector). The separation performance of prepared membrane was characterized using following equations:

$$\text{Separation Factor } (\alpha) = \frac{P_W/PI}{F_W/FI} \quad (2)$$

Where PW , PI , FW , and FI are the weight fractions of water and acetic acid in the permeated solution and the feed solution, respectively. In addition, the flux was calculated by following equation:

$$\text{Flux } (J) = \frac{Q}{A.t} \quad (3)$$

Where Q is the weight of permeated solution collected in the cold trap and the flux is calculated with respect to effective area (A) in time t .

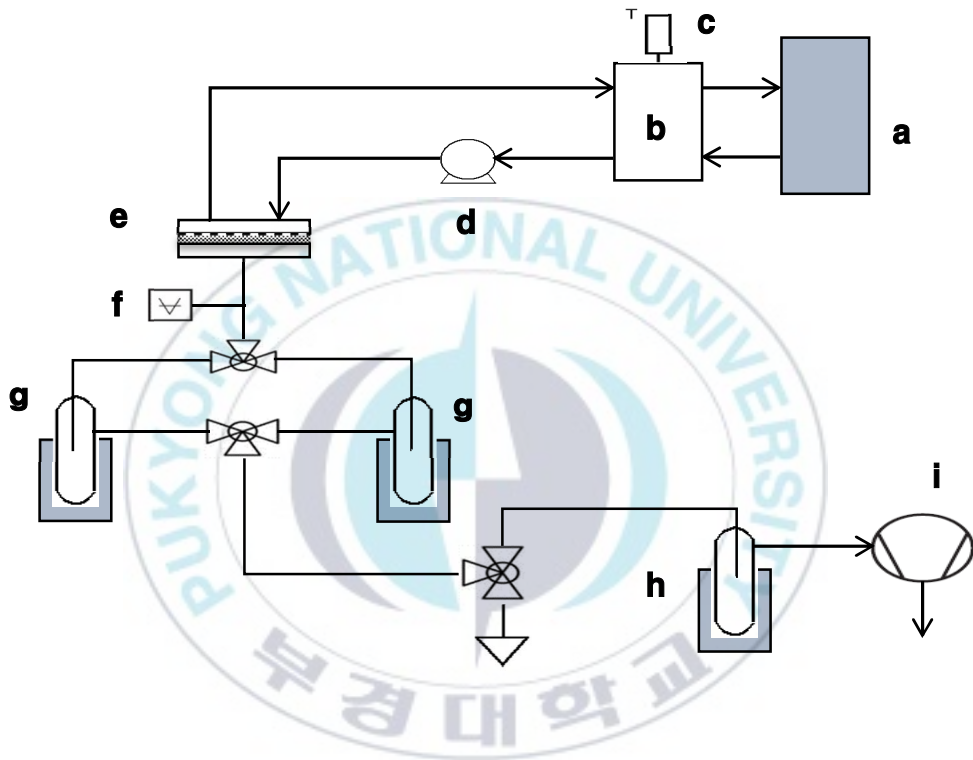


Figure 3.1 Schematic diagram of pervaporation apparatus: (a) water bath, (b) feed tank, (c) temperature indicator (d) circulation pump, (e) membrane cell, (f) vacuum gauge, (g), (h) cold trap + liquid nitrogen (i) vacuum pump

3.3 Results and Discussion

3.3.1 Membrane Characterization.

IR spectroscopy

The FTIR spectra of PVA and crosslinked PVA are shown in Figure 3.3 (a). Characteristic bands at 3320–3300 cm^{-1} , corresponding to the O-H stretching vibration of the PVA hydroxyl groups, are observed in both spectra. Figure S1 (a), shows the crosslinking reaction of PVA using glutaraldehyde as a crosslinking agent. After the crosslinking of PVA, the intensity of the peak corresponding to OH (3300 cm^{-1}) decreased, while that of the C=O peak at 1720 cm^{-1} increased slightly. Additional peaks at 2840 and 2750 cm^{-1} , attributed to the C-H stretching of the aldehyde, were observed owing to the presence of unreacted glutaraldehyde. IR stretching peaks at 1080–1135 cm^{-1} , attributed to the formation of acetal linkages, were observed in the spectrum of the PVA crosslinked membrane, while, in the spectrum of virgin PVA, a peak at 1085 cm^{-1} was observed. These additional peaks at 1135 cm^{-1} are related to the formation of acetal linkages attributed to the aliphatic ether after crosslinking with glutaraldehyde [27]. Figure 3.3 (b), shows the IR spectra of the PVA film and PVA/PVAm blended uncrosslinked and crosslinked membranes. The IR spectrum of the PVA/PVAm blend shows that, after blending with PVAm, the intensity of the OH peak increased; this increase arises because the addition of PVAm adds amine groups, whose vibrations fall in the same frequency range as those of OH groups; consequently, a more intense and broader peak was observed. In addition, a peak at 1580 cm^{-1} , which corresponds to NH_2 [28] bending vibrations, was observed, confirming that PVA and PVAm are compatible at the molecular level. In the IR spectrum of the PVA/PVAm blended glutaraldehyde crosslinked membrane, a peak at 1680 cm^{-1} , which corresponds to the C=N [29] imine linkage resulting from the crosslinking of the C=O groups of glutaraldehyde with the PVAm NH_2 and PVA OH groups, was observed. Based on the IR spectral changes on blending and crosslinking, a postulated reaction scheme is shown in Figure 3.2

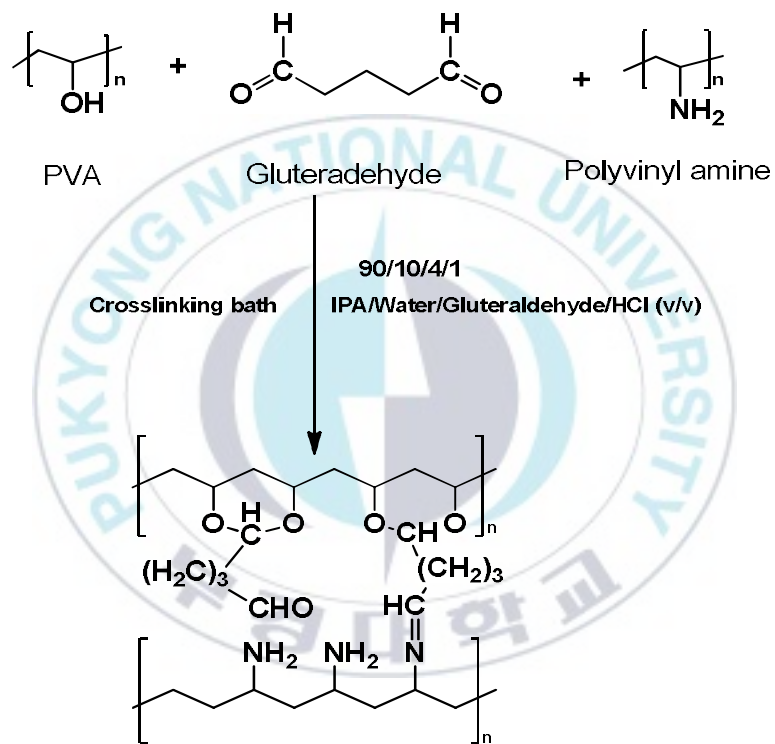


Figure 3.2 Proposed Chemical crosslinking reaction for PVA/PVAm blend membranes

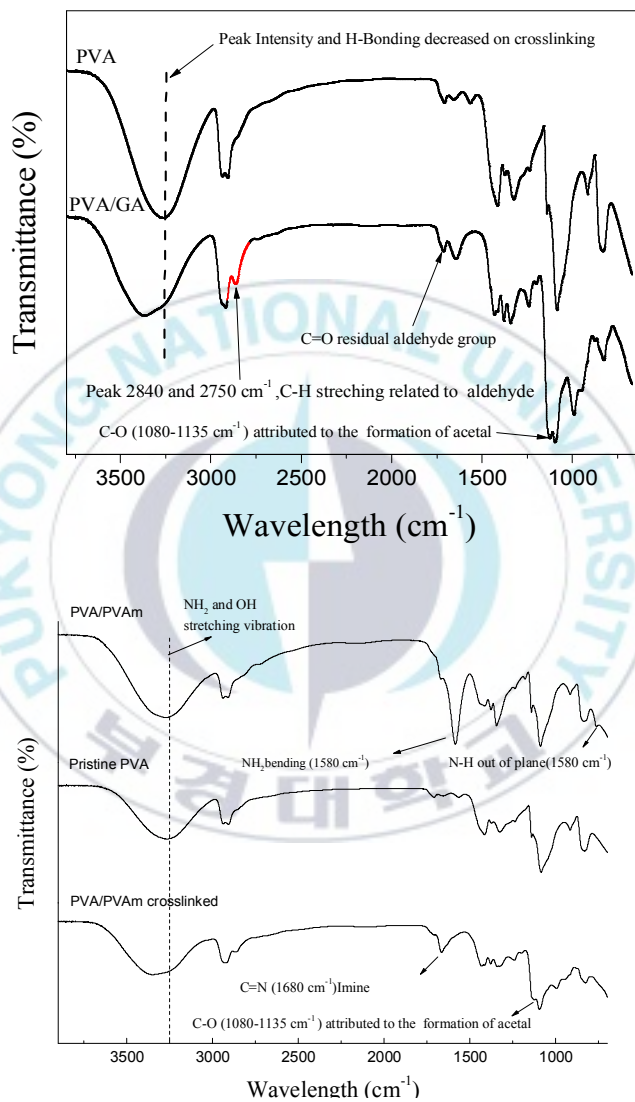
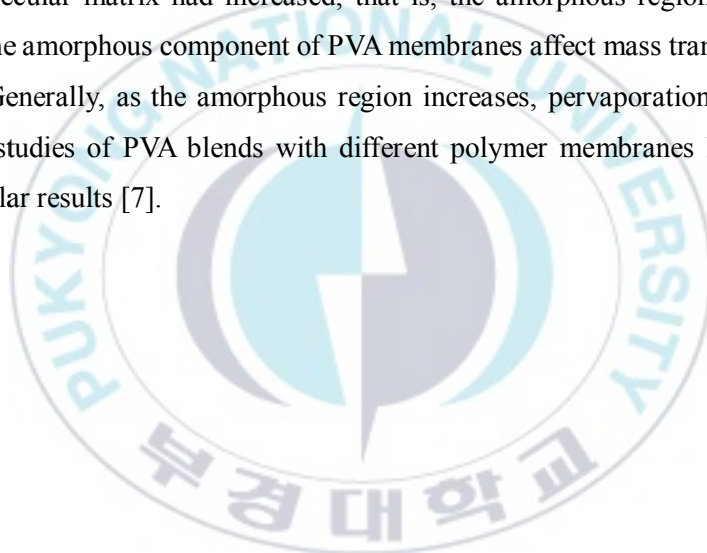


Figure 3.3 FTIR (ATR mode) spectra for PVA and PVA crosslinked membrane a) and PVA, PVA/PVAm blend uncrosslinked and crosslinked membranes b).

X-ray diffraction studies of the blended membranes

The structural changes to the PVA semi-crystalline domain on blending with PVAm were investigated using XRD measurements. Figure 3.4, Shows the XRD patterns of the PVA, crosslinked PVA, and blended PVA/PVAm membranes. All diffraction patterns contain a peak at $2\theta = 20^\circ$, which corresponds to the 101 plane of the crystalline PVA backbone, reflecting the presence of crystalline atactic PVA. This structure results from the intramolecular hydrogen bonding of the OH groups [30]. On crosslinking, the peak intensity decreased, and the peak broadened. This trend continued with the further addition of PVAm to the membrane. These changes suggest that the entropy (or disorderliness) of the PVA molecular matrix had increased; that is, the amorphous region had increased. Changes in the amorphous component of PVA membranes affect mass transport across the membrane. Generally, as the amorphous region increases, pervaporation flux improves. Other XRD studies of PVA blends with different polymer membranes have found and reported similar results [7].



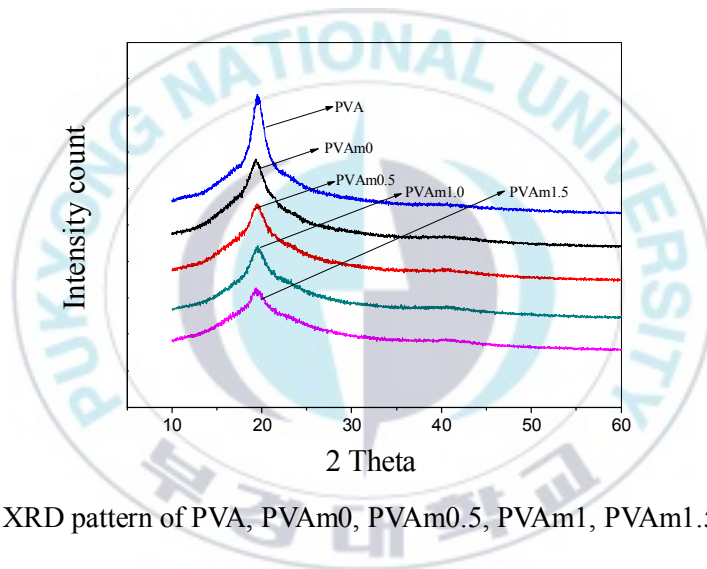
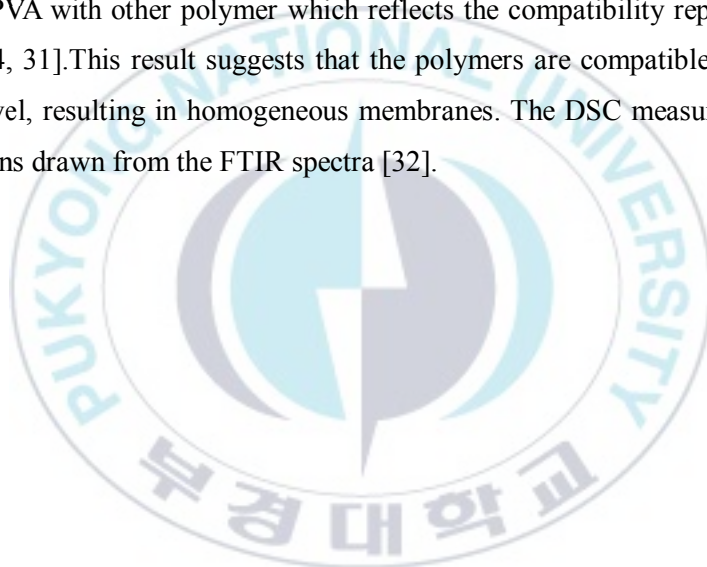


Figure 3.4 XRD pattern of PVA, PVAm0, PVAm0.5, PVAm1, PVAm1.5 membranes.

Differential scanning calorimetry

As both polymers (especially PVAm) are crystalline, the apparent glass transition temperature (T_g) could not be detected in the DSC curve. However, from the endothermic peak observed in the DSC curve, it was possible to determine the melting temperature. Figure 3.5, shows the DSC curve for the PVA and the PVA/PVAm blend membranes. For the PVA membrane, only one melting point (200 °C) was observed; furthermore, it is different from the melting point of the blend membrane. In blended membrane the melting point of membranes shifted to slightly higher values (PVAm0.5= 204 °C, PVAm0.5= 206 °C, and PVAm1.5=208 °C) was observed. The melting temperature transition was caused by the blending of PVA with other polymer which reflects the compatibility reported in several literature. [24, 31]. This result suggests that the polymers are compatible and mix at the molecular level, resulting in homogeneous membranes. The DSC measurements support the conclusions drawn from the FTIR spectra [32].



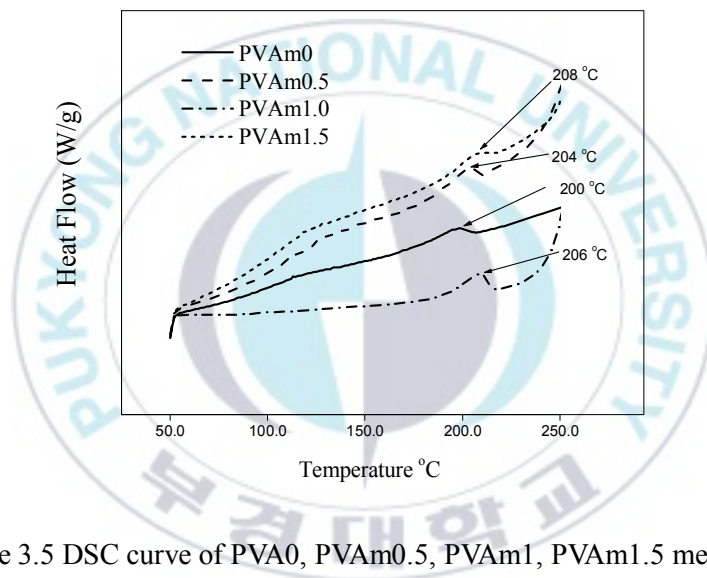
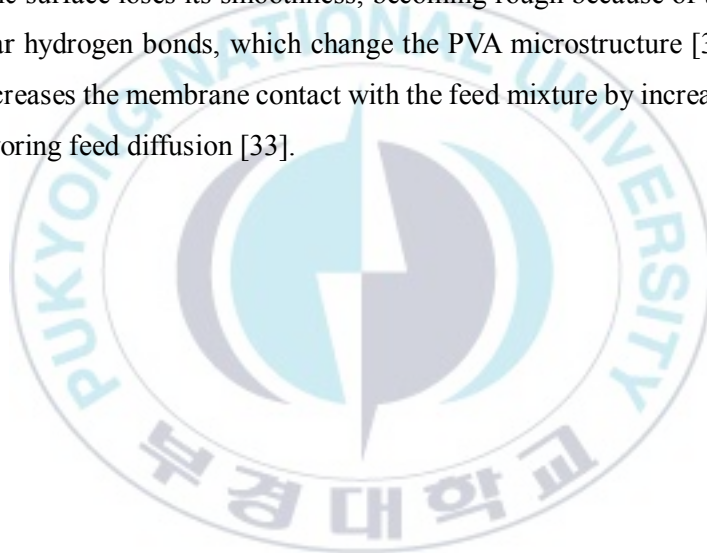


Figure 3.5 DSC curve of PVA0, PVAm0.5, PVAm1, PVAm1.5 membranes

Scanning electron microscopy

The surface morphologies of the PVA and PVAm1.5 blend membranes were investigated by SEM. The surface images and cross-sectional images for PVAm0 and PVAm1.5 films are shown in Figure S4. Figure 3.6, shows that, upon blending with PVAm, a continuous and compact homogeneous surface structure with no voids or phase separation was obtained. This result confirms that both polymers have good compatibility and are mixed at the molecular level due to the presence of hydrogen bonds between the NH_2 and OH groups. This conclusion is also supported by the DSC and IR studies. The micrograph shows that the PVA surface is smooth, but upon introduction of PVAm to the blend membrane, the surface loses its smoothness, becoming rough because of the formation of intermolecular hydrogen bonds, which change the PVA microstructure [32]. The surface roughness increases the membrane contact with the feed mixture by increasing the surface area, thus favoring feed diffusion [33].



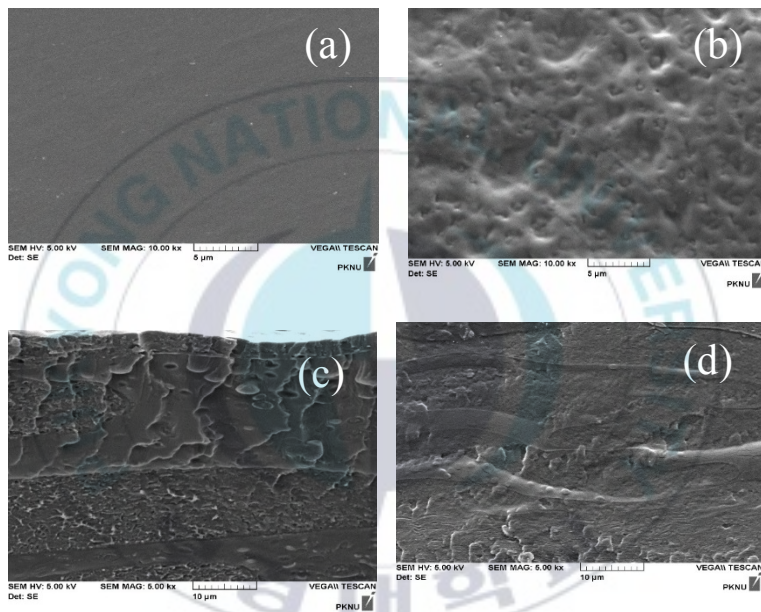


Figure 3.6 SEM (surface and cross-sectional) micrographs for PVA (a, c) and PVAm1.5 (b, d).

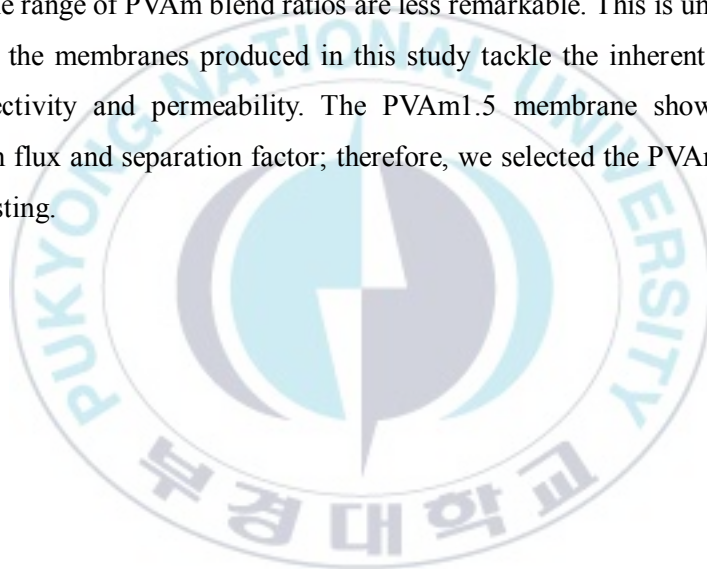
3.3.2 Pervaporation

3.3.2.1 Effect of PVAm addition

In the early 1950s, Flory and Rehner reported [34] that the extent of membrane swelling in specific liquids depends on the crosslinking density, the morphology of the membrane, and the free volume available in the membrane matrix, which strongly affects the sorption mechanism. Therefore, it is important to measure the degree of swelling because, in the PV process, this controls the transport of the permeating molecules under a chemical potential gradient. Therefore, we measured the swelling degree (SD) of the PVA and blended membranes in an 85 wt. % aqueous IPA feed solution at 30 °C, as shown Figure 3.7, The SD values of the membranes increased with increasing PVAm concentration in the PVA/PVAm blend. The increasing SD arises because both polymers are very hydrophilic (i.e., they have a high content of hydrophilic functional moieties), which increases their affinity for water, causing membrane swelling. Similarly, Figure 3.8, shows the effect of PVAm addition on the pervaporation flux and separation factor for the water-isopropanol system. As the PVAm addition increased from PVAm0 to PVAm1.5, the flux increased from the 0.023 to 0.10 kg/m²h, respectively. The separation factor decreased initially, then increased. PVA is an aliphatic hydrophilic polymer. On the crosslinking of PVA with glutaraldehyde, the membrane became dense and compact due to shrinkage of the polymer chains, reducing the flux; however, in the blend membrane, the addition of PVAm increased the hydrophilicity of the membrane by introducing a large number of primary amine groups [32]. Based on the fixed carrier theory, the transportation of water molecule through the membrane take place from the one polar site to another [35]. Therefore, the blending process increases the number of hydrophilic functional moieties (NH₂) in the membrane, which enhances the hydrophilic-hydrophilic and hydrogen bonding interactions for water molecule sorption and diffusion. Additionally, as observed from the XRD analysis (Figure 3.4), the increase in the entropy for the PVA molecular matrix due to the entanglement of the polymer chains and crosslinking results in an increase in the amorphous region. In addition, as shown in the SEM images (Figure 2.5),

on blending, surface roughness increased, and the increased surface area resulted in an increase in the permeation flux.

The membranes produced in this study are highly water selective, and a small discrepancy in the permeate concentration might cause large differences in the membrane selectivity. Figure 3.9, shows the total flux and individual flux for water and IPA and the percentage water in permeate as a function of PVAm addition. The total flux and water flux almost overlap over all PVAm blend ratios; in contrast, the change in the flux of IPA was almost negligible. In addition, the water percentage in permeate was greater than 99.5% for all PVAm blend ratios, as shown in Figure 3.9. Therefore, the differences in the separation factor over the range of PVAm blend ratios are less remarkable. This is unusual because it signifies that the membranes produced in this study tackle the inherent trade-off effect between selectivity and permeability. The PVAm1.5 membrane showed the highest pervaporation flux and separation factor; therefore, we selected the PVAm1.5 membrane for further testing.



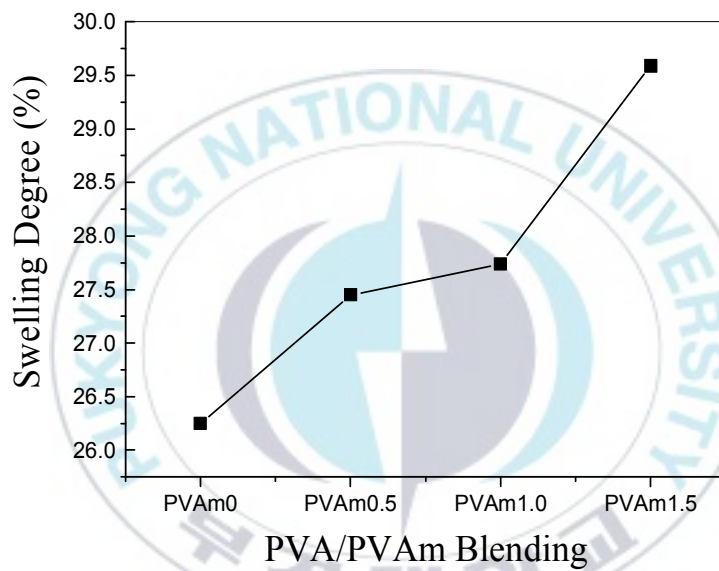


Figure 3.7 Effect of PVAm addition on the degree of swelling using a feed composition of 85 wt. % IPA at 30 °C, thickness: 70 μ m.

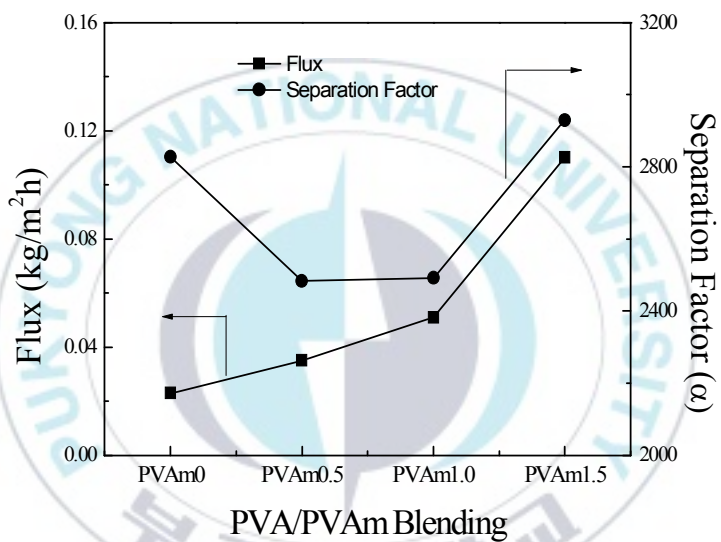


Figure 3.8 Effect of PVAm addition on the pervaporation flux and separation factor. Feed composition: 85% IPA, 70 μm thickness at 30 °C.

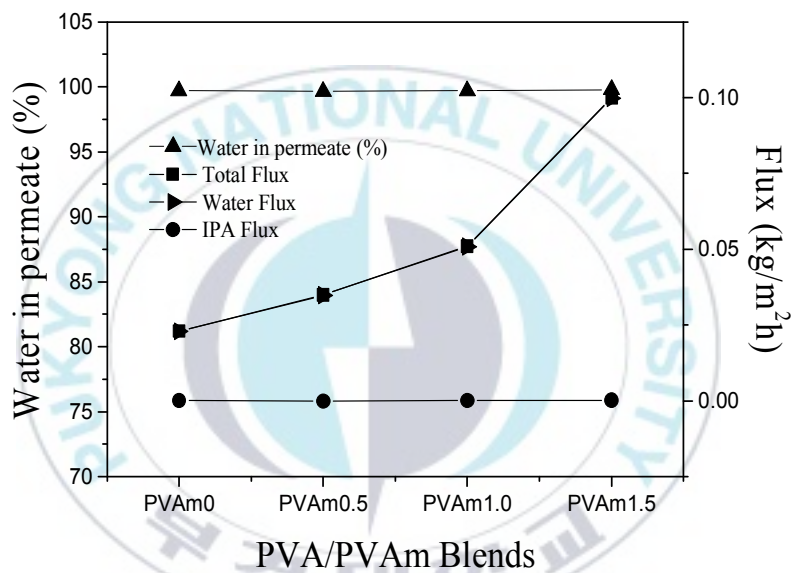


Figure 3.9 Total flux and the fluxes of water and IPA as a function of PVAm addition.

3.2.2.2 Effect of Temperature

Figure 3.10, shows the effect of temperature on the pervaporation of through the membrane (PVAm 1.5) at an IPA feed content of 85 wt. %. The figure indicates that, as the feed temperature increased, the flux increased, while there was little effect on the separation factor. The enhancement in the flux value attributed to the increase in the driving force and free volume. According to the free volume theory, increasing the temperature increases the frequency and amplitude of polymer chain jumping (thermal agitation) and, in turn, randomly creates gaps between polymer chains, otherwise known as the free volume. Due to this random increase in free volume, the diffusion of permeants occurs rapidly, resulting in an increase in flux. However, in our case, the free volume term can be removed because the polymer chains are rigid, and, moreover, the glass transition temperatures for the membranes are greater than the operating temperature. Despite this, an increase in the feed temperature could result in an earlier phase transition of the permeants inside the membrane because energy equivalent to the enthalpy of transition is attained when more heat is provided, and diffusion and mass transfer across the membrane are faster. The membranes produced in this study are dense and compact, and the molecular kinetic diameter of the IPA (0.450) is higher than that of water (0.296) [35-36]. Consequently, the effect of thermal agitation on the driving force can be omitted, and the separation factor is constant over the range of temperatures studied. A similar trend has been reported in several studies [20, 37].

The temperature dependence of the permeation flux can be express by an Arrhenius-type equation.

$$\text{Flux } (J) = A_p \cdot e^{-E_p/RT}, \quad (4)$$

Where A_p and E_p are the pre-exponential factor and the overall activation energy for permeation, respectively.

A logarithmic Arrhenius plot of flux against temperature was plotted for each of the mixture components, as shown in Figure 3.11, From the slope of the resulting plot, the activation energies for the permeation of IPA and water were calculated, and the activation energy for the permeation of IPA (17.11 kJ/mol) is higher than that of water (12.46 kJ/mol). From these results, we can conclude that the adsorption and diffusive transport of IPA are

hindered with respect to that of water. Because the temperature has relatively little effect on the separation factor, we studied the effect of feed concentration at 60 °C to determine the most efficient blend membrane.



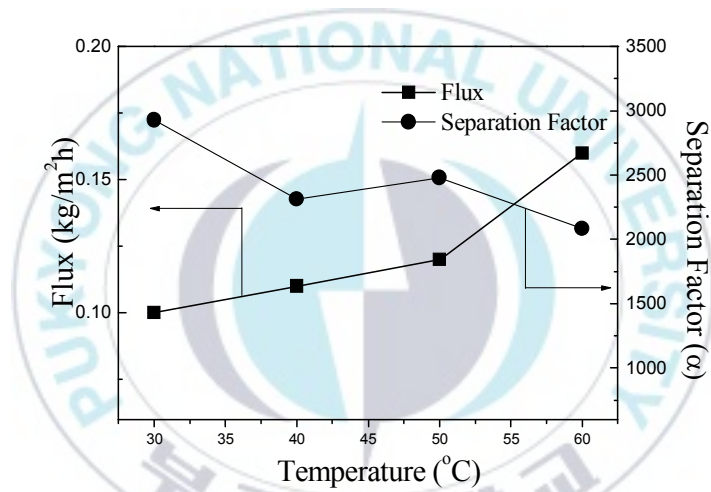


Figure 3.10 Effect of temperature on the pervaporation flux and separation factor. Feed composition: 85% IPA, 70 μm thickness

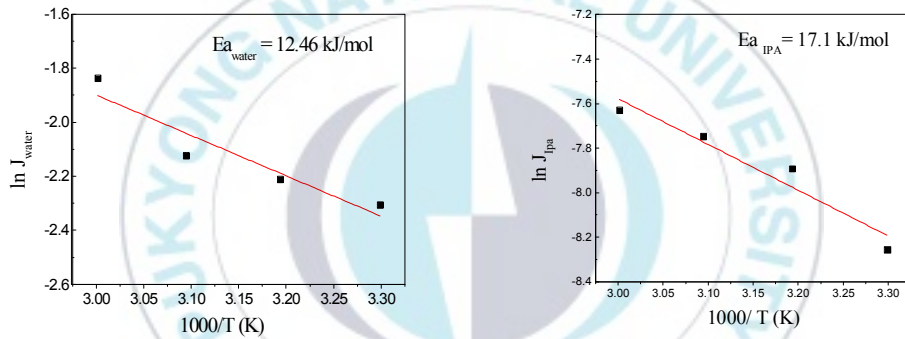


Figure 3.11 Variation of $\ln J_{\text{Water}}$ and $\ln J_{\text{IPA}}$ with temperature for PVAm1.5 membrane, Feed: 85% IPA solution.

3.2.2.3 Effect of feed concentration

Figure 3.12, shows the effect of feed concentration on the swelling degree, flux, and separation factor for IPA separation for feed concentrations ranging from 10 to 20 wt. % water at 60 °C for PVAm1.5. The swelling degree increases linearly with water feed content, and this was attributed to the hydrophilic-hydrophilic interactions arising from the abundant NH₂ and OH groups. The increases swelling with feed concentration implies that the membrane has an increased affinity for water. Similar to the trend in swelling, the total flux increased from 0.032 kg/m²h to 0.28 kg/m²h, as shown in Figure 3.13, this 10-fold increase in the flux arises from the hydrophilicity of the membrane and the increased water driving force due to the higher concentration of water in the feed. Figure 3.7, also shows the separation factor, which decreases as a function of increased water feed composition (4278 to 297.1). The PVAm membrane prepared in this study is highly hydrophilic and selective for water. As the water content increases, the interactions between water and the upstream side of the membrane increase, resulting in swelling and membrane plasticization. The plasticization is a result of adsorbed water and, along with associated molecules of water and IPA, leads to a reduction in the separation factor [17, 20, and 37]. As explained in Section 3.2.1, very small discrepancies in the permeate concentration might cause large differences in the selectivity. However, the percentage of water in permeate was always higher than 98.3% at all feed concentrations. This might be due to the excellent compatibility of the polymers, which resulted in the dense and compact membrane that hinders the diffusion of adsorbed associated molecules in the membrane.

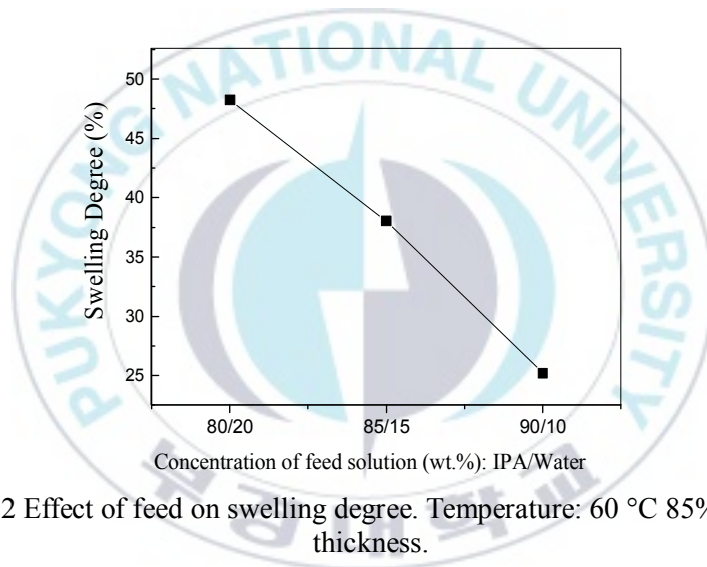


Figure 3.12 Effect of feed on swelling degree. Temperature: 60 °C 85% IPA, 70 μm thickness.

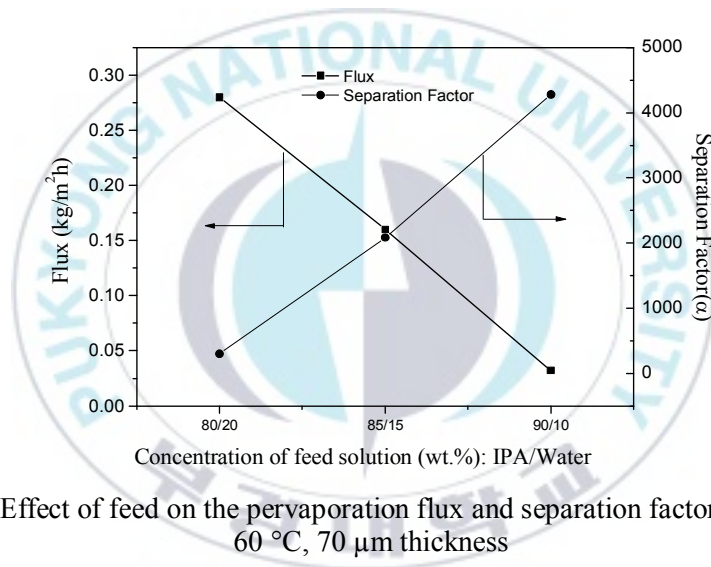


Figure 3.13 Effect of feed on the pervaporation flux and separation factor. Temperature: 60 °C, 70 μm thickness

3.2.2.4 Effect of the membrane thickness

To investigate the effect of membrane thickness, we prepared 35, 50, and 70-micron films of the PVAm1.0 membrane and carried out pervaporation tests at 40 °C with a feed composition of 85/15 IPA/water. We used the PVAm1.0 membrane because the PVAm1.5 membrane was found mechanically unstable with decreased thickness. The solution-diffusion model predicts that the permeation flux is inversely proportional to that of the membrane (Fickian behavior) [2]. Figure 3.14, shows the permeation flux as a function of reciprocal membrane thickness. The permeation flux increases with the reciprocal of membrane thickness in agreement with the prediction from the solution-diffusion model. Moreover, the separation factor can be affected by controlling the thickness. Figure 3.15, shows the effect of the thickness on permeation flux separation factor at an 85/15 IPA/water feed mixture at 40 °C. The separation factor decreased marginally with decreasing membrane thickness. Generally, in the pervaporation process, due to the continuous circulation of feed and the swelling of the upstream side of membrane swelling (and hence plasticization), unrestricted transport across the membrane occurs. In contrast, on the downstream side, due to the continuous evacuation, the membrane becomes dry and forms a restrictive barrier; consequently, only selected feed components can permeate across the membrane. The thickness of the dry layer should increase with increasing membrane thickness, resulting in separation factor enhancement, as observed in the present study. Similar trends for pervaporation performance controlled by membrane thickness have been reported previously [21, 28].

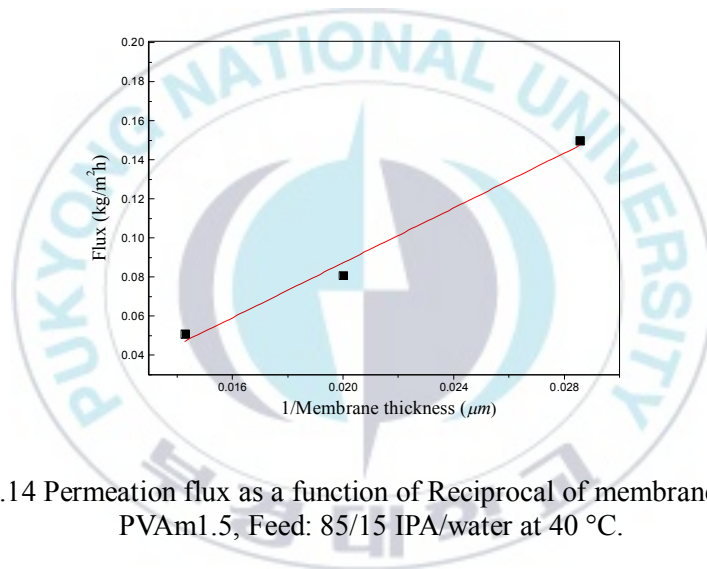


Figure 3.14 Permeation flux as a function of Reciprocal of membrane thickness, PVAm1.5, Feed: 85/15 IPA/water at 40 °C.

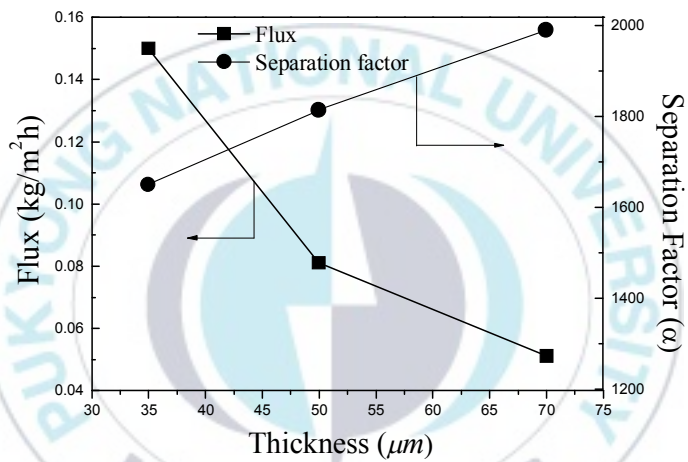


Figure 3.15 Effect of membrane thickness on flux and separation factor. Temperature: 40 °C, Feed: 85% IPA/water.

3.2.2.5 Comparison of PV performance with other studies.

In order to elucidate the pervaporation performance of PVA/PVAm blend membrane system. The result obtained was compared with that of from membrane prepared from the various polymer system and preparation method that have recently studied for IPA dehydration. The Table 3.2 shows the PVAm1.5 showed remarkable selectivity in comparison to the results reported in the other studies however permeation flux was relatively lower compare to PVA/PECs membrane. Nevertheless, as result obtained from PVAm1 explained in the section 3.2.4, for IPA dehydration infer that, by controlling thickness, the PVAm1.5 membrane efficacy also can be enhanced. If it applied to the hollow fiber or supporter for preparation of composite membrane tend to increase the more surface area for contact between feed and membrane, since, that matters the pervaporation performance of membrane [2]. Because, the PVAm1.5 membrane showed highest PV performance throughout the study.

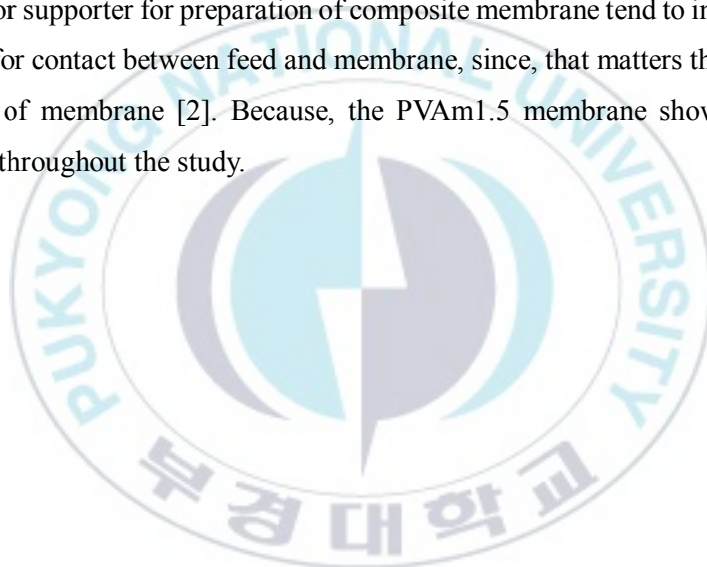


Table 3.2 Pervaporation performances of PVA/PVAm blend membrane compared with other studies.

Polymer	Nature of the membrane preparation method	Feed(%) composition,(w/w) Isopropyl alcohol/Water	Temperature (°C)	Flux(J) (Kg/m ² h)	Separation factor(α)	Thickness (μ)	Ref.
Chitosan	Surface modification of chitosan with PBI	90/10	70	0.25	127	40	[6]
PVA	PVA-PNIPAAm Grafting	12/88	40	0.011	95	90	[17]
PVA	PVA-GTMAC Grafting	90/10	30	0.192	1570	45	[19]
Chitosan	Chitosan/HPC blend membrane	80/20	30	0.341	183	40	[21]
PVA	PVA/PEC (PDDA/CMCNa) Blend membrane	90/10	30	0.32	1491	8	[32]
PVA	PVA/PVAm (PVAm1.5)Blend membrane	85/15	60	0.16	2085	70	Present study
PVA	PVA/PVAm (PVAm1.5)Blend membrane	80/20	60	0.28	297	70	Present study

3.4 Conclusion

The blended membranes were prepared by the blending the highly hydrophilic polymers PVA and PVAm, followed by crosslinking with glutaraldehyde. Using IR and DSC, we determined that the polymers are compatible at the molecular level. XRD measurements showed a decrease in the crystalline region of the membrane due to the intermolecular hydrogen bonding between PVA and PVAm. The surface roughness of membrane increased due to the inclusion of PVAm in the membrane, and this was, again, attributed to the increase in intermolecular hydrogen bonding. The pervaporation performance of the membrane was evaluated for the separation of water-isopropanol mixtures. The blended membranes have a good ability for processing water-isopropanol feed mixtures compared to a virgin PVA membrane. As the amount of added PVAm increased from PVAm0 to PVAm1.5, the flux increased from 0.023 to 0.10 kg/m²h at a water/IPA feed ratio of 85/15 at 30 °C, although there was no effect on the percentage of water in the permeate. The driving force for the permeation of water increased with temperature, but the temperature had no effect on IPA permeation because the PVA/PVAm blend membrane is dense and compact. The activation energy for the permeation of both IPA and water were calculated, and that of IPA (17.11 kJ/mol) is higher than that of water (12.46 kJ/mol). Concerning feed concentration, the water content increased linearly with water flux; however, the increase in the flux does not sacrifice the percentage of water in permeate. By controlling the thickness of the blend membrane, a huge improvement in the permeation flux with only a marginal reduction in the separation factor was achieved.

References

- [1] X. Feng, R.Y.M. Huang, *Ind. Eng. Chem. Res.* 36 (1997) 1048–1066.
- [2] J.G. Wiljmans, R.W. Baker, *J. Membr. Sci.* 107 (1995) 1–21
- [3] Q.G. Zhang, W.W. Hu, A.M. Zhu, Q.L. Liu, *RSC Adv.* 3 (2013) 1855–1861
- [4] Y.L. Liu, Y.H. Su, K.R. Lee, J.Y. Lai, *J. Membr. Sci.* 251 (2005) 233–238
- [5] P.D. Chapman, T. Oliveira, A.G. Livingston, K. Li., *J. Membr. Sci.* 318 (2008) 5–37.
- [6] Y. Han, K. Wang, J. Lai, Y. Liu, *J. Membr. Sci.* 463 (2014) 17–23
- [7] L. Lu, F. Peng, Z. Jiang, J. Wang, *J. Appl. Polym. Sci.* 101 (2006) 167–173.
- [8] I. Blume, J. G. Wiljmans, R. W. Baker, *J. Membr. Sci.* 49 (1990) 253–286.
- [9] N. Rodriguez, M. Kroon, *J. Chem. Thermodynamics.* 85 (2015) 216–221.
- [10] V. Hoof, L. Abeele, A. Buekenhoudt, C. Dotremont, R. Leysen, *Sep. Purif. Technol.* 37 (2004) 33–49.
- [11] Q. Zhao, J. Qian, Q. An, Q. Yang, P. Zhang, *J. Membr. Sci.* 320 (2008) 8–12.
- [12] X. Wang, Q. An, Q. Zhao, K. Lee, J. Qian, X. Gao, *J. Membr. Sci.* 415–416 (2012) 145–152.
- [13] M. Zhu, J. Qian, Q. Zhao, Q. An, J. Li, *J. Membr. Sci.* 361 (2010) 182–190.
- [14] Q. Zhao, J. Qian, C. Zhu, Q. An, T. Xu, Q. Zheng., *J. Membr. Sci.* 345 (2009) 233–241.
- [15] Q. Zhao, J. Zhu, Q. An, *J. Mater. Chem.*, 19 (2009) 8732–8740
- [16] K. Halake, M. Birajdar, B. Kim, H. Bae, C. Lee, Y. Kim, S. Kim, S. Ahn, S. An, J. Lee, *J. Ind. Eng. Chem.* 20 (2014) 3913–3918.
- [17] F. Kursun, N. Isiklan, *J. Ind. Eng. Chem.* 41, (2016) 91-104
- [18] S. Chaudhari, Y Kwon, M. Moon, M.Y. Shon, *Bull. Korean Chem. Soc.* 36–10 (2015) 2534–2541
- [19] A. Sajjan, B. Kumar, A. Kittur, M. Kariduraganavar, *J. Ind. Eng. Chem.* 19 (2013) 427–437.
- [20] A. Ariyaskul, R.Y.M. Huang, P. L. Douglas, R. Pal, X. Feng, P. Chen, L. Liu, *J. Membr. Sci.*, 280 (2006) 815–823.
- [21] R.S. Veerapur, K.B. Gudasi, T.M. Aminabhavi, *J. Membr. Sci.*, 304 (2007) 102–111.

- [22] R. Pelton, Polyvinyl amine: A tool for engineering interfaces, *Langmuir* 30 (2014) 15373–15382.
- [23] L. Deng, T. J. Kim, M. Sandru, M. B. Hagg, *Proceeding of the 1st Ann. Gas Sympo. Elsevier.* (2009) 247.
- [24] L. Deng, T. J. Kim, M. B. Hagg, *J. Membr. Sci.* 340 (2009) 154-163.
- [25] L. Deng, M. B. Hagg, *J. Membr. Sci.* 363(2010) 295-301.
- [26] S. Han, Y. Zhang, D. Lawless, X. Feng, *J. Membr. Sci.* 417 (2012) 34–44.
- [27] H. Mansur, C. Sadahira, A. Souza, A. Mansur, *Mater. Sci. Eng. C* 28 (2008) 539–548.
- [28] P. Rao, B. Smitha, S. Sridhar, A. Krishnaiah, *Sep. Purif. Technol.* 48 (2006) 244–254.
- [29] E. Campos, P. Coimbra, M.H. Gil, *Polym. Bull.* 70 (2013) 549–561.
- [30] R. Ricciardi, F. Auriemma, C. Rosa, F. Laupretre, *Macromolecules*, 37 (2004) 1921–1927.
- [31] S. El-Sayed, K.H Mahmoud, A. A. Fatah, A. Hassen, *Physica B*, 406 (2011) 4068.
- [32] G. Zhu, F. Wang, K. Xu, Q. Gao, Y. Liu, *Polimeros* 23 (2013) 146–151.
- [33] Q. Zhang, Q. Liu, F. Shi, Y. Xiong, *J. Mater. Chem.* 18 (2008) 4646–4653.
- [34] P.J. Flory, *Principles of polymer chemistry*, Cornell University press, Ithaca, NY, 1953, p-509.
- [35] P. Shao, R. Huang, *J. Membr. Sci.* 287 (2007) 162–179.
- [36] S. Kuila, S. Ray, *Chem. Engi. Res. Design.* 91 (2013) 377–388
- [37] Q. Zhao, J. Qian, Q. An, M. Zhu, M. Yin, Z. Sun, *J. Membr. Sci.* 343 (2009) 53–61.

4. Pervaporation dehydration of acetonitrile by using the blend membrane prepared from the PVA and PVAm

4.1 Introduction.

The distillation, low-temperature crystallization, adsorption, extraction are the conventional separation techniques, where for separation of azeotropes the distillation is common. However, due to their high energy process, negative environmental impact and complex operation procedure these techniques are generally commercially fail for separation of azeotropes. In comparison new technique, pervaporation, a membrane based separation process, it is a clean technology for molecular scale liquid separation [1, 2, and 3]. Based on the solution diffusion model, [4] separation is achieved by partial pressure difference between upstream and downstream sides of membrane. The membrane allow to transport across the permeants with higher diffusivity and higher affinity through it preferentially. In addition there is no additional extraction agent and extensive heat involved during the separation process. Most importantly, superior separation efficiency to most other traditional separation processes can generally achieved by pervaporation process.

Acetonitrile is an organic chemical, it has a numerous application in chemical process such as an extracting solvent for separation of olefin and diolefin mixtures and C4 hydrocarbons in petrochemical industries [5]. In laboratory, it is used as medium polarity solvent that is miscible with water in all proportion and range of organic solvent but not with saturated hydrocarbon hence used as a HPLC column solvent [6]. It is key solvent in pharmaceutical industry for drug analysis and manufacture.[7]. It forms a azeotropes with water, gives a mixture having boiling point 76.5 °C contain around 82.2 wt.% of acetonitrile under atmospheric pressure[8]. In order to separate the water acetonitrile mixture, heterogeneous distillation[9,10], extractive distillation, solvent extraction [5] was used. The recovery of

solvent and solute from extract phase usually done by additional distillation process. So these processes are leads to uneconomical pathway. Zerry et.al had explored the novel hybrid method pervaporation and distillation for water acetonitrile separation [11]. They were concluded that, hybrid process was economical in comparison to conventional approach.

Generally, hydrophilic polymeric materials are widely studied as pervaporation membrane for acetonitrile dehydration. Among them, PVA is most popular material, iron oxide nano composite membrane was prepared by Mandal.et.al. [12] and they have reported that Fe containing PVA polymer matrix showed improved flux and selectivity for acetonitrile dehydration. Zeolite filled sodium alginate and poly vinyl alcohol-poly aniline semi-interpenetrating polymer network membrane was prepared by Naidu et.al for pervaporation dehydration of water acetonitrile mixture [13]. M.khayat et.al studied separation of acetone, acetonitrile and ethanol from aqueous solution using pervap@4060 membrane. They have found that organic selectivity of membrane was in order of acetone>acetonitrile>ethanol [14]. Recently Das et.al prepared co-polymer membrane from synthesized acrylonitrile and itaconic acid and used for dehydration of acetonitrile [15]. However from all these membrane they have obtained selectivity but improvement of flux was not remarkable.

In order to increase the water stability, mechanical strength of membrane prepared from the hydrophilic polymer crosslinking of polymer is common, however degree of crosslinking affect the pervaporation performance adversely since it became stiff [16]. Hence PVA incorporation with inorganic filler in order to reduce swelling in aqueous medium were studied however, such membrane limited by uniform dispersion of filler in polymer matrix. Poor dispersion influence the pervaporation performance of membrane severely. Blending of material is one of the more efficient way to amend its appropriate property by adjusting polymer blending ratio owing to its intermolecular interaction. PVA blending membrane have been studied for dehydration of several organics [17]. Spatially chitosan/PVA membrane showed remarkable performance in pervaporation dehydration of various organic solvents. It could possible to obtain homogenous membrane through blending them since they are miscible at molecular level. [18, 19]. Similarly PVA/PVP, [17]

membrane, Sodium alginate/PVP [20] membranes were also been investigated for the pervaporation dehydration of various organic water mixtures. In their study they have reported that permeation improved without appreciably reducing the selectivity. These studies prompted us to explore and extend the pervaporation dehydration study by preparing blend membrane from the PVA. Because PVA has been frequently employed in the preparation of hydrophilic membrane. Since it has high hydrophilicity, excellent processability and available hydroxyl groups for easy post modification [17]. Polyvinyl amine (PVAm) is highly crystalline polymer having abundant of amine group derive from the hydrolysis from Poly N-vinyl formamide (PNVF).[21]. As the among the chitosan, poly (elthyleneimine), poly(allyl amine), the poly(vinyl amine) contain highest amount of NH_2 groups could confer more hydrophilic membrane surface[22]. Since membrane prepared from PVAm (Commercially available as PVAm HCl) usually sticky, swollen and high viscosity fluid therefore not possible to form a film using poly (vinyl amine). Contrary to that PVA have excellent film forming ability, higher tensile strength flexibility and stable in the organic solvent. Both polymers PVAm and PVA are hydrophilic as they possesses amine (NH_2) and OH functional moiety in their backbone, so their combination can be the excellent pervaporation membrane in dehydration process. Hu and X. Feng et.al have studied the PVA/PVAm blending membrane incorporated with carbon nanotube for the dehydration of ethylene glycol but focus of their study was on the effect of CNT in to the membrane on PV performance. [23]. Furthermore, as observed from the PVA/chitosan blend membrane separation pervaporation performance, the filed lacks a pursuance explanation for why the optimal ratio of membranes is different for different feed system. In order to reduce excessive swelling, annealing or crosslinking of polymer blending membrane is common, nevertheless it has an influence on pervaporation performance of membrane. [24]

In this study our focused on the preparation of membrane blend membrane from the PVA and PVAm and crosslinked with glutaraldehyde at mild temperature for pervaporation of dehydration of water acetonitrile mixtures. We kept PVA as base polymer and added PVAm in various proportion. As author's literature survey concern, no such kind of study has been reported still now. The resulting membrane characterization was done by, swelling studies,

SEM analysis, differential scanning calorimetry, IR spectroscopy, X-ray diffraction. Finally applied for the pervaporation separation binary mixture of water and acetonitrile mixture. The effect of PVAm addition, effect of feed concentration and effect of temperature were studied for optimization of membrane performance.

4.2 Experimental

4.2.1 Preparation of the crosslinked PVA/PVAm blend membrane.

Details of membrane preparation have discussed in the chapter 3, section 3.2.2. Three different type of membrane were prepared by changing the PVAm content in the PVA membrane. The membrane composition and abbreviation has shown in table 4.1.

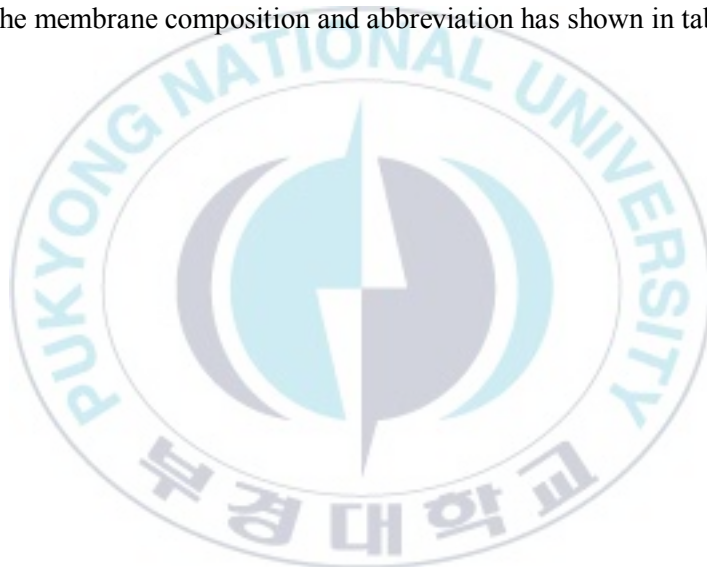


Table.4.1 Abbreviations of blended PVA and PVAm membranes for water/acetonitrile separation

Abbreviation	Ratio in the membrane (g/g)	
	PVA (Polyvinyl alcohol)	PVAm(polyvinyl amine)
MB0	100	0
MB0.5	100	10
MB1.0	100	20
MB1.5	100	30

4.2.2 Degree of membrane sorption in acetonitrile/water feed mixture.

The dried membrane samples were weighed (m_d) and immersed in bottle containing the 50cm³ of different water/acetonitrile mixtures for 48 h, at a 30°C temperatures. They were then removed from the solutions, wiped with dry tissue paper, and the weight of the swelled membrane was measured immediately (m_s). In order to minimise the errors, three time such measurements were done and average value average value was reported. The swelling degree (degree of sorption) was calculated using the following equation:

$$SD = \frac{m_s - m_d}{m_d} \quad (1)$$

Where, m_s and m_d are the mass of the swelled and dried membranes, respectively.

4.2.3 Pervaporation apparatus and measurements

The pervaporation apparatus designed for present study is shown in chapter 3, section 3.3.8. Briefly, the membranes were placed in a membrane cell and fixed. The effective area of membrane was 19.64 cm². The membrane cell was made up of two compartments –, one connected to the downstream side (vacuum pump) and other connected to a feed tank. The feed tank was maintained at the desired temperature (30 to 60 °C) in water bath. In order to avoid concentration polarization feed mixture was continuously circulated using a pump (100 rpm) through the membrane cell. The downstream side pressure was maintained less than 10 mbar using a vacuum pump (Edwards, RV8). The permeants solution was collected in a cold liquefied nitrogen trap and then weighed. The feed mixture composition was ranged from 5-20wt. % of acetonitrile in water. The gas chromatography (with TCD detector) (Perkin) was used to determine the composition of permeants solution concentration. The separation performance of prepared membrane was characterized using following equations:

$$Flux (J) = \frac{Q}{A \times t} \quad (2)$$

Where Q is the weight of permeated solution collected in the cold trap and the flux is calculated with respect to effective area (A) in time t.

$$Separation Factor (\alpha) = \frac{P_{Water}/P_{Acn}}{F_{Water}/F_{Acn}} \quad (3)$$

Where P_{Water} , P_{Acn} , F_{Water} , and F_{Acn} are the weight fractions of water and acetonitrile solution in the permeated solution and the feed solution, respectively. In addition, the flux was calculated by following equation:

$$\text{Pervaporation Separation Index (PSI)} = J \times \alpha \quad (4)$$

Where J and α are the permeation rate and separation factor, respectively. Each pervaporation test was carried out in duplicate average values were reported.



4.3 Results and Discussion

4.3.1 Membrane Characterization.

Details about the membrane characterization has described in the chapter 2, section 2.3.1.

4.3.2 Membrane swelling and sorption study.

The solution diffusion model can explain the pervaporation transport mechanism [4]. Therefore membranes preferential sorption property should be studied. Sorption of desired component in a membrane is significant for pervaporation dehydration because it determines the membrane permselectivity and controls the transport of permeating molecules under chemical potential gradient. Figure 4.1 reflects the effect of PVAm addition and feed concentration of water/acetonitrile on the membranes swelling degree. It is observed from the figure that membrane degree of swelling increases (sorption) with increasing the PVAm content in the PVA/PVAm blending membrane and water content in the feed. Hydrophilic groups of membrane such as OH, NH₂ are generally responsible for preferential sorption of water molecules. Blend membranes consist of abundant such hydrophilic moieties, increasing the hydrophilic-hydrophilic interaction between feed water and membrane hence increase in swelling degree and it can fascinate the pervaporation transportation phenomenon for water-acetonitrile dehydration that has further explained in the next sections.

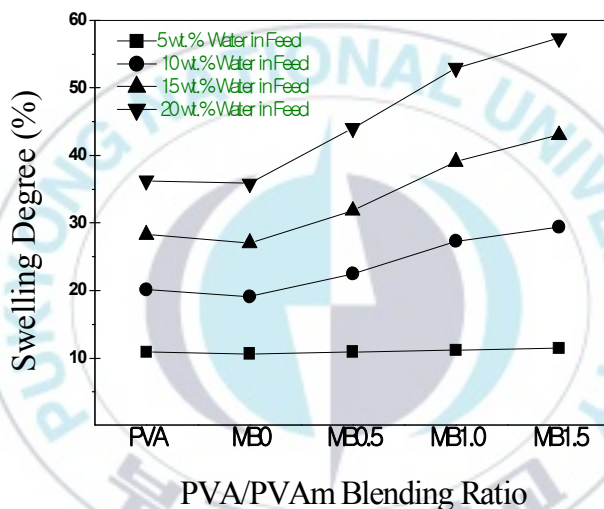


Figure 4.1 Variation of degree of swelling with different wt. % of water in the feed for different PVAm blend membranes.

4.4 Pervaporation

4.4.1 Effect of PVAm content in PVA/PVAm ratios on PV performance for water/ACN mixture

The effect of PVAm contents in blend membrane as function of permeate flux and separation factor from feed composition 80/20 acetonitrile/water at 30 °C as shown figure 4.2. The blending of PVAm with PVA had a significant effect on the permeation flux and separation factor. When the addition of PVAm increased from MB0 to MB1.5 the permeation flux increased which was consistent with the sorption study reflected in section 4.3.2 of the membrane. The changing the trend of PVA crystallinity was an important factor which affect the flux. From the XRD study it was observed that with addition of PVAm result in increases amorphous region in the due to the intermolecular hydrogen bonding interaction. Therefore the more free volume available diffusion of permeants which increases the permeation flux. Whereas the PVAm content increases from the MB0 to MB1.5 the separation factor increased from the 81.2 to 100.84. The increased in separation factor with flux simultaneously is very uncommon phenomenon in pervaporation process [12,16,25]. This is because PVAm is highly crystalline polymer have compact network, additionally crosslinking reinforces the closed compact nature of the membrane consequently less access to acetonitrile having larger molecular size than water. Furthermore the addition of PVAm adds the hydrophilic moieties such as NH₂ responsible for increasing the affinity for water molecule. So it boost the absorption of more water molecules from the feed boundary layers rather acetonitrile and subsequently diffuse through the membrane. Similar result trend was reported in the dehydration of caprolactam using the NaAlg-PVP blend membrane by T. Zhu et.al [20]. For more insight of result obtained in this study we have plotted the individual fluxes water, acetonitrile as function of PVAm content in the membrane as shown in figure 4.3. The figure 4.3 reflects that the total flux and water are overlapping to each other and monotonously increases with PVAm content, however increase in the acetonitrile flux is marginal. It has also seen from the figure that the concentration of water in permeants was greater than 94.5% over the content of acetonitrile. The increase in the acetonitrile flux with PVAm addition was relatively low,

nevertheless it might have been due to the polar nature of the membrane of due to formation of C=N linkage increases the affinity of hydrophobic acetonitrile absorption. In order to optimization of the membrane blending ratio we had calculated the pervaporation separation index (PSI) [26] the figure 4.4 shows PSI as function of PVAm content in the blend membrane. The figure implies that, MB1.5 membrane showed the highest PSI, so further test were done by using the MB1.5 membrane.



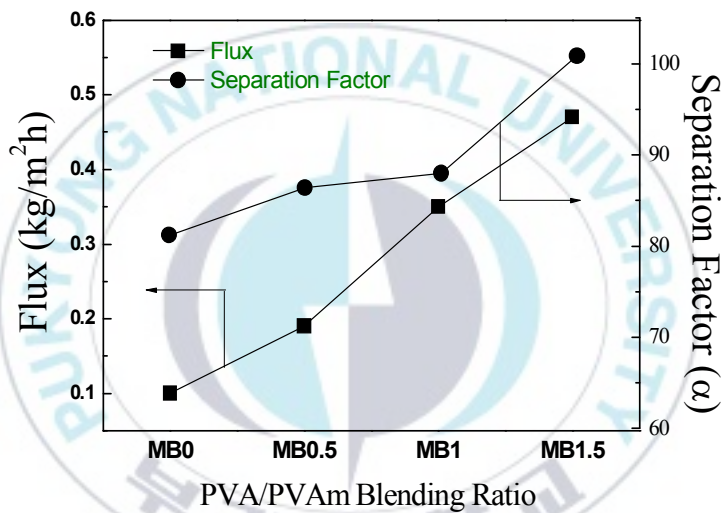


Figure 4.2 Influence of PVAm content in blend membranes of PVA on permeation flux and separation factor for Acetonitrile dehydration at 30 °C, thickness ~65 μ.

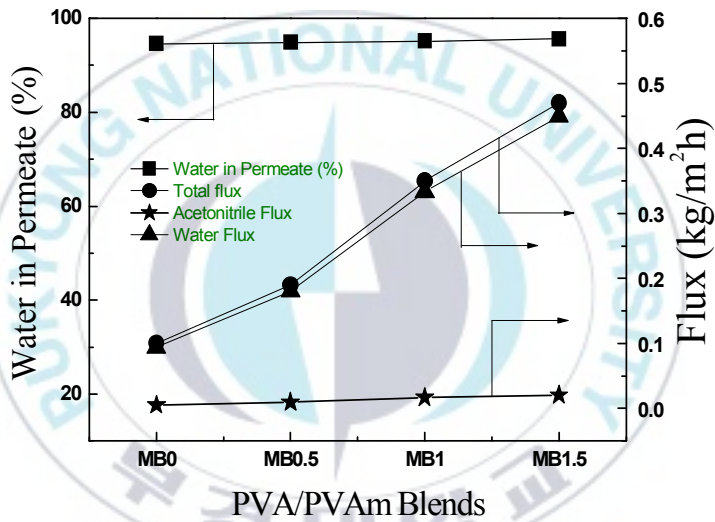


Figure 4.3 Effect of PVAm content in blend membranes of PVA on individual fluxes of water, acetonitrile and water wt. % in permeate

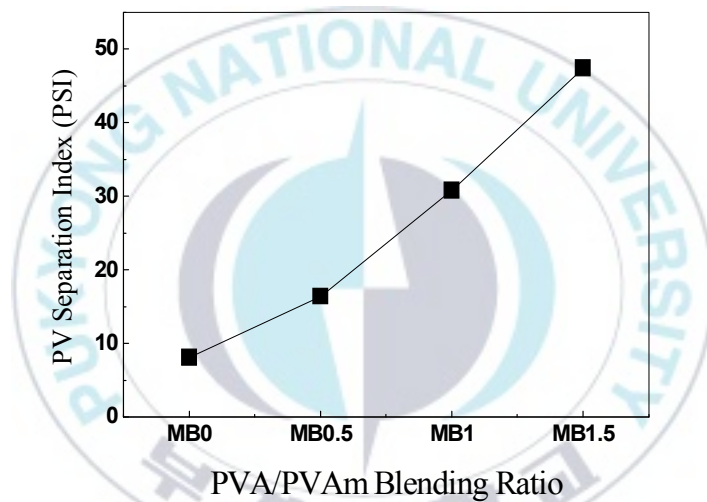


Figure 4.4 Influence of PVAm content in blend membranes of PVA on pervaporation separation index (PSI).

4.4.2 Effect of feed composition on separation performance for water/ACN mixture

The effect of acetonitrile-water concentration on the pervaporation performance in terms of flux and separation factor was tested. The all the pervaporation test were performance with MB1.5 membrane at 30 °C obtained as shown in figure.4.5. The figure indicate that not only the flux but also the separation factor strongly influence by the feed composition. The acetonitrile exhibits azeotropes with at 82.2% at 76.5 °C under atmospheric pressure, therefore the pervaporation were carried out from water contents range from the 5 to 20 wt. % in the feed mixtures. It can be seen from the figure 4.5, that with water content increases from the 5wt. % to 20 wt. % the total flux increased from the 0.01 to 0.47 kg/m²h while separation factor drops from the 5050 to 100.84. The increasing flux with water in feed can be explained by higher swelling in the blend membrane due to the strong affinity of PVA and PVAm towards the water which was observed in the sorption study of the membrane in section in 4.3.2. The figure 4.6 reflects the individual fluxes of water and acetonitrile as function of water content in the acetonitrile feed mixture. It can be seen from the figure that the acetonitrile flux is insignificant, however it was increased with water feed composition as well as water flux. It has been well known that the water molecule absorbed by membrane occurred due to the presence of hydrophilic moieties in to it. The blend membrane (MB1.5) even though it is crosslinked, till it has an enough NH₂ and OH moieties which result in the swelling of the membrane and assist the permeates transport through membrane [16, 20, 27] However excessive swelling due to the increase in feed water absorption severely affected membrane fragility of membrane. The membrane become plasticized and amorphous region of membrane are more swollen which allows the diffusion of acetonitrile along with water molecules, so it result the in water flux increases but separation factor decreases. The trade-off hurdle between flux and separation factor with water driving force is common [25].

Figure 4.7.demonstrate the water-acetonitrile vapor-liquid equilibrium data reported elsewhere [28], compared with the pervaporation results obtained by using MB1.5.tends to evaluate the separation performance by pervaporation over the distillation. It is obvious that the higher concentration of water in permeate by pervaporation compare to vapor-

liquid equilibrium was provided. It dictates that the higher separation features of the blend membrane (MB1.5) compare to the distillation. Additionally the pervaporation process is less energy intensive over the distillation. The distillation require the entrainer in order to achieve the separation obtained by pervaporation. So it was observed that the membrane acted as third phase to effectively break the azeotropes.



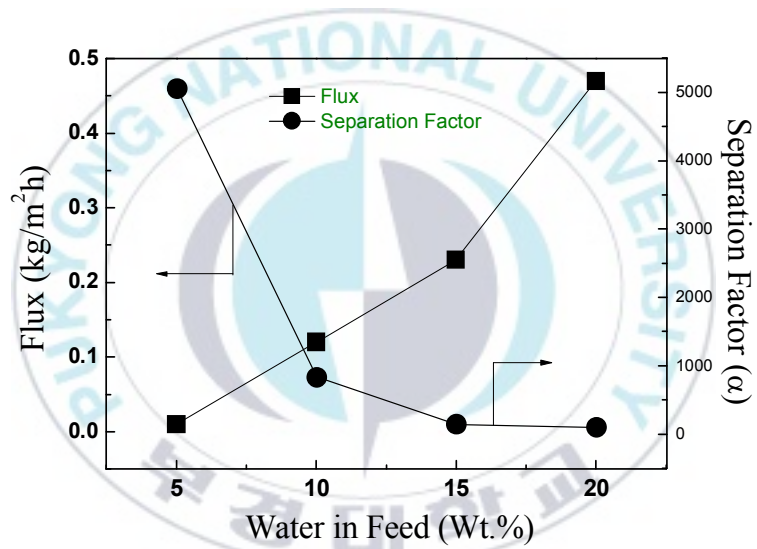


Figure 4.5 Effect of feed composition on pervaporation performance for water-acetonitrile mixture by MB1.5 at 30 °C, 65 μm.

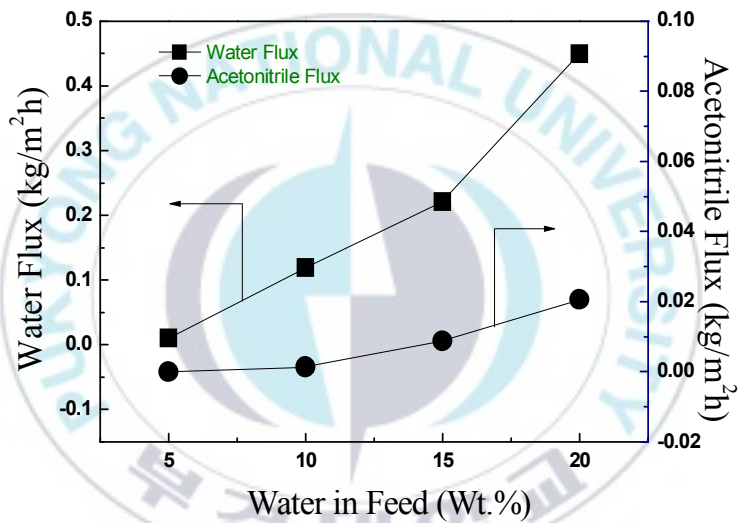


Figure 4.6 Effect of feed composition on pervaporation performance for water-acetonitrile mixture by MB1.5 on individual fluxes of water, acetonitrile.

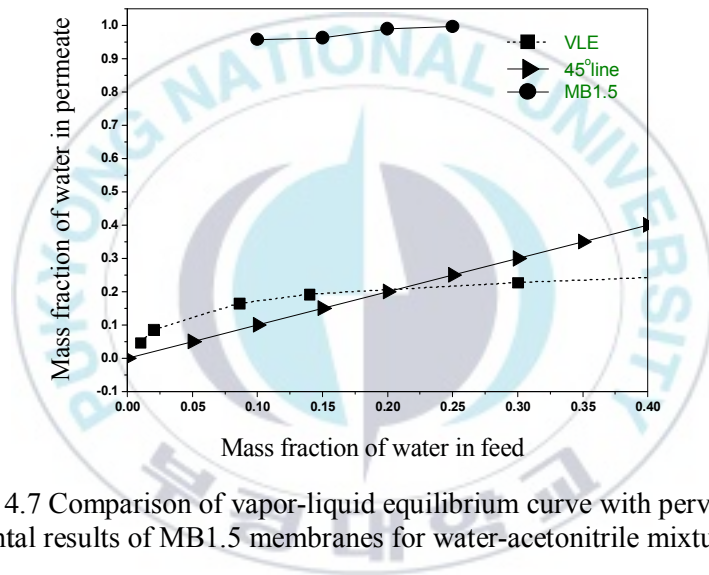


Figure 4.7 Comparison of vapor-liquid equilibrium curve with pervaporation experimental results of MB1.5 membranes for water-acetonitrile mixtures at 30 °C.

4.4.3 Effect of feed temperature on separation performance 4.4.2 for water/ACN mixture

Pervaporation process is a vapor pressure gradients driven process, and hence operation temperature have significant importance in evaluation of membrane performance since it affect both sorption and diffusion rates. The figure 4.8 and 4.9 shows the effect of feed temperature on the pervaporation performance of the membrane at 85/15 w/w and 90/10 w/w acetonitrile/water composition with MB1.5 membrane. It was clearly reveal from the figure that, when temperature increased from the 30 °C to 60 °C the total flux increased from the 0.12 to 0.16 for 90/10 w/w and 0.23 to 0.39 for 85/15 w/w water acetonitrile feed composition. Increased in flux can be ascribed by three reason i) the enhance driving force ii) the free volume increment in the membrane iii) higher molecular diffusivity [29]. Interestingly it was seen from the figures that, the increased in the flux for 85/15 acetonitrile/water feed composition is more significant than that 90/10 it shows hydrophilicity of membrane. Because both the driving force due to temperature and higher feed water increases the sorption and diffusion rate of permeants but on other hand at 90/10 w/w feed composition membrane swelling is fever so only increased vapor pressure difference increases the flux. At instance the flux increased but on other hand separation factor was decreased at the both feed composition. This is because ,according to the free volume theory the increases in temperature increases the thermal mobility of polymer chain, which generates the extra free volume within the polymer matrix, which enhance the permeation water along the acetonitrile thorough the membrane. Which result in the decrease in the separation factor.

The temperature dependence of the permeation flux can be express by an Arrhenius-type equation [30]

$$\text{Flux } (J) = A_p \cdot e^{-E_p/RT}, \quad (4)$$

Where A_p and E_p are the pre-exponential factor and the overall activation energy for permeation, respectively.

A logarithmic Arrhenius plot of flux against temperature was plotted for each of the mixture components, for both 85/15 w/w and 90/10 w/w feed composition as shown in Figure 4.10 and 4.11 From the slope of the resulting plot, the activation energies for the

permeation of acetonitrile and water through MB1.5 were calculated. The activation energy for the permeation of acetonitrile (15.17 kJ/mol) and water (14.38 kJ/mol) for 85/15 w/w and that of 38.56 kJ/mol and (7.81 kJ/mol) for 90/10 w/w water/acetonitrile feed composition was observed. The higher difference in the activity energies at 90/10 w/w than 85/15 w/w feed composition implies that retardation of acetonitrile permeation is more significant at 90/10w/w feed composition shows the more hydrophilic nature of the membrane.



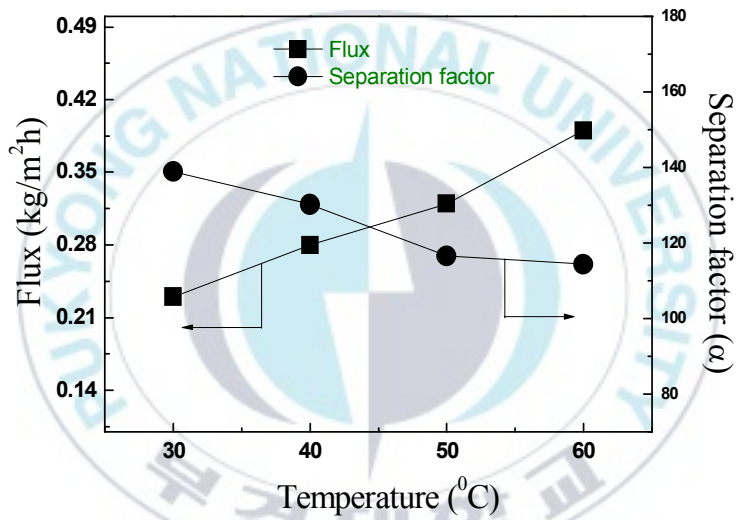


Figure 4.8 Effect of temperature on pervaporation flux and separation factor for water acetonitrile by MB1.5 membrane, feed composition: 85/15 w/w acetonitrile/water.

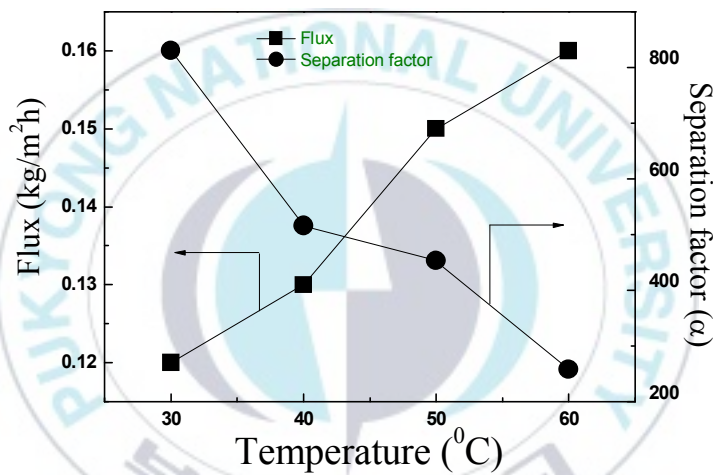


Figure 4.9 Effect of temperature on pervaporation flux and separation factor for water acetone nitrile by MB1.5 membrane, feed composition: 90/10 w/w acetone nitrile/water

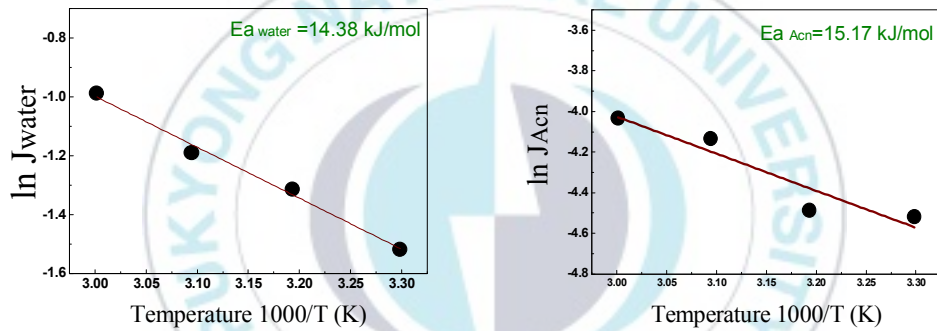


Figure 4.10 Variation of $\ln J_{\text{water}}$ and $\ln J_{\text{Acn}}$ with temperature at 85/15 acetonitrile feed composition.

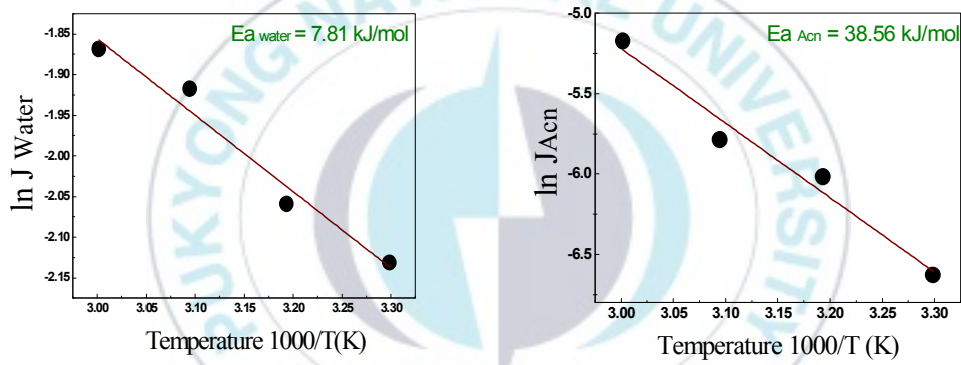


Figure 4.11 Variation of lnJwater and lnJAcn with temperature at 90/10 acetonitrile feed composition.

4.4.4 Comparison of pervaporation results with other studies

A comparison pervaporation results of PVA/PVAm blend membrane system in this study with that reported in the literature is important to evaluate the efficiency of membrane over the existing data. There are least number of study available for acetonitrile pervaporation dehydration in the literature. The Table 4.2 shows the comparison of pervaporation results obtained from the MB1.5 with membrane prepared from the various polymer system and preparation method that have recently studied for acetonitrile dehydration. The Table 4.2 demonstrate that, there is a greater amendment of flux and separation factor in at all composition with MB1.5 membrane for water acetonitrile pervaporation separation as compared to the literature data.

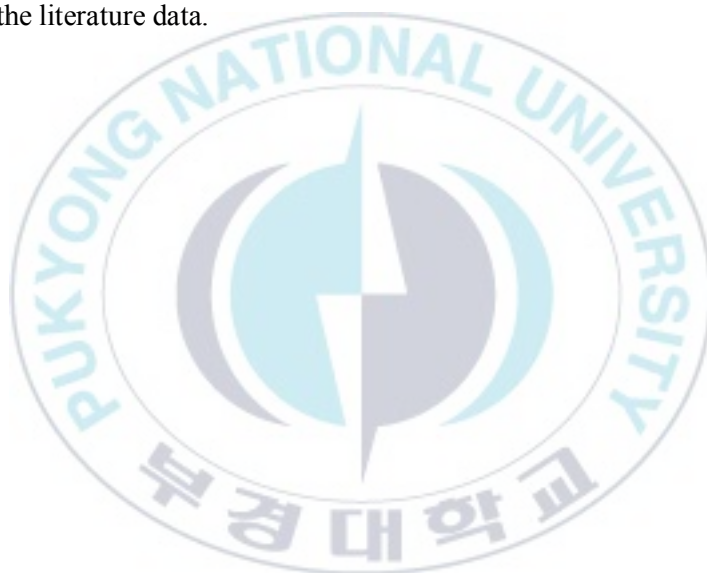


Table 4.2 Comparison table for the pervaporation performance of PVA/PVAm blend membrane with other studies for Acetonitrile separation.

Polymer	Nature of the membrane preparation method	Feed(%) composition,(w/w) Water/Acetonitrile	Temperature (°C)	Flux(J) (kg/m ² h)	Separation factor(α)	Thickness (μ)	Reference
PVA	FeO ₃ /FeO ₂ Incorporation	10-32	35	0.02-0.20	20-700	45	[12]
Na-Alginate	Zeolite filled(PVA/Polyaniline S-IPN)	10-50	30	0.03-0.09	3-69	40	[13]
PAN-IA	PAN-IA-Copolymerization	1.2-24	30	0.028-0.23	35-409	40	[15]
PVA	PVA/PVAm (MB1.5)Blend membrane	5-20	30	0.01-0.47	100-5050	~65	Present study

4.5 Conclusion

The present study demonstrate that the different blend membranes were prepared by the blending the highly hydrophilic polymers PVA and PVAm in different composition. The glutaraldehyde was used as crosslinking agent. The polymers are compatible at the molecular level was determined from FTIR, SEM and DSC studies. The XRD measurements confirms the decreased in crystallinity of crosslinked PVA/PVAm blend membranes with PVAm addition. The surface roughness of membrane increased due to the inclusion of PVAm in the membrane, and this was, again, attributed to the increase in intermolecular hydrogen bonding. The pervaporation performance of the membrane was tested for the separation of water-Acetonitrile mixtures. All the blend membranes showed excellent pervaporation properties for acetonitrile/ water separation in comparison to the virgin PVA membranes .It was demonstrated that the thorough the introduction of PVAm could enhance membrane hydrophilicity of membranes and is in favors of increasing flux. As the PVAm concentration in blend membrane increases, both the flux from 0.1 to 0.47 kg/m²h and separation increased from the 81.2 to 100.84 was increased. Among all the blend membrane MB1.5 membrane was the best one since it exhibited higher separation index. The increasing flux with water in feed can be explained by higher swelling in the blend membrane due to the strong affinity of PVA and PVAm towards the water which was observed in the sorption study of the membrane. With regards to the temperature effect, the permeation rate increases while suppressing the separation factor with increasing the temperature. However the increased in the flux for 85/15 acetonitrile/water feed composition is more significant than that of 90/10 it shows hydrophilicity of membrane. The activation energy for the permeation of acetonitrile was higher than the water. It concludes the permeation of water through the MB1.5 membrane exhibit with less energy shows membrane have a higher affinity with water than acetonitrile.

References

- [1] L. Y. Jiang, Y. Wang, T. S. Chung, X.Y. Qiao, J. Y. Lai, *Prog. Polymer Sci.* 34 (2009) 1135-1160.
- [2] P. Peng, B. Shi, Y. Lan, *Sep. Sci. Technol.* 46 (2011) 234-246.
- [3] B. Smitha, D. Suhanya, S. Sridhar, M. Ramakrishna, *J. Membr. Sci.* 241 (2004) 1-21.
- [4] J. G. Wiljmans, R. W. Baker, *J. Membr. Sci.* 107 (1995) 1–21.
- [5] I. Acosta-Esquivarosa, I. Rodriguez-Donis, U.J Haza, L. Nuevas-Paz, E. Pardillo-Fontdevila, *Sep. Purif. Technol.* 52 (2006) 95-101.
- [6] T. R. C. Van Assche, T. Remy, G. Desmet, G. V. Baron, J. F. M. Denayer, *Sep. Purif. Technol.* 82 (2011) 76-86.
- [7] I. F. Mc Convey, D. Woods, Moira Lewis, Q. Gan, P. Nancarrow, *Org. Process Res. Dev.* 16 (2012) 612-624
- [8] J. Acosta-Esquivarosa, I. Rodriguez-Donis, U. Jaurgeui-Haza, L. Nuevas-Paz, E. Pardillo-Fontdevila, *Sep. Purif. Technol.*, 52 (2006), pp. 95–101
- [9] I. Rodriguez- Donis, E. Pardillo-Fontdevilla, V. Gerbaud, X. Joulia, *Comput. Chem. Eng.* 25 (2001) 799-806.
- [10] I. Rodriguez- Donis, J. Acosta-Esquivarosa, V. Gerubaud, X. Joulia, *AIChE J.* 49 (2003) 3074-3083
- [11] R. Zerry, J. U. Repke, M. Wusterhausen, G. Wozny, Berlin Technical University, Dep. of Process and Plant Technology, Berlin, Germany, 2005.
- [12] M. K Mandal, S. B. Sant, P. Bhattacharya, *Colloids surface. A* 373 (2011) 11-21.
- [13] B. V. Naidu, S. D. Bhat, M. Sairam, V. Wali, D. P. Sawant, S. B. Halligudi, N. N. Mallikarjuna, T. M. Aminabhavi, *J. Appl. Polym. Sci.* 96 (2005) 1968-1978.
- [14] M. Khayet, C. Cojocar, G. Z. Traznadel, *Sep. Purif. Technol.*, 63(2008), 303-310.
- [15] P. Das, S. K. Ray, *J. Membr. Sci.* 507 (2016) 81-89
- [16] S. Chaudhari, Y. Kwon, M. Moon, M.Y. Shon, *Bull. Korean Chem. Soc.* 36–10 (2015) 2534–2541
- [17] K. Sunitha, Y. V. L. Ravi Kumar, S. Sridhar, *J. Mater. Sci.* 44, (2009) 6280-6285.

- [18] S. Zhang, Y. Zou, T. Wei, C. Mu, X. Liu, Z. Tong, *Sep. Purif. Technol.*, 173 (2017), 314-322.
- [19] M. N. Hyder, P. Chen, *J. Membr. Sci.* 340 (2009) 171–180
- [20] T. Zhu, Y. Luo, Y. Lin, Q. Li, P. Yu, M. Zeng, *Sep. Purif. Technol.*, 74 (2011), 242-252.
- [21] X. Feng, R. Pelton, M. Leduc, *Ind. Eng. Chem. Res.* 45 (2006) 6665-6671.
- [22] R. Pelton, Polyvinyl amine: A tool for engineering interfaces, *Langmuir* 30 (2014) 15373–15382.
- [23] S. Han, Y. Zhang, D. Lawless, X. Feng, *J. Membr. Sci.* 417 (2012) 34–44.
- [24] A. Sharma, S.P. Thampi, S.V. Suggala, P.K. Bhattacharya, *Langmuir* 20 (2004) 4708–4714.
- [25] A. Sharma, S. P. Thampi, S.V. Suggala, P. K. Bhattacharya, *Langmuir* 20 (2004) 4708-4714
- [26] R. Y. M. Huang, *Pervaporation membrane separations processes*, Amsterdam, Oxford, New York, Tokyo 1991
- [27] J. H. Chen, J. Z. Zheng, Q. L. Liu, H. X. Guo, W. Weng, S. X. Li, *J. Membr. Sci.* 429 (2013) 206–213.
- [28] D. F. Othmer, S. Josefowitz, *Ind. Eng. Chem.* 39 (1947) 1175-1177
- [29] K. Cao, Z. Jiang, X. Zhang, Y. Zhang, J. Zhao, R. Xing, S. Yang, C. Gao, F. Pan, *J. Membr. Sci.* 490 (2015) 72-83.
- [30] R. Y. M. Huang, C.K. Yeom, *J. Membr.Sci.*51 (1990)273–292.

5. Pervaporation dehydration of water/isopropanol mixtures using M-STA loaded PVA/PVAm mixed matrix membrane

5.1 Introduction

Conventional processes for separation of liquid mixtures includes many forms of distillation and depends on the vapor-liquid equilibrium of components of the mixture. The key step in these processes is the separation of azeotropes because it consumes a tremendous amounts of energy and leads to higher capital costs and environmental pollution. Another technique, pervaporation, follows solution diffusion principles [1]. It is a vacuum driven process, liquid feed mixture (upstream side) is in contact with membrane surface at atmospheric pressure and output from the either side (downstream side) of the membrane obtained in the vapor phase because low pressure existing on it since it is connected to vacuum as shown in Fig. 1.1 Like the separation of azeotropes using distillation, pervaporation does not require an additional carcinogenic entrainer (e.g. benzene) making pervaporation an economical, clean, eco-friendly, and safe separation technology. Pervaporation applications include the separation of water-organic mixtures such as in alcohol dehydration [2, 3, 4], the separation of organic-organic mixtures [5], and the separation of diluted dissolved organic residues from waste water streams [6, 7].

The dehydration of various alcohols, such as ethanol and isopropanol (IPA), is an example of a commercialized pervaporation application. Isopropanol forms an azeotropic mixture with water, produce a mixture that boils at 80.37 °C at an isopropanol composition of 87.7 wt. %. Consequently, to separate these azeotropes, pressure swing distillation or a third entrainer component is required in extractive or azeotropic distillation [8], both of which are infeasible and expensive and have unfavorable side effects. Therefore, pervaporation or hybrid systems combining pervaporation with distillation have been extensively explored. Hoof et al. reported a hybrid distillation-pervaporation system using a ceramic

membrane that saves 49% of the cost of separation compared to conventional azeotropic distillation [9].

Hydrophilic materials, such as polyvinyl alcohol (PVA), have been employed for the preparation of membranes for dehydration of organics [5, 10], because it has inherent hydrophilicity due to the presence of numerous hydroxyl groups on its backbone. Additionally, PVA has excellent film forming ability as well as thermal stability, making it a promising material for use in membrane preparation. Furthermore, the available hydroxyl functionality can be easily modified using several chemical reagents, making PVA extremely useful for pervaporation membrane applications [10-13]. However, excessive swelling in aqueous media tends to lower the performance of PVA membranes in terms of selectivity in pervaporation applications. To remedy the swelling problem, PVA has been modified using different methods like chemical crosslinking, polymer grafting, blending with different polymers, formation of PVA copolymers, and thermal treatment [14-17]. Membranes prepared from the blending of different polymers have shown promising pervaporation performance. In blended films, the intrinsic chemical, physical, mechanical, and morphological properties of each component can be combined, enabling the fine-tuning of membrane properties. Among commonly blended films such as chitosan, poly(ethylamine), and poly(allyl amine), poly(vinyl amine) (PVAm) contains largest amount of NH_2 groups, and allows the preparation of very hydrophilic membranes [18]. PVAm (commercially available as PVAm HCl) polymers are usually sticky, swollen, and highly viscous, preventing the effective formation of films using PVAm alone. In contrast, PVA has excellent film-forming properties, as well as high tensile strength, flexibility, and stability in organic solvents. Both PVAm and PVA are hydrophilic, containing amine NH_2 and OH functional groups in their main chains, consequently, the combination of these polymers may yield a high-quality pervaporation membrane for use in the dehydration process.

To enhance physicochemical properties as well as the pervaporation performance of pervaporation membranes, incorporation of mesoporous silica [19], inorganic nanoparticles [20], zeolite, and carbon nanotubes [10, 21] in membranes by physical mixing has been explored. A hetero poly acid (HPA) is a type of acid produced from a

specific combination of hydrogen and oxygen with certain metals [M] and non-metals [X] incorporated with different polymers, as has been reported by Aminabhavi et.al [22-24]. HPA based on Keggin units gives a polyanion $[XM_{12}O_{40}]^{n-}$ with a three-dimensional assembly of hetero polyanions which can interact with the protons of water molecules. The formation of hydrates using the interaction of terminal and bridging oxygen atoms on the periphery of the HPA with water, privilege the transportation of water molecule in pervaporation dehydration [23]. Silicotungstic acid is a kind of HPA were investigated for pervaporation [24, 26] as well as different application such as proton conducting membrane [27]. Aminabhavi et.al [24] reported in their study that, 1 wt. % addition of STA into the membrane showed infinite water selectivity over 10 to 25% water feed composite range for water/acetic acid separation since highly hydrophilic in nature. Additionally they were found that dispersion of STA particle in the polymer matrix was possible at molecular level since it is water soluble. However, these HPA membranes are affected by leaching of the HPA during the pervaporation cycles [26], which can have a severe impact on the membrane performance.

Melamine (1,3,5-Triazine) consists of 9 hydrogen bonding sites, the 3 sp^2 -hybridized nitrogen atoms of the thiazine ring can accept hydrogen bonds and hydrogen bond donation by the 3 exocyclic unsubstituted primary amine groups can also occur. Melamine also has an aromatic planar ring structure, capable of pi-pi stacking [28]. In neutral or acidic conditions, melamine can be protonated since it is weak base ($pK_b = 6$), so a hydrogen bond accepting site will be converted to a donating site under these conditions. In this study, modified silicotungstic acid (STA) particles (size range from nanometer to micrometer) were prepared using melamine since STA have a number of terminal oxygen and bridging oxygen. In addition, STA has four acidic hydrogen atoms, which can be donated to the melamine molecule, forming an STA anion. These anions are easily formed by interaction with melamine through hydrogen bonding and electrostatic attraction between the anion and cation, facilitating the formation of the STA supramolecular complex [29]. While the long period of pervaporation separation cycle, these modifications not only prevent the leaching of STA filler from the membrane, but also can increase the hydrophilicity and stability of the membrane.

Many paper have dealt with preparation of mixed matrix membrane using different nanoparticle incorporation [19-24], because the membrane exhibit increased thermal/chemical/mechanical stability and high separation ability with appropriate balance of flux and separation was possible with these nano fillers. However, the efficiency of pervaporation separation is strongly influence with used of appropriate membrane materials. Since silicotungstic acid filler was well explored in pervaporation and showed excellent separation, this prompted us to further upgradation and extension of STA as a filler in pervaporation application. Therefore, in this study, a blend membrane was prepared from PVA and PVAm crosslinked with glutaraldehyde at mild temperatures and loaded with melamine modified silico tungstic (M-STA) particles for the pervaporation dehydration of water-isopropanol mixtures. The resulting M-STA particles and membranes were characterized by FTIR-ATR mode spectroscopy, scanning electron microscopy (SEM), scanning electron microscopy with energy-dispersive spectroscopy (SEM/EDS), atomic force microscopy (AFM), contact angle measurement, X-ray diffraction (XRD), and a swelling study. Finally, the membranes were used in the pervaporation of an isopropanol-water mixture under a range of conditions to determine the optimum conditions for enhancing membrane performance.

5.2 Experimental

5.2.1 Materials

Silico tungstic acid hydrate $[H_4(Si(W_3O_{10})_4)_n \cdot nH_2O]$ and melamine were obtained from the Sigma Aldrich. Poly(vinyl alcohol) with a molecular weight of 88000-97000 and a 98-99% degree of hydrolysis was purchased from Alfa Aesar, USA. Poly(vinyl amine) (PVAm) (Lupamin-9095, M_w 340000, 10 wt.% solution) was donated by BASF Indonesia. Isopropyl alcohol (99.5 wt.%) was obtained from Dae-Jung Chemicals & Metal Co, Korea. For the pervaporation experiment the water/isopropyl alcohol mixtures were prepared in the laboratory by mixing an IPA with Ultrapure water (Puris, Expe-RO EDI water system) predetermined quantity of each (w/w).

5.2.1 Preparation of Melamine modified Silicotungstic acid (M-STA) particles

Modified silicotungstic acid particles were prepared by the precipitation method. In a beaker, 100 mL of a solution of silicotungstic acid (0.01 M) in deionized water was prepared. Similarly, a 0.01 M transparent and homogenous solution of melamine in deionized water was prepared in another beaker. Then, the aqueous solution of STA was added dropwise to the melamine solution with constant stirring at room temperature. After a while, the clear transparent solution of melamine turned cloudy white as a supramolecular salt was precipitated. The resultant solution was allowed to settle for approximately 24 h and the powder was subsequently dried at 70 °C in a hot air oven to complete dryness.

5.2.2. Preparation of the M-STA loaded PVA/PVAm mixed matrix membranes

The M-STA loaded mixed matrix PVA/PVAm membranes were prepared by dissolving 4 g of PVA powder into 96 g of water with continuous stirring at 80 °C for 6 h. The resultant solution was filtered to remove the residual undissolved particles. The resultant solution was kept overnight to remove any effervescence and air bubbles. Similarly, in order to prepare a 4 wt.% solution of PVAm, 40 g of a 10 wt.% solution of PVAm was diluted in 100 g of water in another beaker with constant stirring at room temperature. Both resultant solutions were blended in a 10:3 ratio (PVA/PVAm) and mixed with a magnetic stirrer. In a separate beaker, 0.16, 0.32 and 0.48 g of M-STA particles were dispersed in 20 mL water and sonicated using an ultrasonicator (Branson Sonifier 450) at 20% duty cycle for 30 min, then added dropwise to the above solution with constant stirring. Subsequently, the solution was stirred to ensure uniform mixing, then degassed and the desired quantity of the resultant solution was cast on a Petri dish and dried at 40 °C in an oven. Then dried membrane was then pulled off the petri dished and crosslinked with each film in a crosslinking bath containing 90/10/4/1 vol.% IPA/water/glutaraldehyde solution/hydrochloric acid (catalyst), respectively, at 50 °C for 1 h. The thickness of the membrane was determined to be 65 µm. The resulting membranes were designated as M4-MSTA (4% M-STA loading), M8-MSTA (8% M-STA loading), and M12-MSTA (12% M-STA loading). With loadings higher than 12% M-STA, the prepared membranes were mechanically unstable and brittle, so the maximum membrane loading used in subsequent tests was 12 wt.%. The reference PVA/PVAm crosslinked blend membranes were prepared by the same procedures without loading M-STA in the membrane, and is designated as M0-MSTA. Since all membranes are hydrophilic in nature therefore to avoid the atmospheric moisture absorption, they were stored at 35 °C in a drying oven for 12 hrs. prior to being used. . The membrane composition and abbreviation has shown in table 5.1

Table.5.1 Abbreviations of MSTA loading in PVA/PVAm blended membranes.

Abbreviation	Ratio in the membrane (g/g)		
	PVA (Polyvinyl alcohol)	PVAm(polyvinyl amine)	M-STA (g) (wt.%~ PVA)
M0-MSTA	100	30	0.0/0
M4-MSTA	100	30	0.16/4
M8-MSTA	100	30	0.32/8
M12-MSTA	100	30	0.48/12

Infrared spectroscopy

The melamine, STA and M-STA particles and resulting homogeneous M0-MSTA and M4-MSTA crosslinked blend membranes were analyzed by ATR-FTIR spectroscopy (ATR mode of FT-IR, Nicolet iS10, USA) over a wavenumber range of 400-4000 cm^{-1} for characterization of the membrane. All spectra were collected by aggregating 32 scans at a resolution of 2 wavenumbers.

X-ray diffraction studies

The X-ray diffractogram pattern of the modified STA (MSTA) particles, M0-MSTA, M4-MSTA, M8-MSTA and M12-MSTA membranes were recorded using an X-ray diffractometer (Rigaku Japan, D/Max 2500, $\lambda=1.5406$, Cu $K\alpha$ radiation at 45 kV and 15 mA). For identification of crystal phases in the dried membrane, samples with uniform thickness were mounted on the sample holder, and the patterns recorded in range of 0-60° at a rate of 5°/min.

Atomic force microscopy

Atomic force microscopy was used to visualize the surface of the sample using a tapping mode. (AFM: Bruker, Model-I con-PT-Plus). Membrane films were mounted on a glass slide and were analyzed at scan rate of 0.800 Hz with scan size of 30 μm . The nano scope analysis 1.5 was used to calculate the surface roughness of the membrane.

Scanning electron microscopy and SEM EDS

The surface morphology of the M0-MSTA and M8-MSTA membranes were examined by SEM, which produces an image of a sample by scanning it with a focused beam of electrons (Teskan, Czech, Vega II). The surface morphology of M-STA was also studied by SEM and the elemental composition of the modified STA was evaluated by scanning electron microscopy with energy dispersive X-ray spectroscopy (SEM-EDS). Specimens were prepared by gold coating to make film and particles conductive prior to analysis.

Contact angle measurements

The static contact angles of water on the M0-MSTA, M4-MSTA, M8-MSTA and M12-MSTA membranes were measured using the sessile droplet method and a contact angle analyzer (Phoenix 300, South Korea) equipped with a video camera. The contact angle of the water droplet was measured for each sample ten seconds after placing it onto the membrane. According to the shape of the droplet on the membrane, the corresponding contact angle was calculated with the precision and accuracy provided by the software supplied by the manufacturer.

5.2.3 Swelling degree measurements

The dried M0-MSTA, M4-MSTA, M8-MSTA and M12-MSTA membrane samples were weighed (m_d) and immersed in bottle containing 50 mL of different water/isopropanol mixtures for 48 h, at 60 °C. They were then removed from the solutions, wiped with dry tissue paper, and the weight of the swollen membrane was measured immediately (m_s).

The swelling degree was calculated using the following equation:

$$SD = \frac{m_s - m_d}{m_d} \quad (1)$$

Where, m_s and m_d are the mass of the swollen and dried membranes, respectively.

5.2.4 Pervaporation apparatus and measurements

The pervaporation experiments were carried out using the pervaporation apparatus designed in a previous study [15] is shown in Fig. 1b. The effective area of the membrane (19.64 cm²) was placed in a membrane cell consisting of two compartments. One compartment was connected to a feed tank, and other connected to the downstream side which was connected to a vacuum pump. The desired temperatures (40 to 70 °C) of feed tank was maintained by a thermostatically controlled water jacket. In order to avoid concentration polarization, the feed mixture was continuously circulated through the membrane cell using a pump (100 rpm). The downstream side pressure was maintained at less than 10 mbar using a vacuum pump (Edwards, RV8). The test membrane was equilibrated for 1 h before the actual measurements with the feed mixture. A cold liquefied

nitrogen trap was used to collect the permeated solution. The feed mixture composition was varied from 10 to 20 wt.% isopropyl alcohol in water. The composition of the permeated solution was analyzed using gas chromatography with a TCD detector (DS Sci. DS7200). The separation performance of prepared membranes was evaluated by measuring the flux (J) and the separation factor(α):

$$\text{Separation Factor } (\alpha) = \frac{P_W/PI}{F_W/FI} \quad (2)$$

Where PW , PI , FW , and FI are the weight fractions of water and IPA in the permeated solution and the feed solution, respectively. In addition, the flux was calculated by following equation:

$$\text{Flux } (J) = \frac{Q}{A.t} \quad (3)$$

Where Q is the weight of permeated solution collected in the cold trap, and the flux is calculated with respect to effective area (A) over a certain period of time, t .

5.3 Results and Discussion

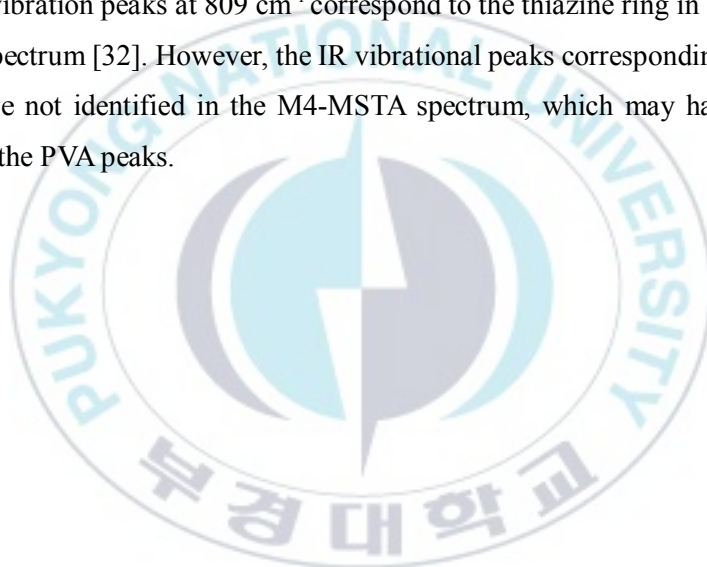
5.3.1 Membrane Characterization

FTIR spectroscopy

Fig. 5.1 a. shows the FTIR spectra of pure STA, melamine and the modified STA particles. The modified STA particles exhibit an infrared vibrational frequency band close to that of the parent STA and melamine (Fig. 2a). Vibrational frequencies in range of 700 to 1200 cm^{-1} were observed in the FTIR spectra of the M-STA particles and pure STA which indicates the presence of Keggin structure [30]. The structure was not altered due to modification of the STA with melamine. The peak intensity of the vibrational frequencies at 3120 and 3321 cm^{-1} corresponding to the primary amine bending vibration and those at 3416 and 3467 cm^{-1} corresponding to the amine stretching vibration in melamine were decreased in the spectra of the modified STA particles. Additional IR vibrational peaks at 1510 cm^{-1} and 1620 cm^{-1} (weak band) were observed in the M-STA particle spectra arising from NH_3^+ deformation of melamine after protonation [31]. Therefore, it can be concluded from the FTIR analysis that the modification of STA with melamine was successful due to

electrostatic attraction between the protonated melamine (cation) and the STA anion in water.

The FTIR spectra of the M0-MSTA and M4-MSTA membranes are shown in the Fig. 5.1 b. Characteristic IR stretching vibration peaks at 3500 to 3100 cm^{-1} were observed arising from the amine in PVAm and OH groups in the PVA. In the M0-MSTA spectrum, the peak at 1680 cm^{-1} corresponds to the C=N groups formed by the crosslinking of NH_2 with glutaraldehyde, and the peaks at 1085-1135 cm^{-1} arise from the acetal ring formed by the crosslinking reaction of the OH in PVA with glutaraldehyde. Upon blending of the M-STA with the membrane, two additional peaks at 906 cm^{-1} arise due to the Si-O band [31] and the bending vibration peaks at 809 cm^{-1} correspond to the thiazine ring in melamine in the M4-MSTA spectrum [32]. However, the IR vibrational peaks corresponding to the Keggin structure were not identified in the M4-MSTA spectrum, which may have been due to overlap with the PVA peaks.



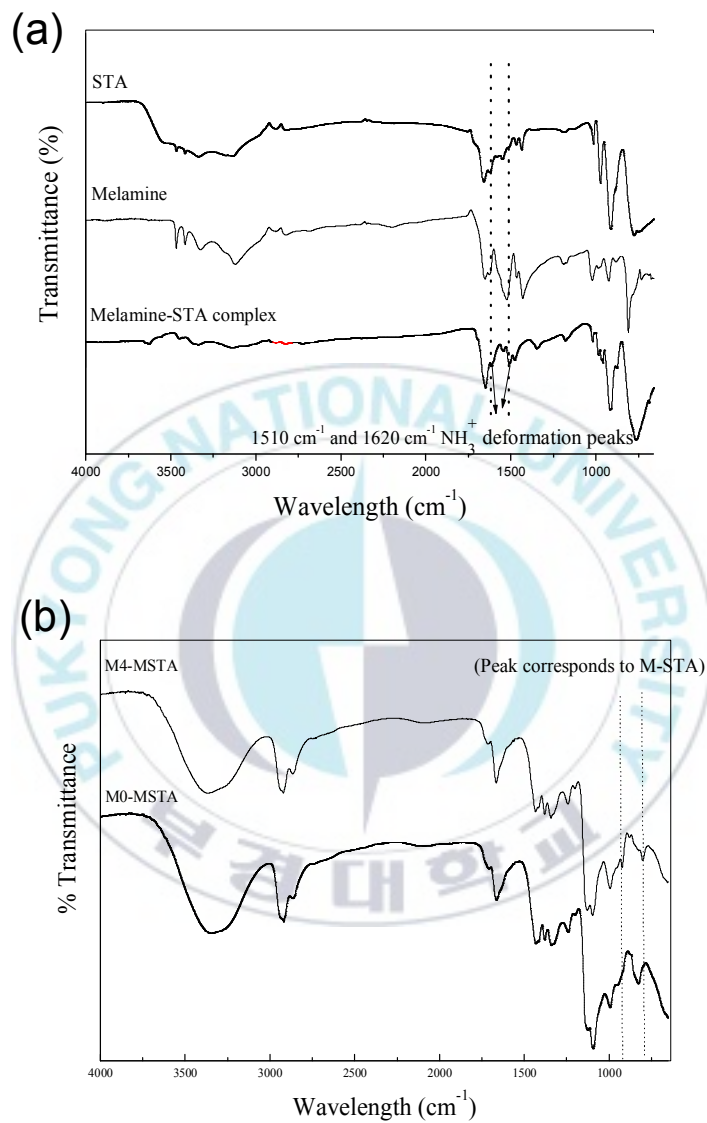
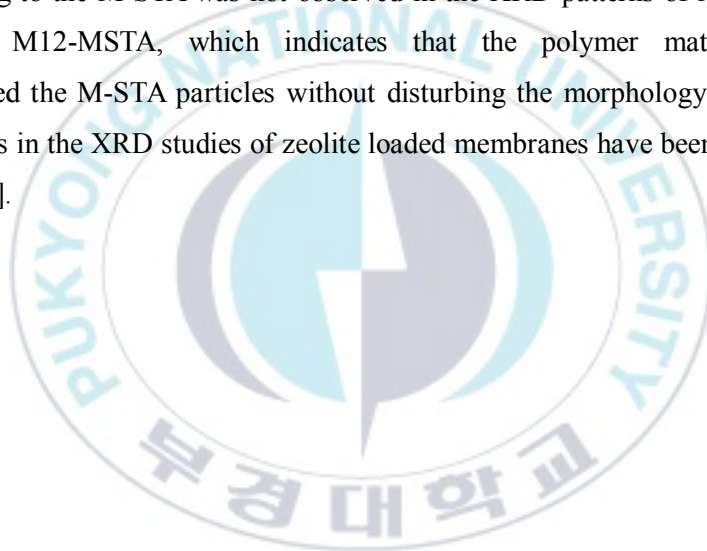


Figure 5.1 FTIR (ATR mode) spectra for (a) STA, melamine and melamine- STA complex crosslinked membrane and (b) M4-MSTA, M0-MSTA membranes.

X-ray diffraction studies

Fig. 5.2 shows the XRD patterns of the M-STA Particles, M0-MSTA and M-STA composite membranes. The crystalline nature of the M-STA particles was exhibited by the sharp diffraction peaks in the XRD pattern. An important factor that affects the molecular transport properties in pervaporation is the crystallinity of the polymers. It is well known that crystalline phase of the polymer can hinder the permeation of the components to be separated. In general, permeation flux obtained from a semi crystalline polymer membrane is lower than that of an amorphous membrane owing to space confinements for diffusion and more complicated diffusion paths around the crystallites [22]. The characteristic peak corresponding to the M-STA was not observed in the XRD patterns of M4-MSTA, M8-MSTA and M12-MSTA, which indicates that the polymer matrix completely accommodated the M-STA particles without disturbing the morphology of membranes. Similar trends in the XRD studies of zeolite loaded membranes have been reported in the literature [33].



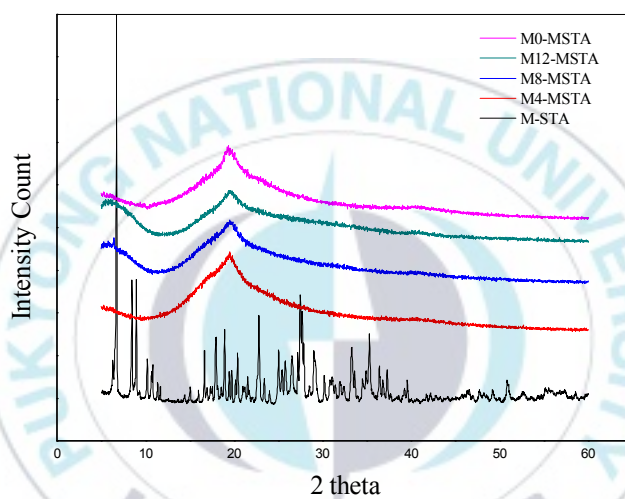


Figure 5.2 XRD patterns for M-STA particles and M0-MSTA, M4-MSTA, M8-MSTA and M12-MSTA membranes.

Morphology of the membrane and M-STA particles

AFM and SEM analysis of the membrane were used to investigate its morphology. Fig. 5.3 shows the SEM micrograph for the M-STA particles, M0-MSTA and M8-MSTA membranes. It can be seen that the particle sizes range from micron (less than 5μ) scale. At higher magnification of the M-STA particles, the elemental composition was measured by EDS analysis as shown in Fig.5.4 The signals correspond to electron excitation in the atoms by the X-ray and could be assigned to C, O, N and W (Atomic %= C-18.79%, O-43.7%, N-24.9%, W-12.62%). The presence of these elements in the spectrum confirms the modification of STA occurred through the H-bonding and electrostatic attraction to melamine. However, Si was not observed because has an excitation signal at same position as W, and is present in smaller amounts. These results supported the explanation given in the FTIR studies (section 3.1.1).

Fig. 5.3 also shows the SEM surface micrograph for the M0-MSTA and M8-MSTA membranes. A uniform distribution of M-STA particles in the membrane can be seen in the image, with the rough surface of the M0-MSTA due to intermolecular H-bonding between PVA and PVAm, was changed to smooth. Fig. 5.4 shows the 3D AFM image of the M0-MSTA and M-STA composite membranes. The root mean square roughness (R_q) values decreased with the addition of M-STA particles to the membrane, which indicates a homogeneous and uniform distribution of the particles in the membrane [24]. Declined in the surface roughness of membrane with M-STA loading, might have been due to the stronger crosslinking reaction rate and intra and intermolecular hydrogen bonding interaction between PVA and PVAm chains resulted in to the valley on the membrane surface during the membrane drying hence M0-MSTA membrane showed rough surface. However the M-STA particles consist of oxygen (bridging and terminal) and amine functional moiety from the melamine interact with both of polymers and acquire interstitial space between the polymers chain leads to lower the rate of crosslinking reaction rate and producing smooth surface without creating valley during membrane drying. It is well known that the surface roughness affects the membrane permeation properties since a rough surface provides more surface area to contact the feed solution and facilitate faster permeation of the mixture components.

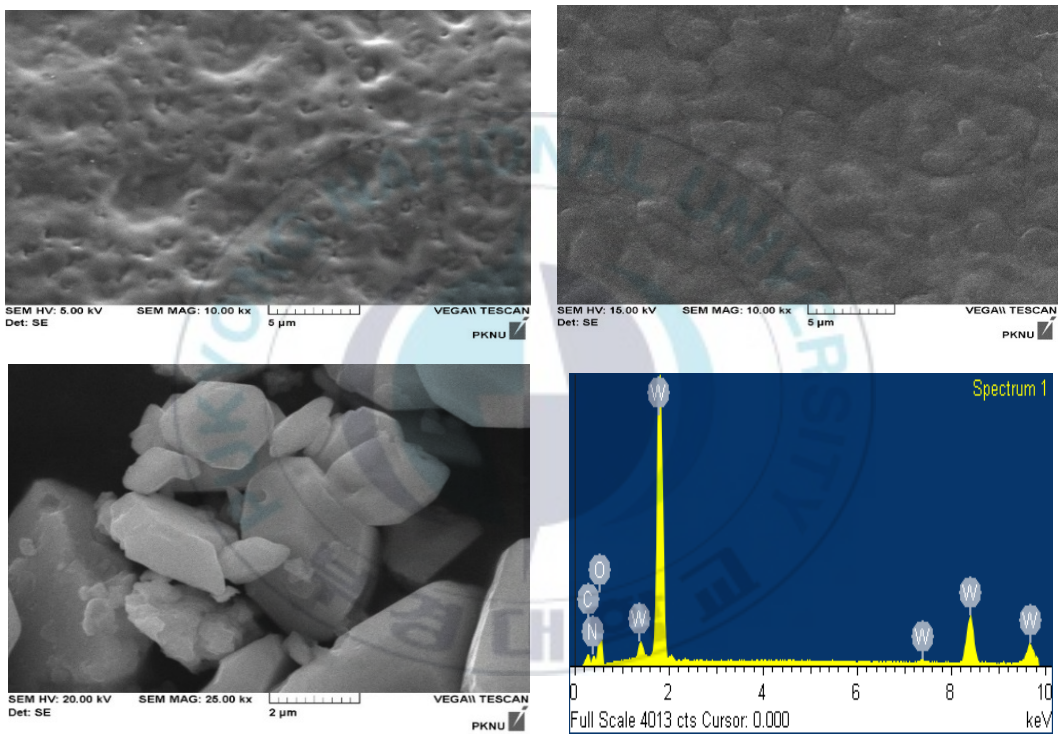


Figure 5.3 SEM surface micrographs for (a) M0-MSTA (b) M8-MSTA membranes and (c) M-STA particles and (d) SEM-EDS spectra for M-STA particles.

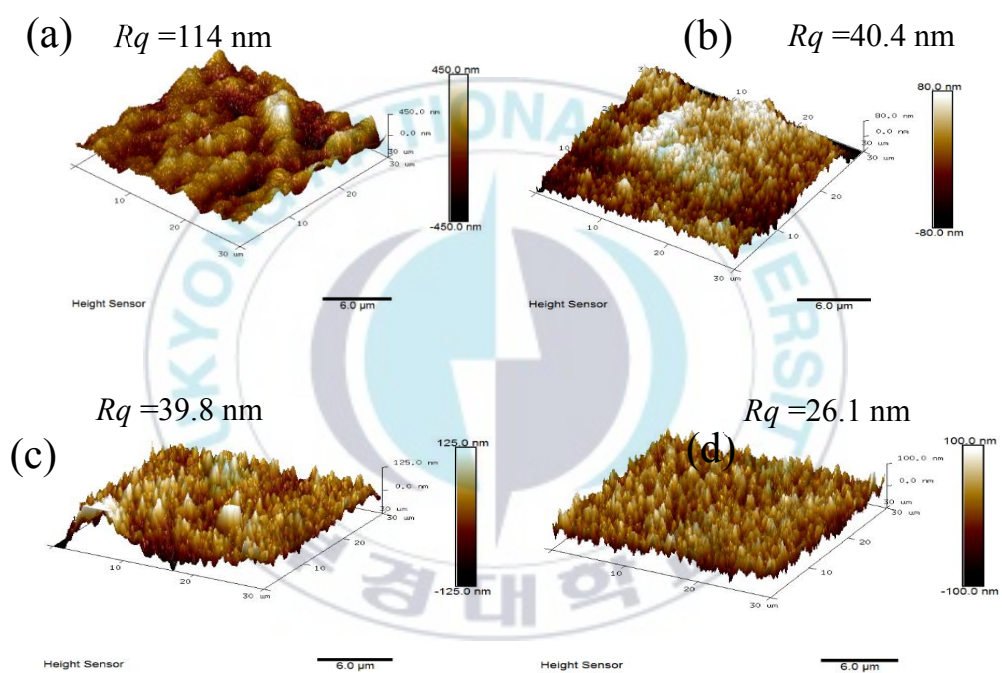


Figure 5.4 3D AFM images for (a) M0-MSTA, (b) M4-MSTA, (c) M8-MSTA (d) M12-MSTA membranes.

Swelling and contact angle measurements

It is well known that the free volume availability, degree of crosslinking and morphology of the membrane determines the extent of its swelling in certain liquids [34]. The degree of swelling, which reflects sorption capacity, is important to determine as it is one of the major mechanisms in the solution-diffusion model. [1] Fig.5.5 shows the degree of swelling as function of M-STA loading in the composite membrane. As can be seen in Fig. 5.5 the degree of swelling decreases with when content of M-STA in the membrane increases.

Fig 5.5 also shows the water contact angle on the membrane surface as function of M-STA loading. Generally, in PVA based membranes as the crosslinking proceeds, hydrophilicity is depressed due to the condensation of the OH groups on the surface. The contact angle measurement is a measure of the surface hydrophilicity of membrane. Interestingly, the water contact angle on membrane surface decreased with M-STA loading in the membrane. The simultaneous decrease in swelling and contact angle is an uncommon phenomenon. This is because the increase in hydrophilic functionality, due to the M-STA particles, increases the affinity for water and hence decreases the contact angle at membrane surface. On the other hand, the degree of swelling, which is a bulk property, decreases with M-STA loading, due to the reduced free volume of the membrane by M-STA occupation of the interstitial space between polymer chains [21].

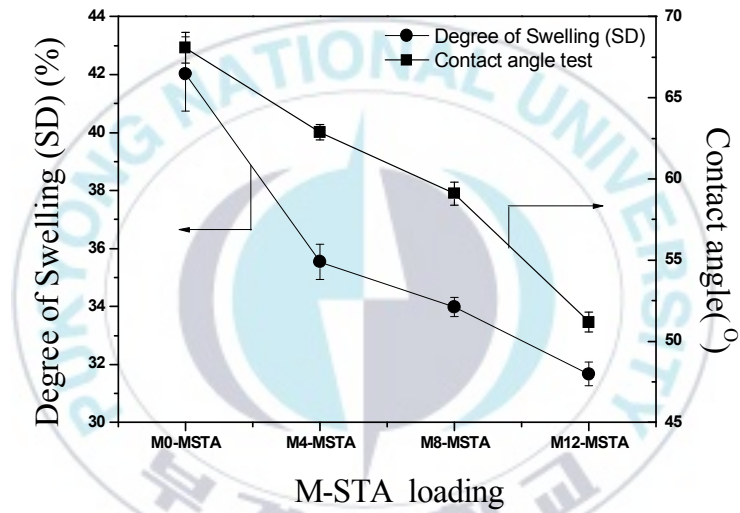


Figure 5.5 Effect of M-STA loading on contact angle of water and swelling degree of the membranes

5.4 Pervaporation

5.4.1 Effect of M-STA loading

The pervaporation flux and separation factor for the 20 wt.% IPA feed separation at 60 °C as a function of M-STA loading in the membranes is shown in Fig. 5.6 It can be clearly seen that the pervaporation flux slightly increased with M-STA loading up to 8 wt.% M-STA (M8-MSTA), and thereafter it marginally decreased. However, the overall fluxes for all M-STA composite membranes were higher than that of the unmodified membrane (M0-MSTA). In addition, the water separation factor was significantly enhanced with M-STA loading. To interpret the results more clearly, the individual concentrations for each of the mixture components in permeate as function of M-STA loading was plotted in Fig. 5.7 The figure clearly indicates that the enrichment of water in the permeate increased with M-STA loading, and, in contrast, the IPA concentration declined continuously with M-STA loading. The presence of the M-STA particles in the membrane matrix confers more hydrophilic character to the modified membrane. Since the M-STA particles consist of a number of hydrophilic moieties (terminal and bridging oxygen, NH₂) and facilitate the hydrophilic-hydrophilic interaction and cluster formation with water molecules [22-24]. It is well known that the transportation in pervaporation dehydration involves shuttling from one polar site to another [19]. However, due to the increase in hydrophilic character of the membrane, the permeation path of IPA was restricted and, therefore, the concentration of IPA declined in the permeate. The separation factor of the two-component mixture increased continuously with M-STA loading. The flux varied with M-STA loading, with the flux of 0.28 kg/m²h for the M0-MSTA increasing to 0.36 kg/m²h for M8-MSTA, then decreasing to 0.30 kg/m²h for M12-MSTA. This is likely caused by the M-STA particles occupying the interstitial space in polymer matrix and restricting the flux at higher loading. Additionally, the M-STA/polymer interaction through hydrogen bonding of M-STA functional groups with the hydroxyl and amino groups on the PVA and PVAm increased the rigidity of membrane and restricted diffusion of the permeating components. Therefore, a marginal decrease in flux above the 8 wt.% loading of M-STA was observed. Nevertheless, the membranes showed improved overall pervaporation performance

compared to the unmodified membrane. Therefore, it was confirmed that the modification of STA with melamine enhances the membrane performance by increasing the number of hydrophilic sites in the membranes. The M8-STA membrane showed the best pervaporation performance, hence for further tests, the M8-MSTA membrane was used.



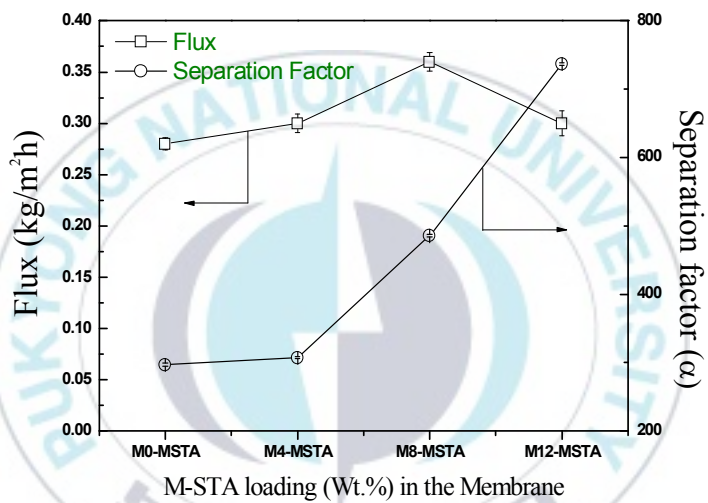


Figure 5.6 Effect of M-STA loading on the pervaporation flux and separation factor. Feed composition: 80% IPA, at 60 °C

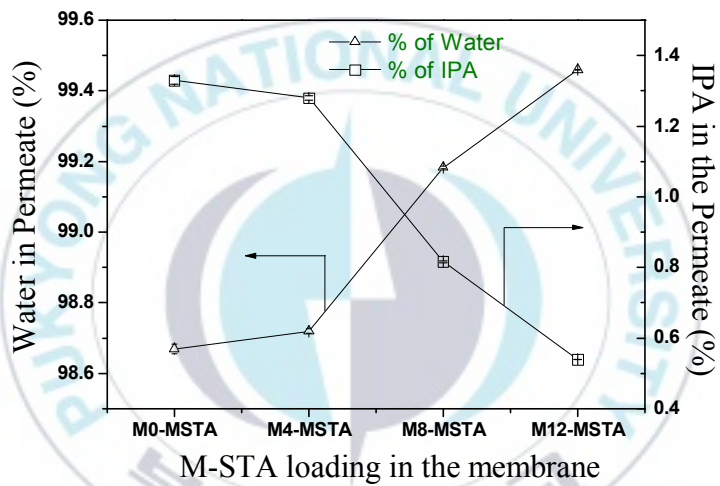


Figure 5.7 Effect of M-STA loading on the individual contents of water and IPA (%) in the permeate solution. Feed composition: 80% IPA, at 60 °C.

5.4.2 Effect of feed concentration

The effect of the feed composition on pervaporation performance of the membrane is an important to the pervaporation process [1]. The Fig. 5.8 and Fig. 5.9 shows the plot of concentrations of water/IPA (10/90 to 20/80 w/w) in the feed versus pervaporation flux and separation factor at 60 °C using M0-MSTA and M8-MSTA membrane. It can be seen that the flux and separation factor were strongly influenced by the feed composition. For instance, the flux value for 90/10 (IPA/water) composition was 0.032 and 0.033 kg/m²h, which was increased 10 fold to 0.28 and 0.36 kg/m²h for 80/20 (IPA/water) for the M0-MSTA and M8-MSTA membranes, respectively. On the other hand, the separation factor declined from 4278 to 297.1 for M0-MSTA and from 6425 to 485.6 for the M8-MSTA membrane for same feed composition at 60 °C. From Fig. 9 and 10, it is clear that the MSTA composite membrane showed a higher flux and separation factor than the blend membrane. Additionally, the differences in flux value for the M0-MSTA and M8-MSTA membranes were more significant for the feed with higher water content. Moreover, in the 10 wt.% water content feed, the separation factor obtained from the M8-MSTA membrane was higher than the M0-MSTA membrane. Therefore, it was confirmed that the presence MSTA particles in the membrane significantly increases the hydrophilicity and hence affinity for water of the membrane. This result is complementary to the explanation given in the section 5.3.2.1. The increase in the permeation flux and decreased separation factor with higher water content in the feed solution is common for hydrophilic membranes [10, 15, 23-25]. Additionally, the upstream side of membrane swells greatly due to the plasticization effect of the water, which creates indiscriminate channels. These channels allow the transportation of both molecules in the feed mixture through the membrane resulting in a decrease in separation factor. Overall, the MSTA composite membrane exhibited improved pervaporation performance over the azeotropic feed composition range.

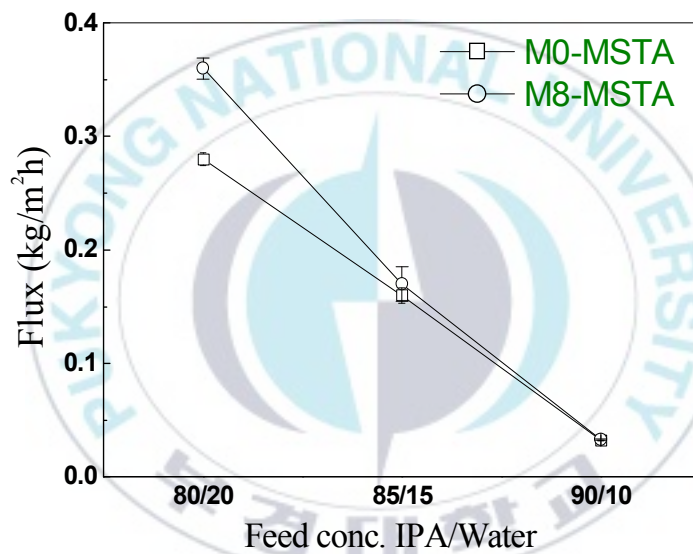


Figure 5.8 Effect feed composition on the pervaporation flux, M0-MSTA and M8-MSTA membranes, at 60 °C.

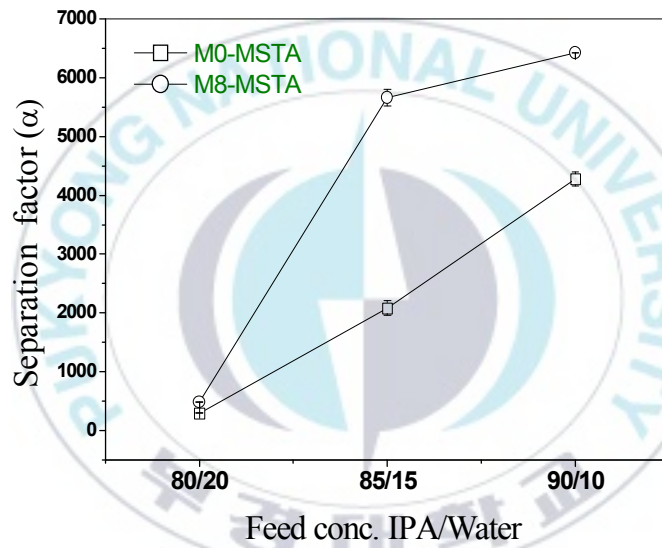


Figure 5.9 Effect feed composition on the separation factor, M0-MSTA and M8-MSTA membranes, at 60 °C.

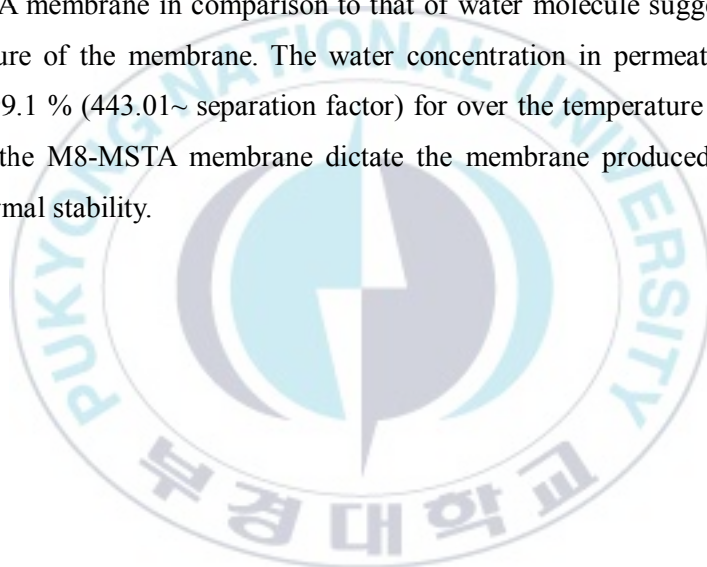
5.4.3 Effect of operation temperature on the membrane performance in pervaporation.

It is well known that, the pervaporation process is sensitive to the operating temperature. It has been stated that, operating temperature magnify permeation by two aspect, one is driving force which is a thermodynamic property and second is intrinsic membrane permeability (diffusion) which is kinetic property. Fig. 5.10 shows the effect of temperature on the pervaporation performance of membrane (M0-MSTA) at feed content 80 wt. % of IPA. Fig. 5.10 infer that as the feed temperature increases from 40 °C to 70 °C, the flux increases from 0.29 to 0.47 kg/m²h, while the separation factor decreases sharply up to 60 °C (2171 ~ 485.6) then with the slower rate (from 485.6 to 443.01). Enhancement in the flux value attributed to the increase in driving force as well as free volume. As operating temperature increased on feed side the saturated vapor pressure of feed component increases and either side (permeate side) of membrane has a vacuum so may not be greatly affected which result in the enthalpy for phase transition of components in membrane achieved with the faster rate. Additionally an increase in temperature leads to increase the energy of permeants and also the frequency and amplitude of polymer chain jumping (thermal agitation), and in turn, randomly creates the transition gap between polymeric chains, otherwise known as the free volume. Due to this, diffusion of permeants occurs rapidly through these this random increase in free volume, resulting in an increase in flux and decreased in the separation factor was observed [4, 7, 23, and 24]. Fig.5.11 reflects the individual fluxes of water and IPA as function of temperature. It has seen from the figure that, the effect of temperature on the water flux was more significant in comparison to IPA flux, this is due to the presence of STA in the membrane, which can form the protonated cluster at higher temperatures [22]. Moreover, the molecular kinetic diameter of the IPA (0.450) is higher than that of the water (0.296) owing to diffusion of water molecule take place with faster rate over the isopropanol. Therefore the separation factor declined at slower rate when the temperature was increased from the 60 °C to 70 °C. The temperature dependence of the permeation flux can be express by an Arrhenius-type equation.

$$\text{Flux } (J_i) = A_p \cdot e^{-E_p/RT} \quad (4)$$

Where, J_i ($\text{kg}/\text{m}^2\text{h}$) is the flux of component i , T (K) is the absolute temperature, R (J/mol K) is the universal gas constant and A_p ($\text{kg}/\text{m}^2\text{h}$) and E_p (kJ/mol), are the pre-exponential factor and the overall activation energy for permeation, respectively.

A logarithmic Arrhenius plot of flux against temperature was plotted for each of the components of the mixture, as shown in Figure 5.12. From the slope of the resulting plot the activation energy for the permeation of both IPA and water can be calculated, and it can be seen that the activation energy for the permeation of IPA (64.31 kJ/mol) is fivefold higher than that of water (13.65 kJ/mol). From these results, we can conclude that the adsorption and diffusive transport of IPA molecule required higher energy and hindered by the M8-MSTA membrane in comparison to that of water molecule suggesting the water selective nature of the membrane. The water concentration in permeate achieved was higher than 99.1 % (443.01~ separation factor) for over the temperature range (40 to 70 °C) through the M8-MSTA membrane dictate the membrane produced in this has an excellent thermal stability.



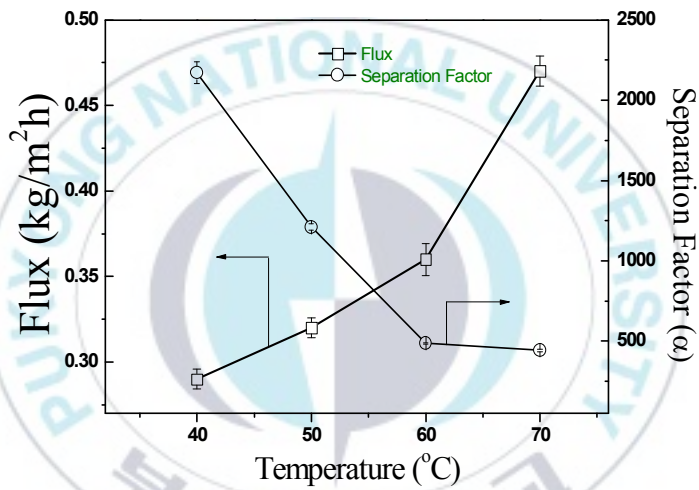


Figure 5.10 Effect of temperature on pervaporation flux and separation factor, M8-MSTA membranes, Feed composition: 80% IPA.

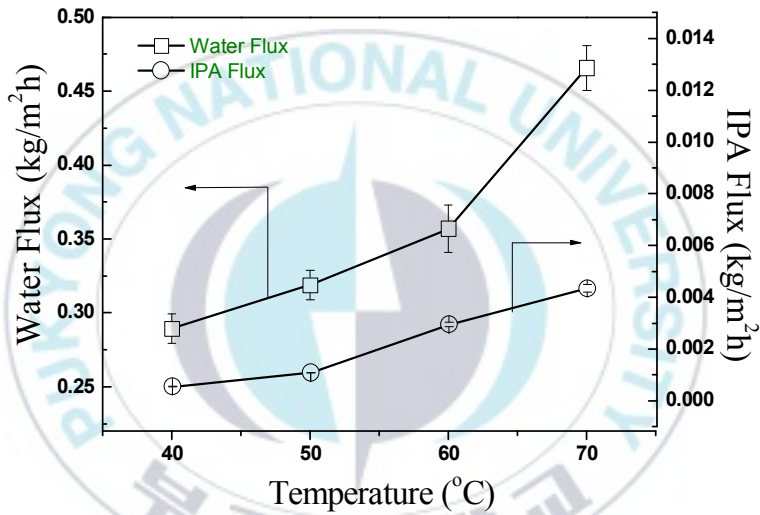


Figure 5.11 Individual fluxes of water and IPA as function of temperature, M8-MSTA membranes, Feed composition: 80% IPA.

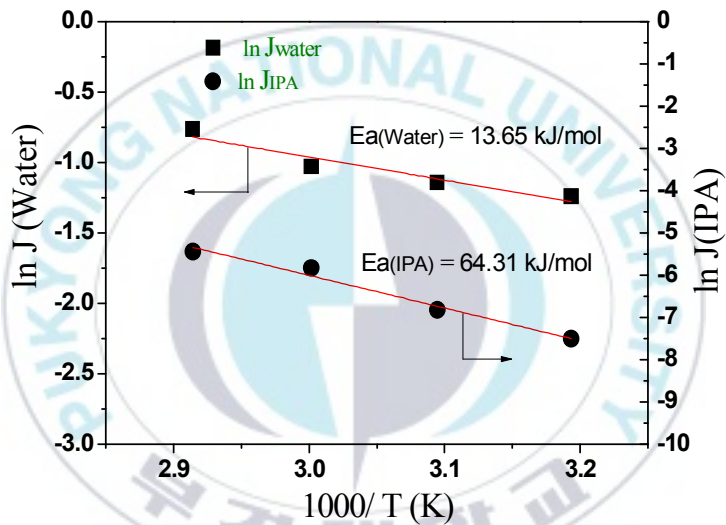


Figure 5.12 Variation of $\ln J_{\text{Water}}$ and $\ln J_{\text{IPA}}$ with temperature for M8-MSTA membrane, Feed: 80% IPA solution.

5.4.4 Membrane durability study

Due to the leaching of unmodified STA from the membrane, previous membranes have suffered from poor mechanical stability [26]. Additionally, the polymeric material has intrinsic characteristics, such as relaxation, which can result in the unstable pervaporation performance [35]. Hence, in this study long term stability of the membrane (M8-MSTA) was tested by long periods of pervaporation operation with the feed liquid (86/14, IPA/water) continually circulated through the membrane cell at 30 °C (the temperature was kept low to avoid concentration polarization since test performed at low circulation speed (50 rpm) for 10 d. Testing of the pervaporation performance indicators was carried out each day. Fig. 5.13 shows a plot of the pervaporation flux and water content in permeate as function of time. It can be seen that, over the experimental range, the water content in the permeate was always higher than 99.0% and the flux obtained was around 0.12 kg/m²h, only marginally deviating with time. Such deviation can be explained by conditioning [36] and relaxation effects [37], which are commonly observed in PVA membranes. It can be concluded that the modification of STA with melamine prevents the leaching of STA particles from the membrane. Therefore, the membrane produced in this study showed a constant and reproducible pervaporation performance throughout the lengthy operation period used in this study.

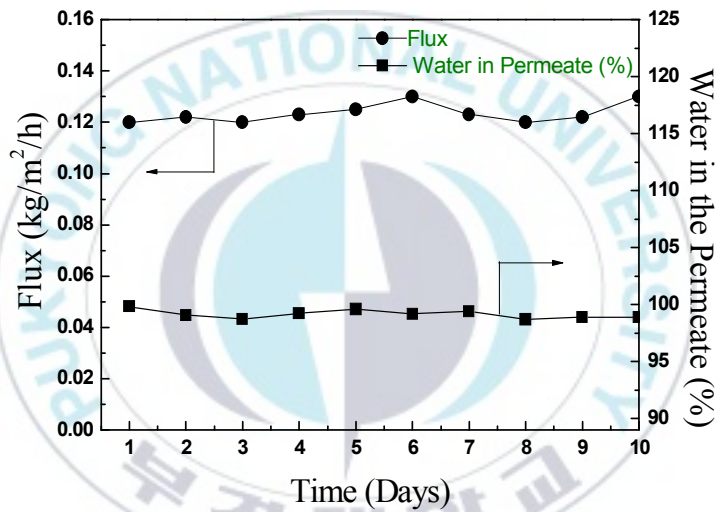


Figure 5.13 Plot of time against flux and water in the permeate (%) for durability of membrane (M8-MSTA) at Feed composition: 86/14 IPA/water (w/w), at 30 °C.

5.5 Conclusion.

For separation of a water-IPA mixture, M-STA loaded membranes consisting of PVA/PVAm crosslinked with glutaraldehyde were developed. From the FTIR, SEM and EDS studies of the M-STA particles, it was concluded that STA particle was successfully modified with melamine. The SEM and AFM studies showed uniform distribution of the particles within the membranes. It was observed from the contact angle measurements that the surface hydrophilicity of the membrane increased due to incorporation of modified M-STA particles. The flux varied with M-STA loading, with the flux of 0.28 kg/m²h for the M0-MSTA increasing to 0.36 kg/m²h for M8-MSTA, then decreasing to 0.30 kg/m²h for M12-MSTA was observed. The overall flux obtained for all M-STA composite membranes was higher than that of the unmodified membrane (M0-MSTA) observed. The water separation factor was significantly enhanced with M-STA loading, from 297.1 for M0-MSTA to 736.7 for M12-MSTA at 80% IPA, at 60 °C were observed. The effect of temperature on permeation of water and IPA were investigated. With increased of temperature from the 30 to 70 °C at 80 wt. % IPA composition, the water flux influenced more significantly in comparison to IPA flux that was attributed to the presence of M-STA particles in the membrane. Permeation flux for water and IPA followed the Arrhenius trends over the investigated range of temperature. The activation energy for the permeation of IPA (64.31 kJ/mol) was fivefold higher than that of water (13.65 kJ/mol) observed. From the stability data it was concluded that the modification of STA with melamine prevented the leaching of STA from the membrane during extended periods of pervaporation operation.

Reference

- [1] J.G. Wiljmans, R.W. Baker, The solution diffusion model: a review, *J. Membr. Sci.* 107 (1995), 1-21
- [2] P.D. Chapman, T. Oliveira, A.G. Livingston, K. Li., *J.Membr.Sci.*318 (2008) 5-37.
- [3] Y. Han, K. Wang, J. Lai, Y. Liu, *J. Membr.Sci.*463 (2014) 17-23.
- [4] M. Hosseini, E. Ameri, *Vacuum* 141 (2017) 288-295
- [5] L.Lu, F. Peng, Z. Jiang, J. Wang, *J. Appl. Polym, Sci.* 101 (2006)167-173.
- [6] I. Blume, J.G. Wiljmans, R.W. Baker, *J.Membr.Sci.*49 (1990) 253-286.
- [7] M. Olukman, O. Sanli, E.K. Solak, *Vacuum*, 120 (2015) 107-115
- [8] N. Rodriguez, M. Kroon, *J. Chem. Thermodynamics.* 85 (2015) 216-221.
- [9] V. Hoof, L. Abeele, A. Buekenhoudt, C. Dotremont, R. Leysen, *Sep. Purif. Techno.*37 (2004) 33-49
- [10] A. Malekpour, B. Mostajeran, G.A. Koohmareh, *Chem. Engi. Proc. Intensi.* 118 (2017) 47-53.
- [11] B. Baheri, M. Shahverdi, M. Rezakazemi, E. Motaee, T. Mohammadi, Performance of PVA/NaA mixed matrix membrane for removal of water from ethylene glycol solutions by pervaporation, *Chem. Eng. Commun.* 202 (2015) 316–321.
- [12] T. Narkkun, W. Jenwiriyakul, S. Amnuaypanich, *J. Membr. Sci.* 528 (2017) 284-295.
- [13] A.M. Sajjan, B.K. Jeevan Kumar, A.A. Kittur, M.Y. Kariduraganavar, *J. Ind. Eng. Chem.* 19 (2013) 427-437.
- [14] F. Kursun, N. Isiklan, *J. Ind. Eng. Chem.* 41 (2016) 91-104.
- [15] S. Chaudhari, Y. Kwon, M. Moon, and M. Y. Shon, *BKCS* 36-10(2015), 2534-2541
- [16] A. Ariyaskul, R.Y.M. Huang, P.L. Douglas, R. Pal, X. Feng, P. Chen, L. Liu, *J. Membr. Sci* 280 (2006) 815-823.
- [17] R.S. Veerapur, K.B. Gudasi, T.M. Aminabhavi, 304 (2007) 102-111.
- [18] R. Pelton, *Polyvinyl amine: Langmuir*, 30 (2014) 15373-15382.
- [19] E.J. Flynn, D.A. Keane, P.M. Tabari, M.A. Morris, 118 (2013) 73-80.
- [20] P. Das, S.K. Ray, *J. Membr. Sci* 507 (2016) 81-89.
- [21] S. Hu, Y. Zhang, D. Lawless, X. Feng, *J. Membr. Sci.* 417 (2012), 34-44.

- [22] S.B. Teli, G.S. Gokavi, M. Sairam, T.M. Aminabhavi, *Sep. Purif. Techno.* 54 (2007) 178-186.
- [23] V.T. Magalad, G.S. Gokavi, K.V.S.N. Raju, T.M. Aminabhavi, *J. Membr. Sci.* 354 (2010), 150-161.
- [24] V.T. Magalad, G.S. Gokavi, C. Rangnathaiah, M.H. Burshe, C. Han, D. D. Dionysiou, M. N. Nadagouda T. M. Aminabhavi, *J. Membr. Sci.* 430 (2013), 321-329.
- [25] J. Chen, J. Zheng, Q. Liu, H. Guo, W. Weng, S. Li, *J. Membr. Sci.* 429 (2013), 206-213.
- [26] S.G. Adoor, S.D. Bhat, D.D. Dionysiou, M.N. Nadagouda, T.M. Aminabhavi, *RSC adv.* 4 (2014) 52571-52582.
- [27] S. Shanmugam, B. Viswanathan, T.K. Varadarajan, *J. Membr. Sci.* 275 (2006), 105-109.
- [28] B. Roy, P. Bairi, A.K. Nandi, *RSC adv.* 4 (2014) 1708-1734.
- [29] J. Shen, Q. Cai, Y. Jiang, H. Zhang, *RSC Chem. Commun.* 46 (2010) 6786-6788.
- [30] A.H. Jadhav, H. Kim, *RSC Adv.* 3 (2013) 5131-5140.
- [31] M. Llusar, G. Monros, Cecile Roux, J. Pozzo, C. Sanchez, *J. Mater. Chem.* 13 (2003) 2505-2514.
- [32] D. Merline, S. Vukusic, A. Abdala, *Polym. J.* 45 (2013) 413-419.
- [33] S.S. Kulkarni, S.M. Tambe, A.A. Kittur, M.Y. Kariduraganavar, *J. Membr. Sci.* 285 (2006), 420-431.
- [34] P.J. Flory, J. Rehner, *J. Chem. Phys.* 11 (1943) 521.
- [35] Q. Zhao, J. Qian, Q. An, Q. Yang, P. Zhang, *J. Membr. Sci.* 320(2008), 8-12.
- [36] Z. Huang, Y. Shi, R. Wen, Y. Guo, J. Su, T. Matsuura, *Sep.Puri.Tech.* 51 (2) (2006)126-136.
- [37] A.S.E. Otsuka, *Prog. Coll. Poly Sci.* 136 (2) (2009)121-126.

6. Pervaporation separation of a water/acetic acid mixture using in situ synthesized silver nanoparticles in PVA/PAA membrane

6.1 Introduction

Due to the global consumption demand, the worldwide production of the chemical, pharmaceutical, food, and other industries has been increasing. Making these industrial production processes more efficient, economical, and sustainable has always been challenging. Membrane processes have come into the picture as an additional category of separation processes besides the well-established thermal processes, being advantageous due to their high selectivity, low energy consumption, mild separation conditions, etc. Among the membrane separation processes, pervaporation has received much attention due to its application in the separation of azeotropes [1]. It involves partial vaporization of a liquid-liquid mixture through a selective membrane, and owes its name to the simultaneous processes of permselective transport and evaporative phase change [2].

Pervaporation has been used for the dehydration of organic substances, separation of organic-organic mixtures, and removal of water from the organic phase [1–5]. Thus, the selection of a potential membrane material depends on its application, e.g., hydrophilic materials are used for dehydration and hydrophobic ones for dewatering of the organic phase. Acetic acid is an important chemical reagent and industrial chemical, used in the production of various synthetic fibers and other polymers such as polyethylene terephthalate, cellulose acetate, and polyvinyl acetate. The global demand for acetic acid has been estimated at around 6.5 million metric tons per year, with approximately 1.5 Mt/year produced by recycling. Pervaporation can be an effective alternative to distillation in the recycling processes, helping obtain more concentrated acetic acid, and has been perceived as a clean process [6, 7].

Membranes play a key part in the pervaporation process. Several methods have been used to explore pervaporation membranes in relation to the separation of desired components, namely blending, cross-linking, and grafting [8–10]. Poly (vinyl alcohol), or PVA, is a semi-crystalline material [11] used as a base chemical and frequently employed for the preparation of hydrophilic membranes. This material is inherently hydrophilic due to the abundant hydroxyl groups in its polymer chain and is a suitable candidate for the preparation of membranes, owing to its excellent chemical stability and film forming ability [12–14]. Similarly to PVA, poly (acrylic acid), or PAA, is also an anionic hydrophilic biocompatible polymer, due to the presence of carboxyl groups. Cross-linked PVA/PAA provides a classical system for the fabrication of dense pervaporation membranes. This material has been frequently employed in the pervaporation separation of multi-component mixtures, e.g., acetic acid/fused oil [15–17], since membranes produced from this polymer showed promising selectivity and stability.

Pervaporation membranes always feature a trade-off between hurdle, flux, and selectivity, since it is impossible to optimize all terms simultaneously. Thus, numerous membrane types have been prepared to tackle the process, namely composite and mixed matrix membranes. Mixed matrix membranes contain porous fillers, e.g., hydrophilic metal oxide nanoparticles embedded in the polymer (zeolites, TiO_2 , Fe_3O_4 , and SiO_2) [6, 18–21]. These fillers are known to exhibit hydrophilic and molecular sieving properties, imparting mechanical strength to the membrane. Silver nanoparticles have received much attention due to their diverse applications in optics, solar cells, catalysts, and antimicrobial agents, enabled by their unique properties [22–26]. Metal nanoparticles incorporated in the polymers constitute new hybrid materials offering numerous applications. Polymers are considered good host materials for metal nano colloids, providing a protective layer; at the same time, the embedded nanomaterials impart new properties to the polymer. PAA molecules offer abundant carboxylic groups on both sides of the polymer chain, which can form complexes with metal atoms by charge transfer [27]. On the other hand, PVA molecules have numerous hydroxyl groups, which can reduce the metal ion and form stabilized metal nanoparticles, preventing their agglomeration [28]. The hydroxyl group can coordinate the Ag ion using its lone pairs and successfully reduce it to metallic Ag.

Metal nanoparticles embedded in the organic pervaporation membrane have been reported to provide selective transport and impart hydrophilicity [5, 29].

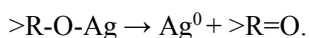
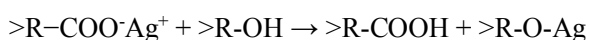
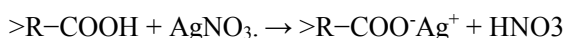
This study focuses on the in situ preparation and stabilization of dispersed silver nanoparticles in the PVA/PAA membrane using its functional groups without addition of any reducing agent. This study does not dwell on the highest possible membrane efficacy, but rather concentrates on its successful preparation and assessment of the silver nanoparticle capability to enhance the pervaporation transport. Thus, we have chosen a PVA/PAA ratio for a less selective membrane instead of a more selective one by using a larger amount of PVA during the membrane preparation. Because in more selective crosslinking composition where greater than 99% of water in the permeate due to that, it is difficult to find out the effect of Ag nanoparticle since small change in the feed or flow rate affect the results but that can be random and regardless of particle. The membranes obtained were characterized by UV spectroscopy, IR spectroscopy, X-ray diffraction (XRD), scanning electron microscopy (SEM), energy-dispersive X-ray spectroscopy (EDS), contact angle measurements, membrane absorption and swelling degree measurements, and were used for the separation of a water/acetic acid mixture by pervaporation.

6.2 Experimental

6.2.1 Membrane preparation.

PVA powder (7 g) was dissolved in water under continuous stirring at 75 °C for 6 h. The resulting solution was filtered to remove the residual undissolved particles. A 2.0 g aliquot of the 35 wt. % PAA solution was diluted to 90 mL with water under constant stirring at 50 °C. Subsequently, aqueous AgNO₃ (0.0525 g in 10 mL) was added to the PAA solution under continuous stirring. The color of the reaction mixture changed to dark yellow, which is characteristic of complex formation between Ag⁺ and COO⁻ groups of PAA. Later on, both PVA and PAA solutions were mixed together and stirred for ca. 48 h. The final solution color was dark brown, characteristic of silver nanoparticle formation. The obtained homogenous solution was filtered and sonicated for about 30 min to disperse the Ag nanoparticles. The resulting dispersion was stored overnight to remove effervescent air bubbles, cast into a Petri dish, and dried at 40 °C. Subsequently, the membrane was separated from the Petri dish and cured in an oven at 140 °C for 2 h. The final concentration of silver with respect to PVA was 0.75 wt. %. The amount of silver was varied (0, 1.5, and 2.25 wt. %), and the corresponding membranes were designated as MAg0, MAg0.75, MAg1.5, and MAg2.25.

Upon dropwise addition of AgNO₃ with constant stirring to the Poly (acrylic acid) at 50^o, the COOH groups in the PAA molecules dispersed the Ag⁺ cation in the polymer matrix. In the second step of PAA dispersed Ag⁺ cation solution blended with the Poly (vinyl alcohol). Under the magnetic stirring at room temperature, causes the microstructure of refreshed reactive PVA molecules, with OH-groups free from the H-bonding. Due to the internal friction between PVA layers in relative motion refines the PVA molecules. So the magnetic stirring with PVA of Ag⁺ dispersed PAA provide the driving force to drive the Ag⁺→Ag⁰ reaction. [30] A postulated reaction as shown is shown below.



Here >R-OH and >R-COOH represent the PVA and PAA respectively.

Infrared spectroscopy

The observed functional changes due to incorporation of silver nanoparticles into membranes were characterized by ATR-FTIR spectroscopy (ATR mode of FTIR, Nicolet iS10, USA) in the range of 400–4000 cm^{-1} . Averaging over 32 scans was carried out for each sample spectrum.

Contact angle measurements

The contact angles of water on the membrane were measured using the sessile droplet method with the help of a contact angle analyzer (Phoenix 300, South Korea) equipped with a video camera. The contact angle of the water droplet was measured for each sample ten seconds after placing it onto the membrane. According to the shape of the droplet on the membrane, the corresponding contact angle was calculated with the precision and accuracy provided by the supplied software.

UV spectrophotometry

Proof of successful silver nanoparticle formation was provided by measuring the membrane absorbance in the 200–400 nm range on a Shimadzu UV (Jasco V-670) spectrophotometer with a resolution of 0.2 nm.

SEM and SEM-EDS characterization

The surface morphology and elemental composition of PVA/PAA and silver composite membranes were investigated by SEM and SEM-EDS analysis, whereby sample imaging was carried out by scanning with a focused electron beam [Teskan, Czech, Vega II, and LSU]. Specimens for analysis

6.2.2 Membrane absorption study

A membrane absorption study was performed. The weight of all membranes was recorded prior to immersing them in water. At specific time intervals, the membranes were removed, wiped, immediately weighed, and re-immersed in water until equilibrium absorption was achieved. The % increase in the membrane mass compared was calculated using the following equation.

$$\% \text{Increase} = \frac{\text{Mass gained at time } t}{\text{Initial mass}} \times 100 \quad (1)$$

6.2.3 Swelling degree measurements

The dried membrane samples were immersed in water/acetic acid mixtures of different compositions for 24 h at 40 °C. After achieving equilibrium absorption, the samples were removed from the solutions, wiped with dry tissue paper, and the weights of the swelled membranes were measured immediately. The swelled membranes were then dried to constant weight under vacuum at 25 °C. The swelling degree was calculated using the following equation:

$$SD = \frac{m_s - m_d}{m_d} \quad (2)$$

Where m_s and m_d are the masses of the swelled and dried membranes, respectively.

6.2.4 Pervaporation apparatus and measurements

The pervaporation apparatus designed for this study has described in the chapter 3, figure 3.3.8. The membranes were placed in a membrane cell and fixed; the membrane effective area being equal to 19.64 cm². The membrane cell consisted of two parts – one connected to a feed tank, and other connected to the downstream side (vacuum pump). The feed tank was maintained at the intended operating temperature (40 °C) in a water bath, and the feed mixture was continuously circulated (using a pump at 100 rpm) through the membrane cell to avoid concentration polarization. The downstream pressure was maintained at < 10 mbar using a vacuum pump. The permeated vapor was collected, condensed in a glass tube of the liquid nitrogen trap, and then weighed. The feed mixture composition used in the pervaporation experiment was 80 wt. % of acetic acid in water. The respective components in the feed and permeated solution were analyzed by gas chromatography (TCD detector).

The separation performance of the prepared membrane was evaluated using following equation:

$$\text{Separation Factor } (\alpha) = \frac{P_W/P_A}{F_W/F_A} \quad (3)$$

Where P_W , P_A , F_W , and F_A are the weight fractions of water and acetic acid in the permeated and the feed solutions, respectively. In addition, the flux was calculated using the following equation:

$$\text{Flux } (J) = \frac{Q}{A \times t} \quad (4)$$

Where Q is the weight of the permeated solution collected in the cold trap and A is the effective area at time t .

6.3 Results and Discussion

6.3.1 Characterization.

FTIR (ATR mode) spectral analysis

FTIR spectra of virgin PVA/PAA and various silver nanoparticle composite membranes are shown in Fig. 6.1, with all membranes showing characteristic peaks at 1700 cm^{-1} and around $1000\text{--}1300 \text{ cm}^{-1}$, corresponding to C=O and C–O stretches, attributable to the formation of ester groups after PVA/PAA crosslinking [29, 31-33]. The intensity of the peak due to OH stretching around 3300 cm^{-1} remarkably increased in the case of the hybrid membrane, compared to virgin PVA/PAA. The intensity of the peak at 810 cm^{-1} , attributable to out-of-plane PAA OH vibration, marginally increased, and peak broadening due to silver nanoparticle addition was observed. This may be attributable to the interaction of silver nanoparticles with the PVA OH groups and the PAA COOH groups and the formation of hydrogen bonds [29, 34-35]. The increased intensity and broadening of peaks at 1390 and 1260 cm^{-1} was assigned to the symmetric and anti-symmetric stretches of the COO^- groups, revealing that PAA molecules were adsorbed on the surface of silver nanoparticles through the bidentate band [36]. Thus, the FTIR results imply that membrane

hydrophilicity and rigidity was increased by the addition of silver nanoparticles to the PVA/PAA polymer matrix, since it shows hydrophilic character. [29].

Water contact angle measurements

Water contact angles were measured to evaluate the hydrophilicity of the membranes. Figure 6.2 shows a plot of the average contact angle as a function of silver nanoparticle content in the PVA/PAA membranes. A decreased contact angle value implies increased membrane hydrophilicity due to the presence of silver nanoparticles in the membrane.



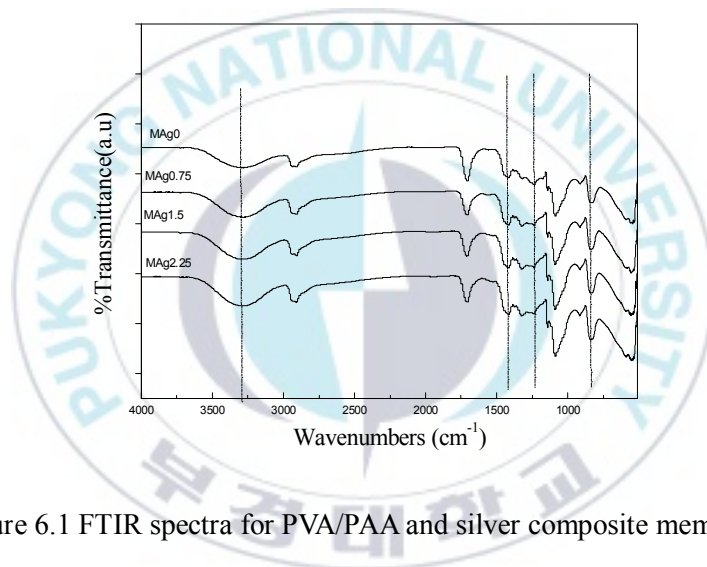


Figure 6.1 FTIR spectra for PVA/PAA and silver composite membranes

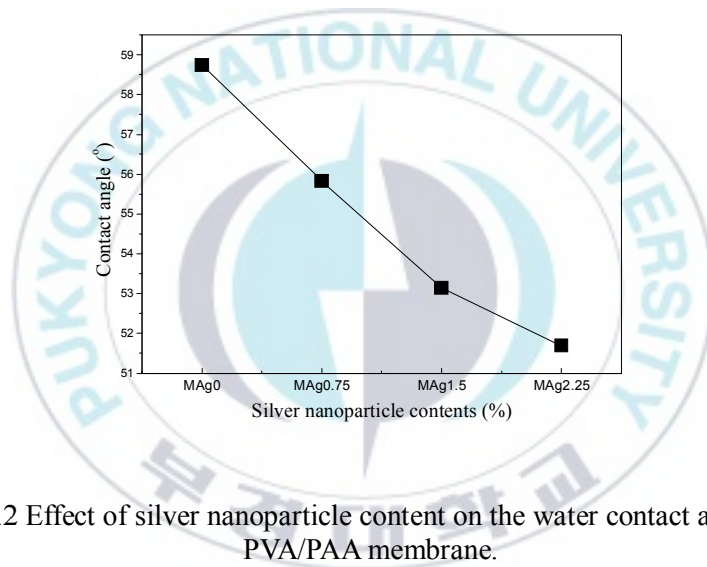
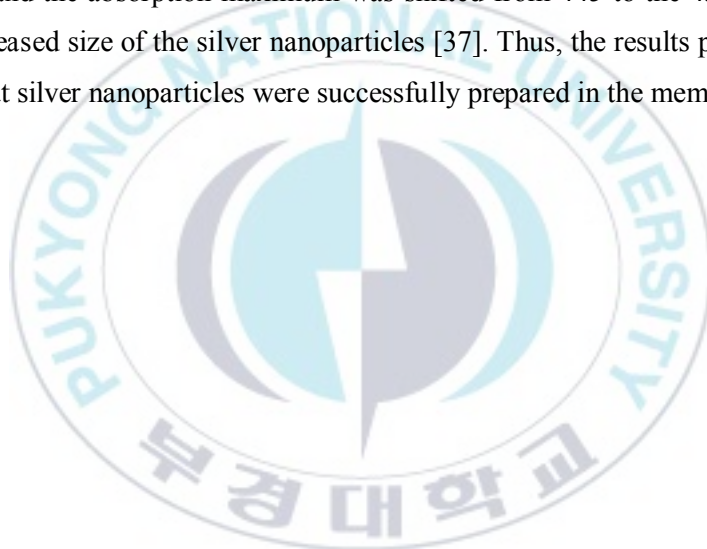


Figure 6.2 Effect of silver nanoparticle content on the water contact angle for the PVA/PAA membrane.

UV-visible spectroscopy

In situ generation of Ag nanoparticles in PVA/PAA has been accompanied by a membrane color change from transparent light-yellow to yellowish-green and gray with increasing AgNO₃ amount, compared to the virgin PVA/PAA membrane. All membrane films were characterized in the UV-visible range (200 to 800 nm). Figure 6.3 shows the absorption spectra of the virgin PVA/PAA and various silver-loaded films. With the exception of the pristine PVA/PAA membrane, all other silver-loaded membranes showed an absorption peak around 445 nm, which is characteristic of the surface plasmon band of silver nanoparticles [37]. Interestingly, the absorption intensity increased concomitantly with the Ag content, and the absorption maximum was shifted from 445 to the 432 nm, possibly due to a decreased size of the silver nanoparticles [37]. Thus, the results presented in Fig. 3 confirm that silver nanoparticles were successfully prepared in the membrane.



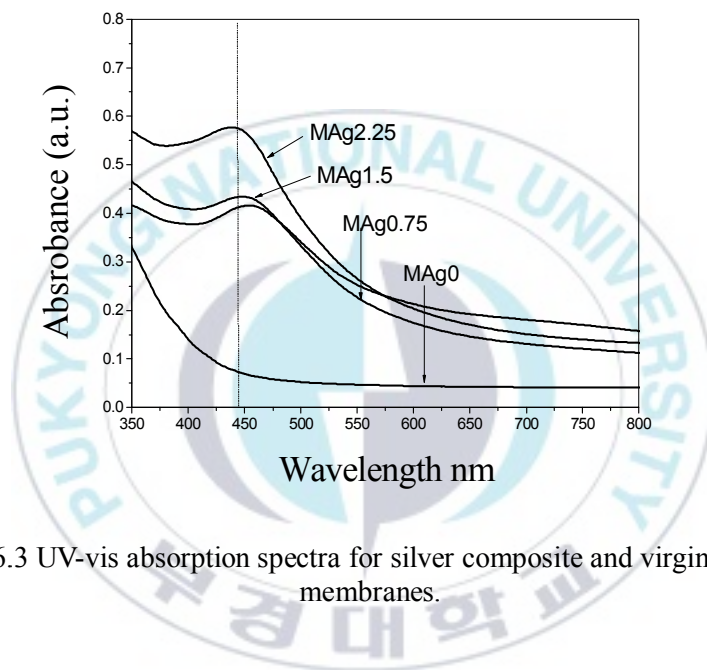


Figure 6.3 UV-vis absorption spectra for silver composite and virgin PVA/PAA membranes.

SEM and SEM-EDS characterization

Figure 6.4 shows SEM micrographs for PVA/PAA and the silver composite membranes (MAg0 to MAg2.25). It can be seen from Figure 2.15 that the silver nanoparticles are uniformly and homogeneously distributed throughout the PVA/PAA polymer matrix for all concentration of silver in the PVA/PAA membrane. The figure 6.4 also shows that the membranes are dense with no voids observed, which is good for pervaporation applications. Figure 6.5 shows the EDS spectrum of the MAg0.75 membrane, revealing a signal of back-scattered electrons corresponding to silver at approximately 3 keV, due to surface plasmon resonance [35]. Therefore, the presence of elemental silver at low concentration (MAg0.75) was confirmed, being representative for all silver composite membranes.



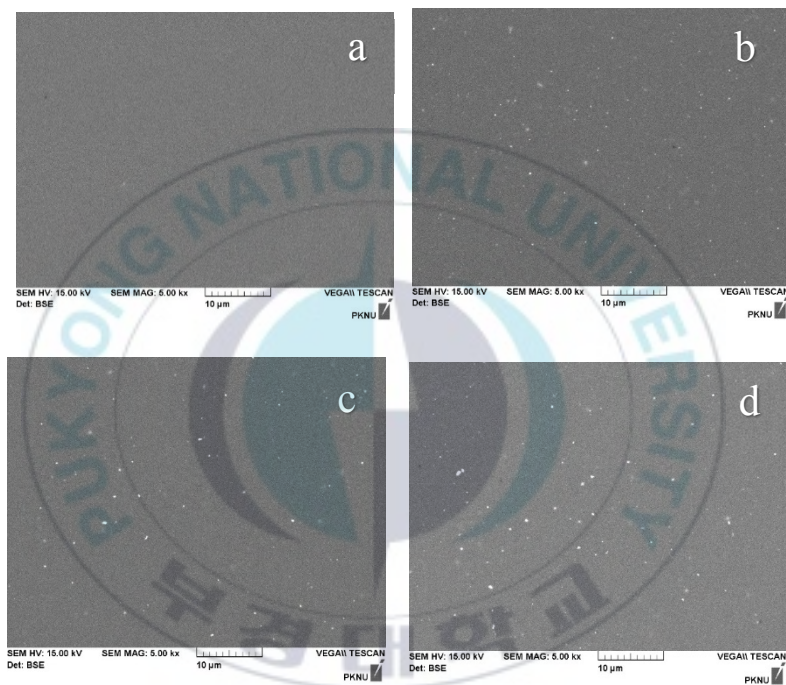


Figure 6.4 SEM micrographs of PVA/PAA (a) and silver composite membranes (MAg0.75 – (b), MAg 1.5 – (c), MAg2.25 – (d)).

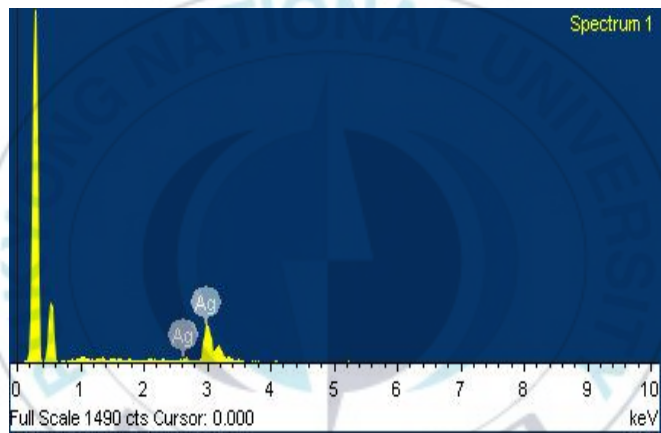


Figure 6.5 SEM-EDS spectrum of the in situ synthesized Ag nanoparticles in the PVA/PAA composite membrane (MAg0.75).

Membrane absorption.

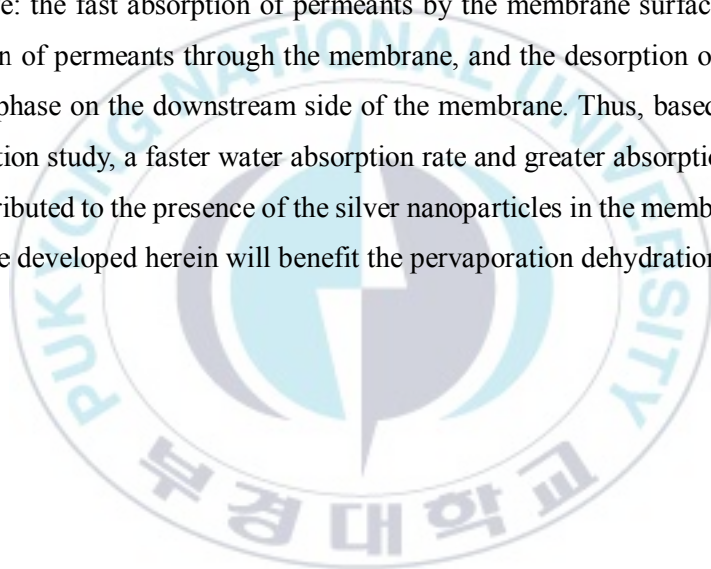
Figure 6.6 shows absorption as a function of time and the maximum absorption achieved in water for virgin PVA/PAA and various silver-loaded membranes. All membranes achieved maximum water absorption after 20 min, showing a constant value at later times. Virgin PVA/PAA (MAg0) membrane showed a maximum absorption of 150.5% of its original mass, while the corresponding values for MAg 0.75, MAg1.5, and MAg 2.25 are 177.1, 187.3 and 190.6%, respectively. Thus, the water uptake capacity is increased for silver-loaded membranes. Additionally, the rate of the membrane water absorption also increased due to the Ag nanoparticles present in the membrane. Thus, increased membrane hydrophilicity due to the Ag nanoparticles in the membrane matrix was observed. Abdel and El. Sawy prepared a composite membrane using PAA/Ag nanoparticles/chitosan [38] and obtained similar trends for water absorption as a function of silver nanoparticle content. The silver nano particle have a high surface energy of, a high hydrophilicity is expected for surface covered with the silver nano particle. Silver nanoparticle can release the silver ions in aqueous phase by oxidating and silver ion can simultaneously adsorbed on the silver nanoparticles surface, in the formation of hydration silver ion, which is the possible cause for the silver nanoparticle hydrophilicity. The dissolve the oxygen concentration in in deionized water is 9.1 mg/l under air saturated condition which is enough for the silver oxidation release. Additionally the as per the silver ion release mechanism, the silver ion released rate have been demonstrated to inversely proportional to the pH during the oxidation release process of silver. In the present study PVA and PAA are the fixation site for the silver nano particle, moreover the due to the presence of the PAA in the membrane creates the relatively low pH condition for the silver ion release.

The J. Li. and Q. Zhang et.al have reported the effect of silver nanoparticle nps on the PVDF membranes in terms of the hydrophilicity and antifouling performance [39], they have the found similar type of result. However in their study they have reported that further increased in the silver nanoparticle concentration leads to the decreased in the hydrophilicity due to the aggregation of silver nanoparticles therefore we have attempted to prepare the silver nanoparticle in situ in PVA/PAA matrix. Even though silver

nanoparticle have high surface energy, if mixed the silver nanoparticle in the PVA/PAA membrane the dispersion of particles would have been not easy.

Also, the effective interaction of Ag nanoparticles with the OH group of PVA. It forms the complex COO^- from PAA molecule. Additionally, while the in situ formation and growth of silver nanoparticles in the membrane matrix is due to the OH group of PVA, the adsorption of some PAA molecules on the surface of Ag nanoparticles [40] creates electrostatic interactions with water, resulting in increased water affinity and hydrophilicity. IR analysis data for the corresponding membranes support this explanation.

According to the solution diffusion model [31], the pervaporation process consists of three steps selective: the fast absorption of permeants by the membrane surface, the relatively slow diffusion of permeants through the membrane, and the desorption of the permeants in the vapor phase on the downstream side of the membrane. Thus, based on the present water absorption study, a faster water absorption rate and greater absorption capacity was observed, attributed to the presence of the silver nanoparticles in the membrane, and hence the membrane developed herein will benefit the pervaporation dehydration process.



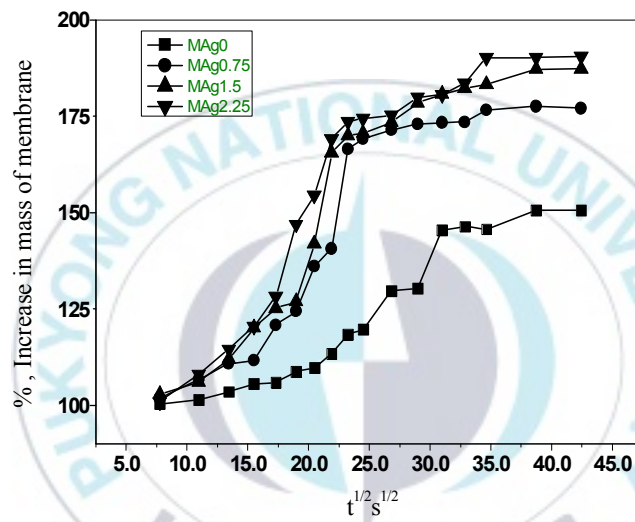


Figure 6.6 Membrane water absorption as a function of time ($s^{1/2}$) for the PVA/PAA and silver composite membranes.

6.4 Pervaporation.

6.4.1 Effect of Ag nanoparticles on the pervaporation performance of the PVA/PAA membrane.

Figure 6.7 summarizes the flux and selectivity data for the pervaporation separation of the water/acetic acid (80/20, w/w) feed mixture at 40 °C as a function of different silver nanoparticle content in the membranes. While showing a dramatic increase for the MAg0.75 silver composite membrane (0.14 kg/(m² h)), the permeation flux of the virgin membrane is 0.04 kg/(m² h), implying that the three-fold increase of flux sets the trend that continues with the increase of the silver nanoparticle content in the membrane. The separation factor, on the other hand, decreased from 75.8 to 27, and the marginally decreased to the 22 (MAg0 to MAg0.75- MAg2.25). The swelling study was performed under the same conditions as the pervaporation study. Figure 6.8 shows a plot of the swelling degree as a function of silver nanoparticle content. Similarly to the pervaporation permeation flux, it can be seen that the swelling value increased concomitantly with the silver nanoparticle content of the PVA/PAA polymer matrix.

To assess the effect of silver nanoparticles on the pervaporation performance of the composite membrane, the individual fluxes of water and acetic acid as functions of the silver nanoparticle content are shown in Figure 6.9. Figure 6.9 implies that the total flux is very close to the flux of water, increasing concomitantly with the silver nanoparticle content, while that of acetic acid is quite low and marginally increases with increasing silver nanoparticle content. Pervaporation experimental results indicate that the presence of silver nanoparticles increase the permeation of water compared to acetic acid.

Silver nanoparticles possess high surface energy and are thermodynamically unstable; therefore, they need to be stabilized. During stabilization, their surface properties (hydrophilicity or hydrophobicity) can be controlled depending on the groups present in the stabilizing molecule [42]. PVA molecules act as both reducing and capping agents in the preparation of Ag nanoparticles. Continuous magnetic stirring refines PVA molecules of refreshed reaction surface in smaller molecule which operate a controlled Ag⁺ to Ag reaction. PAA molecules stabilize the prepared Ag nanoparticles by means of COOH group

and adsorbed on the surface of its [40]. As is observed in the FTIR study of the composite membranes, both PVA and PAA interact with silver nanoparticle (utilizing OH and COOH groups, respectively), forming a protective layer and preventing nanoparticle aggregation. Since the membrane synthesis is conducted in aqueous media, particles with hydrophilic surface are generated [43]. Thus, membrane hydrophilicity is expected to increase due to the presence of the silver nanoparticles. Contact angle measurements and absorption data support this explanation. It has been proposed that dehydration of the organic phase take place in a unique manner. Amongst the feed components, unlike the random path of the less polar component (organics), water is transported by jumping from the one polar to another, meaning that each feed component takes a different path in the membrane. Thus, the presence of silver nanoparticles increased the membrane hydrophilicity and hence the water affinity responsible for the constant separation factor. The permeation flux also increased concomitantly with the silver nanoparticle content. A separation factor drop from 75 to 27 was observed for the silver composite membrane due to the plasticization of water on the PVA/PAA polymer matrix responsible to the dissolution of associated water acetic acid molecule and subsequently diffused through it, since the membrane water affinity has been increased.

In this study we have prepared different silver nanoparticle embedded (MAg0.75, MAg1.5, and MAg2.25) hybrids membrane to evaluation of pervaporation performance, further addition of silver nanoparticle resulted in to the extraction of nanoparticle during the pervaporation test ,since pervaporation experiment carried out at relatively elevated temperature comparison to the ambient condition, hence we stopped at MAg2.25 as optimal content. Nevertheless in our next study, have plan to optimize the size of the nano particle in the PVA/PAA polymer membrane to obtain the optimal pervaporation performance.

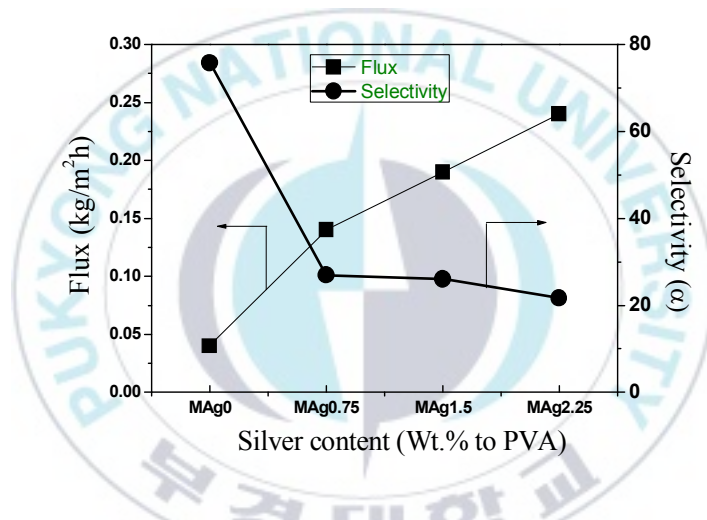


Figure 6.7 Effect of silver nanoparticle content on the pervaporation flux and separation factor. Feed composition: 80 wt. % Acetic acid, 50 μ m thickness at 40 °C.

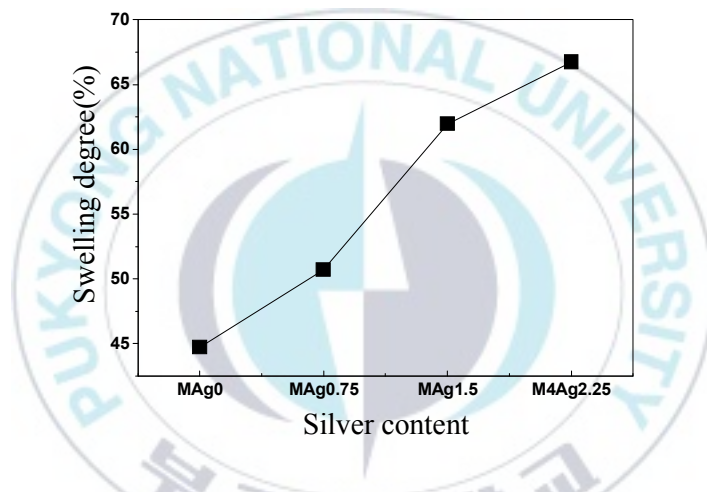


Figure 6.8 Effect of silver nanoparticle content on the degree of swelling for PVA/PAA membranes using a feed composite of 80 wt. % acetic acid at 40 °C, thickness: 50 μ m.

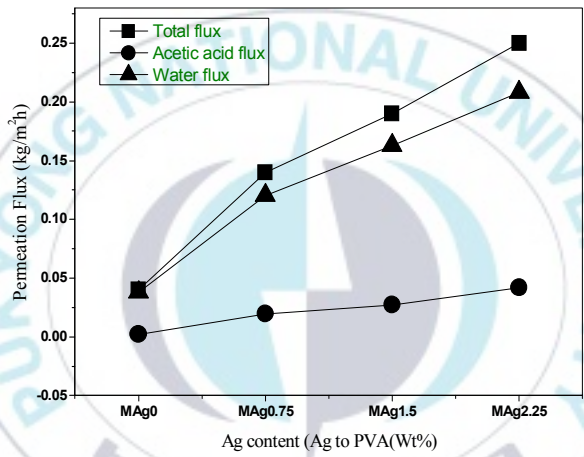


Figure 6.9 Total flux and the fluxes of water and acetic acid as a function of silver nanoparticle content.

6.5 Conclusions

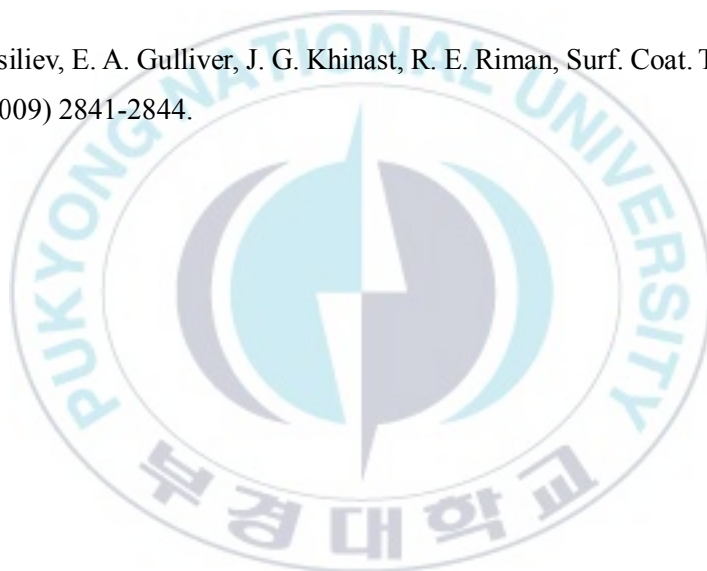
In the present study, in situ generation of silver nanoparticles in PVA/PAA polymer membranes in absence of reducing agent and their effect on the pervaporation of a water/acetic acid mixture was investigated. Based on UV, SEM, and SEM-EDS characterization, it was concluded that silver nanoparticles have been successfully prepared and well dispersed in the polymer matrix. The hydrophilicity of the PVA/PAA membrane was increased due to the presence of silver nanoparticles, and was confirmed by FTIR, contact angle, and membrane absorption studies. Pervaporation data for the composite membrane showed a three-fold increase of the flux value, while the separation was initially decreased prior to obtaining a constant value. This work shows the ease of preparation and stabilization of silver nanoparticles in membranes. The presence of Ag nanoparticles significantly influences the pervaporation performance of the membrane. This type of membrane fabrication can be highly beneficial if optimized for better pervaporation performance by controlling the PVA/PAA polymer ratio and the silver nanoparticle particle size/shape.

References.

- [1] V. Van Hoof, L. A. Van den Abeele, A. Buekenhout, C. Doutremount, R. Leysen, Sep. Purif. Technol. 37 (2004)133-49
- [2] R.W. Baker, Membrane Technology and Application, second ed. John Wiley and son's ltd. (2007) England,
- [3] Kalyani S, Smitha B, Sridhar S, Krishnaiah A, Desalination, 229 (2008) 68-81.
- [4] S. Ray, S. K. Ray, J. Membr.Sci. 285 (2006)108-119,
- [5] Y. Li Y, Verbiest T, Strobbe R and.Venkelecom Ivo F.J, J. Mater. Chem. A, 1, (2013) 15031.
- [6] N. Jullok, R. V. Hooghten, P. Luis, A. Volodin, C. V. Haesendonck, J. Vermant, B. V. Bruggen, J. Clean. Prod. 112 (2016) 4879-4889.
- [7] J. S. Kim , B. G. Lee, C. H. Lee, S. W. Kim, H. S. Jee, J. H. Koh, A.G. Fane, J. Clean. Prod. 5 (1997) 263-267
- [8] Zhu Y, Xia S, Liu F, Jin WJ. Membr. Sci. 349, ,(2009) 341-348.
- [9] A. V. Penkova, S. F. A. Acquah, M. E. Dmitrenko, B. Chen, K. N. Semnov, H. W. Kroto, Carbon, 76 (2014) 446-450.
- [10] Chen Z, Yang J, Yin D, Li Y, Wu S, Lu J ,Wang J,(2010), J. Membr.Sci. 349, 1-2: 175-182.
- [11] A. Rosa, L. Heux, J. Cavaille, K. Mazeau, Polymer 43 (2002) 5665–5677
- [12] S. Khoonsoop, S. Amnuaypanich, J. Membr.Sci. 367 (2011) 182-189.
- [13] M. Amirilargani, M. A. Tofighy, T. Mohammadi, B. Sadatnia, Ind. Eng. Chem. Res. 53 (2014) 12819-12829.
- [14] S. Rao, P. Smitha, B. Sridhar, S. Krishnaiah, Sep. Purif. Technol. 48 (3) (2006) 244–254
- [15] G. Asman, O. Sanli, Sep. Sci. Tech. 41 (2006) 1193-1209.
- [16] J. W. Rhim, S. W. Yeom, S. W. Kim, K. H. Lee, J. Appl. Polym. Sci. 63 (1997) 521-527.
- [17] C. Vaclair, H. Tarjus, P. Schaetzel, J. Membr.Sci.125 (2) (1997) 293-301.

- [18] S.S. Kulkarni, S. M. Tambe, A. A. Kittur, M. Y. Karuduraganavar, *J. Membr.Sci.* 285 (2006) 420-431
- [19] B. Baheri, M. Shahverdi, M. Rezakazemi, E. Motae, T. Mohammadi, *Chemical Engi. Communication*, 202 (2015) 316-321.
- [20] G. Dudek, M. Gnus, R. Turczyn, A. Strzelewicz, M. Krasowska, *Sep. Purif. Technol.* 133 (2014) 8-15.
- [21] M. Sairam, M. B. Patil, R. S. Veerapur, S. Ravindra, S. A. Patil, T. M. Aminabahi, *J.Membr.Sci.*281 (2006) 95-102.
- [22] A. Sivanesan, H. K. Ly HK, J. Kozuch, “*Chemical Communications*, 47, (2011) 3553–3555.
- [23] K. Liu, S. Qu, X. Zhang, F. Tan, Z. Wang, *Nanoscale Research Letters*, 8, (2013) 1–6,
- [24] H. Zhu, M. Du, M. Zhang, *Biosensors and Bioelectronics*, 49 (2013) 210–215,
- [25] P. Zhang, C. Shao, Z. Zhang, *Nanoscale*, 3 (2011) 3357–3363,
- [26] W. A. Ismail, Z. A. Ali, R. Puteh, *Journal of Nanomaterials*, (2013) Article ID 901452, 6 pages,
- [27] H. Kaczmarek, A. A. Szalla, Photochemical transformation in poly (acrylic acid)/poly (ethylene oxide) complexes. *J. Photochem. Photobiol*, 180 (2006) 46–53.
- [28] N. Mahanta, S. A. Valiyaveetil, *RSC advances* 2 (2012)11389- 11396.
- [29] F. G. Premakshi, A. M. Sajjan, A. A. Kittur, M. Y. Kariduraganavar, *J.Appl.Polym.Sci.*132 (2015) 41248.
- [30] A. Gautam, P. Tripathi, S. Ram, *J. Mater. Sci.* 41, (2006) 3007-3016.
- [31] H. Mansur, C. Sadahira, A. Souza, A. Mansur, *Mater. Sci. Eng. C* 28 (2008) 539–548.
- [32] P. Rao, B. Smitha, S. Sridhar, A. Krishnaiah, *Sep. Purif. Technol.* 48 (2006) 244–254.
- [33] E. Campos, P. Coimbra, M.H. Gil, *Polym. Bull.* 70 (2013) 549–561.
- [34] J. B. Gonzalez-campos, E. Provkhorov, G. Luna-Barcenas, I. C. Sanchez, J. Lara-Romero, M. E. Mendoza-Duarte, F. Villasenor, L. Guevara-Olvera, *J.Polym.Sci.Part B: Polym.Phys.* 48, (2010) 739-748
- [35] S. Chalal, N. Haddadine, N. Bouslah, A. Benaboura, *J. Polym.Res.*0024-1(2012) 10965.

- [36] Z. Ni, Z. Wang, L. Sun, B. Li, Y. Zhao, *Mate. Sci. Eng. C* 41(2014) 249-254.
- [37] M. K. Choudhary, J. Kataria, S. S. Cameotra, J. Singh, *Appl. Nanosci.* 6, (2015) 105-111.
- [38] A. Mohdy, A. Okeil, S. El-Sabagh, S. M. El-Sawy, *Int. J. Chem. Mol. Nucl., Mat., and Metall. Engi.* 9 (2015) 1088-1093.
- [39] J. Li, X. Shao, Q. Zhou, M. Li, Q. Zhang, *App. Sur. Sci.* 265 (2013) 663-670.
- [40] Z. Ni, Z. Wang, L. Sun, B. Li, Y. Zhao, *Mate. Sci. Eng. C*, 41 (2014) 249-254.
- [41] J. G. Wiljmans, R. W. Baker, *J. Membr. Sci.* 107 (1995) 1-21.
- [42] A. Y. Olenin, Y. A. Krutyakov, A. A. Kudrunskil, G. V. Lisichkin, *Coll. Jour.* 70 (2008) 71-76.
- [43] A. N. Vasiliev, E. A. Gulliver, J. G. Khinast, R. E. Riman, *Surf. Coat. Tech. Surf. Coat. Tech.* 203, (2009) 2841-2844.



7. Summary and Conclusion

7.1 Summary

1. Membrane of polyvinyl alcohol and polyvinyl amine blend and mixed matrix membrane from M-STA incorporation in to the PVA/PVAm were synthesized and In-situ synthesized PVA/PAA membrane were prepared. They were characterized by FTIR, XRD, and SEM, contact angle measurement of membrane surface, AFM study for membrane surface, DSC and SEM-EDS analyses. Swelling (Sorption) characteristic in water/AA and water/IPA and water/acetonitrile mixtures also studied.
2. Pervaporation dehydration of IPA, Acetonitrile and Acetic acid were performed using above prepared membranes and PV performance of membrane were evaluated in terms of flux and separation factor.
3. PVAm/PVA blended and M-STA loaded MMM (mixed matrix membrane) and Ag-PVA-PAA membranes showed high separation selectivity with good flux for water in comparison to that of acetic acid, IPA, and acetonitrile from the IPA-water, acetonitrile/water and acetic acid-water mixtures.
4. An optimum mixing ratio of PVA/PVAm 100/30 (PVAm1.5), and M8-MSTA were determined.
5. Improved PV performance from M-STA loaded MMM in comparison to the PVA/PVAm blend membrane was obtained.
6. From the Pervaporation data for the composite membrane (PVA/PAA-Ag NPs) showed a three-fold increase of the flux value, while the separation was initially decreased prior to obtaining a constant value.
7. All the membrane showed good mechanical and thermal stability was observed. The activation energy for permeation each of water, acetonitrile and isopropanol using an Arrhenius equation calculated and with a higher activation energy being was observed for isopropanol and acetonitrile than that for water.

7.2 Conclusion

PVA based hydrophilic dense membranes (flat sheet) was developed for the PV dehydration of Acetic acid and isopropanol and acetonitrile feed system. It was concluded from the all studies that, membrane developed can be used to dehydrate the isopropanol, acetonitrile and acetic acid of their azeotropic composition range.

Since the membranes prepared in this study had a higher thickness because of laboratory scale preparation using solution casting technique. However with increasing the membrane surface area by decrease in membrane thickness, it can possible by coating or applying same membrane solutions on the commercial supporter will provide rapid and effective separation.



Acknowledgement

I sincerely express my gratitude to my advisor, Prof. Dr. MinYoung Shon, Department of Industrial chemistry, Pukyong National University, for his invaluable guidance, kind advices and constant inspiration throughout my course of this investigation. I also gracefully express my gratitude to Prof. MyungJun Moon for kindly providing the laboratory to carry out my investigation.

I am grateful to Dr. YouIn Park, Dr. SeungEun Nam, Korea Research Institute of Chemical Technology for granting research fund to perform my investigation.

I would like to thank the examination committee members, Prof. Dr. Lim JunHyuk, Prof. Dr. SeongIl Ryu, Prof. Dr. DongWook Chang for their valuable suggestion and comments.

I would also to thank the all my laboratory members in Department of Industrial Chemistry, Pukyong National University, namely, Enthusiastic DongWook Lee, Hardworking YongSung Kwon, Sincere Bae Duck Hwan, Kind Shin PyongHwa, Lee NamKyu, Lim Taekyu for their moral support and as well as their help in performing the membrane characterization experiments.

I would to acknowledge the all of the instruments department in Pukyong National University for proving facilities to carry out my precise analysis of membrane characterization.

At the submission of my thesis, I express my thanksgiving to my mother, father, mother-in law and father in-law, elder brother and sister in law for their blessing and inspiration during the period of my research. I am grateful to my wife for creating positive environment in home and attitude in me to follow the work.